

MPI-PhT/98-76

September 1998

**Complete Helicity Decomposition of the $Bt\bar{t}$ Vertex
including Higher Order QCD Corrections and
Applications to $e^+e^- \rightarrow t\bar{t}$**

Bodo Lampe

Max Planck Institut für Physik
Föhringer Ring 6, D-80805 München

Abstract

The complete density matrix for all polarization configurations in the process $B^* \rightarrow t\bar{t}$, where B^* is an off-shell Z or photon and t is the top quark, is calculated numerically including oneloop QCD corrections, i.e. virtual *and* real gluon contributions in $O(\alpha_s)$. The analysis is done in the framework of the helicity formalism. The results are particularly suited for top quark production at the Linear Collider, but may be useful in other circumstances as well. Relations to LEP and Tevatron physics are pointed out.

1. Introduction

Since its discovery in 1995 the top quark has been an object of increasing interest. The production process for top quarks has been analyzed in various theoretical studies both for pp and e^+e^- collisions. Early references on the lowest order cross section are [1] for pp collisions and [2] for e^+e^- annihilation. Higher order corrections to the cross section (total cross section, p_T distribution etc.) have been calculated by several groups, [3, 4] for pp and [5, 6] for e^+e^- processes. These total cross sections do not involve information on the top quark polarization. Such spin effects only come in, if one studies distributions of top quark decay products. In some cases, spin effects have been studied, i.e. the distribution of the top quark spin vector, in ref. [7] for pp and in ref. [8] for e^+e^- collisions, but have not been extended to higher orders. An interesting step in this direction has been taken in ref. [6], where a Monte Carlo program including final state spin terms has been written. That article is in fact concerned with higher order corrections to $\tau^+\tau^-$ production in e^+e^- annihilation at lower energies and so does not take into account axial vector couplings. More general results, including axial vector couplings, can be found in [9], but not in the form of a Monte Carlo program. Ref. [9] is an alternative to the approach presented here, although we think that our approach is more enlightening, systematic and complete.

Nothing is known about higher order spin corrections to the processes which induce top quark production in proton collisions (light quark annihilation $q\bar{q} \rightarrow t\bar{t}$ and gluon-gluon fusion $gg \rightarrow t\bar{t}$). In contrast to e^+e^- annihilation, there is initial state gluon radiation and this makes those calculations very difficult. The simplifying feature of QCD corrections to heavy quark production in e^+e^- annihilation is that the problem may be reduced to QCD corrections to the vectorboson-heavy quark vertex. Recently, a method for calculating QCD corrections to this vertex has been developed for the case of top quark decay $t \rightarrow bW$ [10], i.e. the tbW vertex. In the present article this method will be applied and generalized to $e^+e^- \rightarrow B(=Z,\gamma)^* \rightarrow t\bar{t}$. The method is based on the helicity formalism and allows to obtain the QCD corrections to the full spin density matrix of the process in a straightforward and economical way. Furthermore, the results obtained for top quark decay [10] can be easily combined with the results of this paper by

using a master formula Eq. (4) to obtain QCD corrections for any distribution of top quark decay products in e^+e^- annihilation one may be interested in.

Within the Standard Model, all couplings of the top quark to other particles are completely fixed by its mass and by a few quantum numbers. For example, the coupling of the top quark to gluons is a pure vector coupling with strength g_s , the coupling to a vector boson is given by $v_B\gamma_\mu + a_B\gamma_\mu\gamma_5$ with $v_Z = \frac{1}{2} - \frac{4}{3}s_W^2$, $a_Z = \frac{1}{2}$, $v_\gamma = \frac{4}{3}s_Wc_W$, $a_\gamma = 0$ etc. The couplings to the Z-boson and to the photon are particularly important for this article, because the process under consideration proceeds with an intermediate off-shell Z or photon where Z^* and γ^* arise from the annihilation of two massless fermions (e^+ and e^-). As will be seen, this latter fact strongly reduces the number of independent helicity amplitudes and makes the results quite intuitive.

2. Helicity Description

Helicity amplitudes have been considered in many applications of phenomenological importance in high energy physics, like jet production [11], nonstandard effects in top quark processes [12], and many others. The idea is, first to separate a given process into simpler subprocesses and then to explicitly evaluate all the possible spin amplitudes for the subprocesses in special Lorentz and Dirac frames. The results can afterwards be put together with the help of a master formula (to be given below). For example, consider the lowest order helicity amplitudes for top quark production in e^+e^- annihilation through a vector boson B^* with either vector or axialvector couplings v_B or a_B to the top quark. They are given by

$$M_V(H, h, \bar{h}) = v_B \bar{u}_h(p_t) \gamma_\mu v_{\bar{h}}(p_{\bar{t}}) \epsilon_H^\mu \quad (1)$$

$$M_A(H, h, \bar{h}) = a_B \bar{u}_h(p_t) \gamma_\mu \gamma_5 v_{\bar{h}}(p_{\bar{t}}) \epsilon_H^\mu \quad (2)$$

where $h = \pm\frac{1}{2}$, $\bar{h} = \pm\frac{1}{2}$ and $H = 0, \pm 1$ label the spin states for the top quark and the B-boson. Note that for off-shell photons there is a longitudinal component with $H = 0$ just as for a massive vector boson. In total, there are 24 amplitudes to be considered, which can in principle be relevant to the process.

Real gluon emission cannot be treated on the amplitude level, but only on the level of the density matrix

$$\rho_{IJ}(H, h, \bar{h}, H', h', \bar{h}') := M_I(H, h, \bar{h}) M_J^*(H', h', \bar{h}') \quad (3)$$

where I and J denote either V (=vector) or A (=axialvector). The gluons are supposed to be unpolarized. After hermiticity one has 78 independent density matrix elements each for the VV , VA and AA case, a total of 234 amplitudes. As will be shown below, only 60 of these are relevant for e^+e^- annihilation. Note that the amplitudes are only determined up to an overall phase, and that this arbitrariness goes away when forming the density matrix elements.

The full density matrix is in fact needed in the 'master formula', if one considers the combined production and decay process for the top quark. Assume the general case, that top quarks are produced in some process $ab \rightarrow t\bar{t}$ and then decay according to $t \rightarrow W^+b$ and $\bar{t} \rightarrow W^-\bar{b}$, where the W 's further decay to light (massless) fermions, $W^+ \rightarrow f_1\bar{f}_2$ and $W^- \rightarrow f_3\bar{f}_4$. The cross section is then given by the 'master formula'

$$\sigma = \sum_{EXT} \left| \sum_{INT} M(h_a, h_b, h, \bar{h}) M(h, h_{W^+}) M(\bar{h}, h_{W^-}) M(h_{W^+}) M(h_{W^-}) \right|^2 \quad (4)$$

where $EXT = h_a, h_b$ denotes the spins of the external particles and $INT = h, \bar{h}, h_{W^+}, h_{W^-}$ the spins of the internal particles of the process. $M(h_a, h_b, h, \bar{h})$ are the helicity amplitudes for the production process, $M(\bar{h}, h_{W^-})$ for the decay of the antitop quark, and $M(h_{W^+})$ and $M(h_{W^-})$ are the amplitudes for the decay of the W^+ and W^- , respectively. The fact that the formula makes no explicit reference to the spins of the massless fermions f_i , $i=1,2,3,4$, has the same reason as the non-appearance of the b -quark spins. Namely, the h_{f_i} are fixed by the V-A nature of the W decays, just as h_b is fixed by the V-A nature of the top decays (assuming massless b -quarks). Furthermore, if one is not interested in the decay of the antitop or of the W 's, the corresponding amplitudes and helicities will not appear in the above formulas. In that case, the \bar{t} and/or the W 's will be one of the external (EXT) particles, whose spins have to be summed over after taking the square in Eq. (4). Besides neglecting the b -quark mass, it is also a good approximation in Eq. (4) to take the internal particles (top quarks and

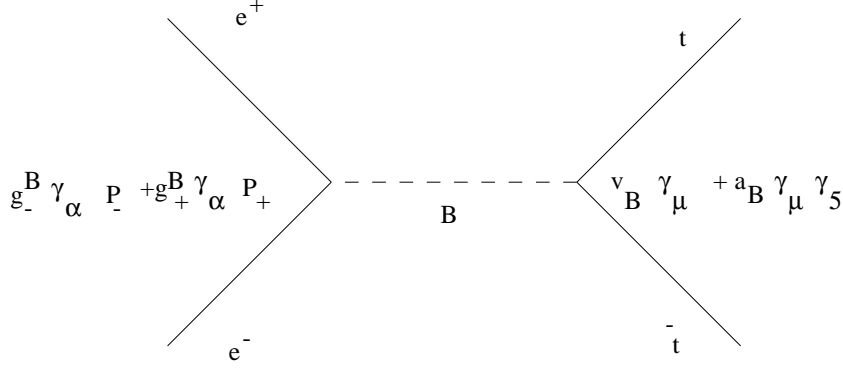


Figure 1: Definition of the couplings

W's) on-shell, because off-shell contributions are suppressed by powers of the width Γ_t and Γ_W .

3. Deconstruction of the e^+e^- Production Cross Section

In contrast, the intermediate vector boson Z and γ must not be taken on-shell. The general spin amplitude for the production part of the process is

$$M(h_p, h_e, h, \bar{h}) = \frac{M_Z(h_p, h_e, h, \bar{h})}{Q^2 - m_Z^2} + \frac{M_\gamma(h_p, h_e, h, \bar{h})}{Q^2} \quad (5)$$

where $h_{p,e}$ are the e^\pm spins and Q^2 is the square of the e^+e^- energy. These amplitudes are now to be decomposed into the elementary amplitudes Eqs. (1) and (2). The decomposition will be on the algebraic level only, and no numerical analysis will be presented in this section, because we just want to show how the elementary amplitudes enter the e^+e^- cross section. Afterwards the complete oneloop QCD corrections to all the elementary amplitudes resp. spin density matrix elements will be given (sections 5 and 6).

The two amplitudes M_Z and M_γ in Eq. (5) have a decomposition of the form

$$M_B(h_p, h_e, h, \bar{h}) = \sum_H M_B(h_p, h_e, H) \frac{1}{Q^2 - m_B^2} M_B(H, h, \bar{h}) \quad (6)$$

where the sum is over the Spins $H = 0, \pm 1$ of the off-shell B-boson. In this way the $Bt\bar{t}$ vertex amplitudes Eqs. (1) and (2) enter the cross section (4).

$M_B(h_p, h_e, H)$ are the spin amplitudes for $e^+e^- \rightarrow B^*$ and have a very simple structure due to the approximate masslessness of e^\pm . Namely, one has

$$M_B(h_p, h_e, H) = \begin{cases} \frac{g_-^B}{\sqrt{2}} & \text{for } (h_p, h_e, H) = (+\frac{1}{2}, -\frac{1}{2}, -1) \\ \frac{g_+^B}{\sqrt{2}} & \text{for } (h_p, h_e, H) = (-\frac{1}{2}, +\frac{1}{2}, +1) \\ 0 & \text{otherwise} \end{cases} \quad (7)$$

where $g_\pm^B = v_e^B \pm a_e^B$ are the left- and right-handed part of the lepton couplings to the B , with $v_e^Z = -\frac{1}{2} + 2s_W^2$, $a_e^Z = -\frac{1}{2}$, $v_e^\gamma = -2s_W c_W$, $a_e^\gamma = 0$. Furthermore, the spin quantization axis has been chosen to be the $+z$ direction. According to Eq. (7) not all of the amplitudes $M_B(H, h, \bar{h})$ are picked up in Eq. (6) to give a nonzero contribution to the e^+e^- amplitudes $M_B(h_p, h_e, h, \bar{h})$. Fig. 1 gives a graphic view about what notations are used for the couplings of the lowest order process. From this figure it becomes clear that the amplitudes $M_B(H, h, \bar{h})$ are a linear combination $\sim v_B M_V + a_B M_A$. Altogether one gets:

$$M_B(h_p, h_e, h, \bar{h}) = \begin{cases} +\frac{g_-^B}{\sqrt{2}}[v_B M_V(-1, h, \bar{h}) + a_B M_A(-1, h, \bar{h})] & h_p = +\frac{1}{2}, h_e = -\frac{1}{2} \\ -\frac{g_+^B}{\sqrt{2}}[v_B M_V(+1, h, \bar{h}) + a_B M_A(+1, h, \bar{h})] & h_p = -\frac{1}{2}, h_e = +\frac{1}{2} \\ 0 & \text{otherwise} \end{cases} \quad (8)$$

One can now combine the contributions from γ and Z (cf. Eq. (5)):

$$M(h_p, h_e, h, \bar{h}) = \begin{cases} v_- M_V(-1, h, \bar{h}) + a_- M_A(-1, h, \bar{h}) & h_p = +\frac{1}{2}, h_e = -\frac{1}{2} \\ v_+ M_V(+1, h, \bar{h}) + a_+ M_A(+1, h, \bar{h}) & h_p = -\frac{1}{2}, h_e = +\frac{1}{2} \\ 0 & \text{otherwise} \end{cases} \quad (9)$$

where we have used the abbreviations $v_\pm = \mp \frac{1}{\sqrt{2}}(\frac{g_\pm^Z v_Z}{Q^2 - m_Z^2} + \frac{g_\pm^\gamma v_\gamma}{Q^2})$ and $a_\pm = \mp \frac{1}{\sqrt{2}} \frac{g_\pm^Z a_Z}{Q^2 - m_Z^2}$. According to Eqs. (4) and (9), if the e^\pm beams are unpolarized, the cross section is a sum of two terms, $\sigma = \sigma_- + \sigma_+$, where the first term is due to e^+e^- helicities $h_p = +\frac{1}{2}$, $h_e = -\frac{1}{2}$ and the second term is due to e^+e^- helicities $h_p = -\frac{1}{2}$, $h_e = +\frac{1}{2}$. One has

$$\sigma_\pm = \left| \sum_{h, \bar{h}} [v_\pm M_V(\pm 1, h, \bar{h}) + a_\pm M_A(\pm 1, h, \bar{h})] D(h, \bar{h}) \right|^2 \quad (10)$$

where the contributions from the decay amplitudes have been summarized as $D(h, \bar{h})$. When one carries out the modulus squared in Eq. (10), it becomes apparent that in general all the density matrix elements of the form $M_I(+1, h, \bar{h})M_J(+1, h', \bar{h}')^*$ and $M_I(-1, h, \bar{h})M_J(-1, h', \bar{h}')^*$ for $IJ = VV, VA + AV$ and AA are needed to calculate the cross section of the decay products. Note that instead of VA we are using the explicitly hermitean combination $VA + AV$. This is no restriction because to all orders in QCD one has $M_V M_A^* = M_A M_V^*$. As will become explicit in section 5, the matrix elements of $H = +1$ and $H = -1$ are related, so that only the first set $M_I(+1, h, \bar{h})M_J(+1, h', \bar{h}')^*$ has to be calculated. For each combination $IJ = VV, VA + AV$ and AA there are 10 independent matrix elements in this set.

4. The Method

The results to be presented were obtained in the helicity formalism. Furthermore, they concern the oneloop QCD corrections to the lowest order matrix elements. The lowest order expressions are usually simple, whereas the oneloop expressions, in particular for the case of hard gluons are quite lengthy for arbitrary spin orientations of B , t and \bar{t} (the gluons are assumed to be unpolarized)¹. Furthermore, the hard gluon contributions cannot be treated on the level of amplitudes, because they have to be integrated over the gluon's energy and angles. One really has to go to the level of the (spin) density matrix,

$$\rho(H, h, \bar{h}, H', h', \bar{h}') := M(H, h, \bar{h})M^*(H', h', \bar{h}') \quad (11)$$

to do the phase space integrations. There is, however, one circumstance which simplifies the task. This is related to the fact, that the oneloop QCD corrections to the total (spin-averaged) cross section for top quark production are known [5, 14]. This allows to get rid of the infrared and collinear singularities present in the matrix elements, by forming suitable singularity-free combinations of the spin-dependent and the spin-averaged expressions. The point is that the infrared and collinear singularities are 'universal', i.e. independent of the spin direction,

¹see however ref. [13] for rather compact formulae

so that they will drop out in suitable ratios and differences. To be more explicit, consider the ratio

$$R(H, h, \bar{h}, H', h', \bar{h}') := \frac{\rho(H, h, \bar{h}, H', h', \bar{h}')}{\text{tr}\rho} \quad (12)$$

where the trace of the density matrix is given by

$$\text{tr}\rho = \sum_{H, h, \bar{h}} |M(H, h, \bar{h})|^2 \quad (13)$$

Now assume that each matrix element has the generic form $\rho = T + \alpha K$ where T stands for the tree level term, K for the higher order correction and $\alpha = C_F \frac{\alpha_s}{2\pi}$ is the QCD coupling constant and $C_F = \frac{4}{3}$. Assume similarly, that $\text{tr}\rho$ has the form $\text{tr}\rho = T_{\text{all}} + \alpha K_{\text{all}}$. Then the ratio $\rho/\text{tr}\rho$ is given by

$$R = \frac{\rho}{\text{tr}\rho} = \frac{T}{T_{\text{all}}} + \alpha \frac{KT_{\text{all}} - TK_{\text{all}}}{T_{\text{all}}^2} + O(\alpha^2) = \text{LO} + \alpha \text{HO} \quad (14)$$

It turns out that the difference $KT_{\text{all}} - TK_{\text{all}}$ is free of infrared and collinear (and ultraviolet) singularities. If calculated, it gives an elegant means to determine higher order corrections to the density matrix [15]. In the formulas and figures presented below, R will be written as $R = \text{LO} + \alpha \text{HO}$ where LO and HO will be plotted as a function of m_t/Q .

Finally note that the considerations in this section should in principle be done for the three matrices ρ_{VV} , $\rho_{VA}(= \rho_{AV})$ and ρ_{AA} separately. In the case of VA it turns out that the trace of the density matrix vanishes (in leading order and in higher order). It is therefore convenient to consider a different linear combination, e.g. $VA + AV + AA$ with a nonvanishing $\text{tr}\rho$, and to apply the method Eq. (14) on that. Results for VA can afterwards be reconstructed by taking the difference of $VA + AV + AA$ and AA (see Eq. (31) in the summary section).

5. Lowest Order Amplitudes and Virtual Corrections

I have calculated the eight needed amplitudes $M_I(+1, h, \bar{h})$, $I = V, A$ as defined in Eqs. (1) and (2) using the 'chiral representation' of γ matrices, in which

$\gamma_5 = \text{diag}(-1, -1, 1, 1)$ etc. The results are presented in the rest frame of the virtual B-boson where the momenta are given by

$$p_B = (Q, 0, 0, 0) \quad p_t = \frac{Q}{2}(1, 0, 0, \beta) \quad p_{\bar{t}} = \frac{Q}{2}(1, 0, 0, -\beta) \quad (15)$$

with $\beta^2 = 1 - \frac{4m_t^2}{Q^2}$. An independent set of spinors for the top quarks is then given by

$$\begin{aligned} \bar{u}_{+\frac{1}{2}}(p_t) &= (a_+, 0, a_-, 0) & \bar{u}_{-\frac{1}{2}}(p_t) &= (0, a_-, 0, a_+) \\ v_{+\frac{1}{2}}(p_{\bar{t}}) &= (-a_+, 0, a_-, 0) & v_{-\frac{1}{2}}(p_{\bar{t}}) &= (0, -a_-, 0, a_+) \end{aligned}$$

where $a_{\pm}^2 = \frac{Q}{2}(1 \pm \beta)$. The quantization axis of the B-boson spin is chosen to be at an angle θ w.r.t. the top quark momentum, i.e. the polarization vector for $H = +1$ is given by

$$\epsilon_{+1} = \frac{1}{\sqrt{2}}(0, \cos \theta, -i, -\sin \theta). \quad (16)$$

The most general parametrization of polarization vectors would be

$$\begin{aligned} \epsilon_{-1} &= -\frac{e^{i\phi}}{\sqrt{2}}(0, \cos \phi \cos \theta - i \sin \phi, \sin \phi \cos \theta + i \cos \phi, -\sin \theta) \\ \epsilon_{+1} &= -\epsilon_{-1}^* \\ \epsilon_0 &= -(0, \sin \theta \cos \phi, \sin \theta \sin \phi, \cos \theta). \end{aligned} \quad (17)$$

but for the problem at hand one may choose $\phi = 0$ without restriction. Note further that although the off-shell B-boson has a longitudinal polarization component, there is no contribution from longitudinal $B's$ to the e^+e^- cross section, as has been shown in section 3. Nevertheless, for completeness and curiosity, all

the lowest order amplitudes are given here:

$$\begin{aligned}
M_V(0, -\frac{1}{2}, -\frac{1}{2}) &= -2\frac{m_t}{Q} \cos \theta & M_A(0, -\frac{1}{2}, -\frac{1}{2}) &= 0 \\
M_V(-1, -\frac{1}{2}, -\frac{1}{2}) &= \sqrt{2}\frac{m_t}{Q} \sin \theta e^{i\phi} & M_A(-1, -\frac{1}{2}, -\frac{1}{2}) &= 0 \\
M_V(+1, -\frac{1}{2}, -\frac{1}{2}) &= -\sqrt{2}\frac{m_t}{Q} \sin \theta e^{-i\phi} & M_A(+1, -\frac{1}{2}, -\frac{1}{2}) &= 0 \\
M_V(0, -\frac{1}{2}, +\frac{1}{2}) &= \sin \theta e^{i\phi} & M_A(0, -\frac{1}{2}, +\frac{1}{2}) &= \beta \sin \theta e^{i\phi} \\
M_V(-1, -\frac{1}{2}, +\frac{1}{2}) &= -e^{2i\phi} \frac{1-\cos \theta}{\sqrt{2}} & M_A(-1, -\frac{1}{2}, +\frac{1}{2}) &= -\beta e^{2i\phi} \frac{1-\cos \theta}{\sqrt{2}} \\
M_V(+1, -\frac{1}{2}, +\frac{1}{2}) &= -\frac{1+\cos \theta}{\sqrt{2}} & M_A(+1, -\frac{1}{2}, +\frac{1}{2}) &= -\beta \frac{1+\cos \theta}{\sqrt{2}} \\
M_V(0, +\frac{1}{2}, -\frac{1}{2}) &= \sin \theta e^{-i\phi} & M_A(0, +\frac{1}{2}, -\frac{1}{2}) &= -\beta \sin \theta e^{-i\phi} \\
M_V(-1, +\frac{1}{2}, -\frac{1}{2}) &= \frac{1+\cos \theta}{\sqrt{2}} & M_A(-1, +\frac{1}{2}, -\frac{1}{2}) &= -\beta \frac{1+\cos \theta}{\sqrt{2}} \\
M_V(+1, +\frac{1}{2}, -\frac{1}{2}) &= e^{-2i\phi} \frac{1-\cos \theta}{\sqrt{2}} & M_A(+1, +\frac{1}{2}, -\frac{1}{2}) &= -\beta e^{-2i\phi} \frac{1-\cos \theta}{\sqrt{2}} \\
M_V(0, +\frac{1}{2}, +\frac{1}{2}) &= 2\frac{m_t}{Q} \cos \theta & M_A(0, +\frac{1}{2}, +\frac{1}{2}) &= 0 \\
M_V(-1, +\frac{1}{2}, +\frac{1}{2}) &= -\sqrt{2}\frac{m_t}{Q} \sin \theta e^{i\phi} & M_A(-1, +\frac{1}{2}, +\frac{1}{2}) &= 0 \\
M_V(+1, +\frac{1}{2}, +\frac{1}{2}) &= \sqrt{2}\frac{m_t}{Q} \sin \theta e^{-i\phi} & M_A(+1, +\frac{1}{2}, +\frac{1}{2}) &= 0
\end{aligned} \tag{18}$$

These amplitudes show a lot of symmetry. The most important for us arises from interchanging the role of particle and antiparticle. For $\phi = 0$ this amounts to $\theta \leftrightarrow \theta + \pi$ and interchanges amplitudes of the form $M_I(+1, h, \bar{h}) \leftrightarrow M_I(-1, h, \bar{h})$, $I = V, A$. In fact this relation is induced by CP invariance and it holds including higher order QCD corrections. It reduces the number of independent density matrix elements to be calculated by half from 60 to 30.

Using Eq. (18) one may calculate the trace of the corresponding density matrix Eq. (13):

$$\text{tr} \rho_{VV} = 4 + 8\frac{m_t^2}{Q^2} \quad \text{tr} \rho_{VA} = \text{tr} \rho_{AV} = 0 \quad \text{tr} \rho_{AA} = 4\beta^2 \tag{19}$$

These expressions should take the role of T_{all} in Eq. (12). However, it appears that for the VA interference term the ratio $R_{VA} \equiv \rho_{VA}/\text{tr} \rho_{VA}$ becomes infinite.

Instead of R_{VA} the following combination will be considered in the following
 $R_{VAAVAA} := (\rho_{VA} + \rho_{AV} + \rho_{AA})/\text{tr}\rho_{AA}$.

The next step is to incorporate the corrections from virtual gluon exchange. This can be done on the amplitude level and is quite straightforward, because virtual gluons do not modify the kinematics of the lowest order process. The effect can be condensed to effectively change the vector and axialvector interactions according to

$$\gamma_\mu \rightarrow \gamma_\mu(1 + \alpha f_1) + \frac{i}{2m_t} \sigma_{\mu\nu} p_B^\nu \alpha f_2 \quad \gamma_\mu \gamma_5 \rightarrow \gamma_\mu \gamma_5(1 + \alpha f_A) \quad (20)$$

where $\alpha = C_F \frac{\alpha_s}{2\pi}$ as before and f_1 , f_2 and f_A are functions of β and can be found in [5]. It turns out that $f_2 = f_1 - f_A$. Therefore, the amplitudes Eq. (18) can be easily extended to contain effects from virtual gluon exchange. We here give the result only for the relevant cases $\phi = 0$ and $H = +1$:

$$\begin{aligned} M_V(+1, -\frac{1}{2}, -\frac{1}{2}) &= -\sqrt{2} \frac{m_t}{Q} \sin \theta (1 + \alpha f_+) & M_A(+1, -\frac{1}{2}, -\frac{1}{2}) &= 0 \\ M_V(+1, -\frac{1}{2}, +\frac{1}{2}) &= -\frac{1+\cos\theta}{\sqrt{2}} (1 + \alpha f_-) & M_A(+1, -\frac{1}{2}, +\frac{1}{2}) &= -\beta \frac{1+\cos\theta}{\sqrt{2}} (1 + \alpha f_-) \\ M_V(+1, +\frac{1}{2}, -\frac{1}{2}) &= \frac{1-\cos\theta}{\sqrt{2}} (1 + \alpha f_-) & M_A(+1, +\frac{1}{2}, -\frac{1}{2}) &= -\beta \frac{1-\cos\theta}{\sqrt{2}} (1 + \alpha f_-) \\ M_V(+1, +\frac{1}{2}, +\frac{1}{2}) &= \sqrt{2} \frac{m_t}{Q} \sin \theta (1 + \alpha f_+) & M_A(+1, +\frac{1}{2}, +\frac{1}{2}) &= 0 \end{aligned} \quad (21)$$

where $f_+ = f_1 - \frac{Q^2}{4m_t^2} f_2$ and $f_- = f_A = f_1 - f_2$.

It should be noted that the functions f_1 and f_A merely 'renormalize' the form of the lowest order interactions, cf. Eq. (20), and accordingly they *do not contribute* in the ratios $R_{IJ} = \rho_{IJ}/\text{tr}\rho_{IJ}$, $IJ = VV, VAAVAA$ and AA . The interesting point is that the infrared and collinear singularities are solely contained in the functions f_1 and f_A whereas f_2 is completely finite and given by

$$f_2 = \frac{1 - \beta^2}{2\beta} \ln \frac{1 - \beta}{1 + \beta} \quad (22)$$

The normalized density matrix elements $R_{VV}(+1, h, \bar{h}, +1, h', \bar{h}')$ are given in the table where $\lambda = \frac{1-2m_t^2/Q^2}{m_t/Q}$, $s_t = \sin \theta$ and $c_t = \cos \theta$ and the \star 's follow from the

$h\bar{h} \downarrow h'\bar{h}' \rightarrow$	$(-\frac{1}{2}, -\frac{1}{2})$	$(-\frac{1}{2}, +\frac{1}{2})$	$(+\frac{1}{2}, -\frac{1}{2})$	$(+\frac{1}{2}, +\frac{1}{2})$
$(-\frac{1}{2}, -\frac{1}{2})$	$-4\beta^2 s_t^2 \alpha f_2$	\star	\star	\star
$(-\frac{1}{2}, +\frac{1}{2})$	$-\lambda\beta^2 s_t(1+c_t)\alpha f_2$	$2\beta^2(1-c_t)^2\alpha f_2$	\star	\star
$(+\frac{1}{2}, -\frac{1}{2})$	$\lambda\beta^2 s_t(1-c_t)\alpha f_2$	$-2\beta^2 s_t^2 \alpha f_2$	$2\beta^2(1-c_t)^2\alpha f_2$	\star
$(+\frac{1}{2}, +\frac{1}{2})$	$4\beta^2 s_t^2 \alpha f_2$	$\lambda\beta^2 s_t(1+c_t)\alpha f_2$	$-\lambda\beta^2 s_t(1-c_t)\alpha f_2$	$-4\beta^2 s_t^2 \alpha f_2$

symmetry of the matrix. It is thereby explicit that all corrections are $\sim f_2$ as anticipated.

The density matrix elements of R_{AA} and R_{VAAVAA} do not get any corrections at all from virtual gluon exchange because according to Eq. (21) there are two factors of $1 + \alpha f_-$ both in the numerator and denominator of $\rho_{AA}/\text{tr}\rho_{AA}$ and similarly for R_{VAAVAA} .

6. Real Gluon Emission and Numerical Results for the Corrections to the Normalized Density Matrix

Next we come to the two Feynman diagrams with real gluon emission $B^* \rightarrow t\bar{t}g$. The higher order corrections are calculated in such a way that all gluon d.o.f. are summed and integrated over. This means, for example, the gluon is assumed to be unpolarized. Furthermore, a rather complicated phase space integration has to be performed. In contrast to the tree level process $B^* \rightarrow t\bar{t}$ where the phase space is trivial, one has here two highly nontrivial integrations which I have chosen to perform numerically. This is then straightforward because, as pointed out before, the integrand corresponding to Eq. (14) is completely finite.

The trivial phase space for the lowest order kinematics (15) is given by $\text{PS}(B^* \rightarrow t\bar{t}) = \int \prod \frac{d^3 p_i}{2E_i} \delta^4(p_t + p_{\bar{t}} - p_B) = \frac{\pi}{2}\beta$. With an additional gluon the 4-momenta of the particles become more complicated. First, the energies of t and \bar{t} are not fixed as in lowest order – in fact they are to become the integration variables – and

secondly, there is now an angle ω between the top quark and antitop direction.

$$p_B = (Q, 0, 0, 0) \quad p_t = \frac{Q}{2}x_1(1, 0, 0, \beta_1) \quad p_{\bar{t}} = \frac{Q}{2}x_2(1, \beta_2 \sin \omega, 0, \beta_2 \cos \omega) \quad (23)$$

Here x_1 and x_2 are the (normalized) energies of t and \bar{t} and $\beta_i^2 := 1 - \frac{4m_i^2}{x_i^2 Q^2}$, $i = 1, 2$. ω is not an independent variable but can be related to x_1 and x_2 through the gluon's on-shell condition $p_g^2 = 0$ and 4-momentum conservation $p_g = p_B - p_t - p_{\bar{t}}$. One obtains:

$$0 = 1 + 2\frac{m_t^2}{Q^2} - x_1 - x_2 + \frac{1}{2}x_1x_2(1 - \beta_1\beta_2 \cos \omega) \quad (24)$$

The 2-dimensional phase space integral is given by

$$\text{PS}(B^* \rightarrow t\bar{t}g) = \frac{\pi^2 Q^2}{4} \int_0^{1-2m_t/Q} dy \int_{z_-}^{z_+} dz \quad (25)$$

where

$$y := \frac{2\bar{t}g}{Q^2} = 1 - x_1 \quad z := \frac{2tg}{Q^2} = 1 - x_2 \quad (26)$$

and

$$z_{\pm} = \frac{1}{2} \frac{y}{y + \frac{m^2}{Q^2}} [x_1(1 \pm \beta_1) - 2\frac{m^2}{Q^2}] \quad (27)$$

The polarization vectors Eqs. (16) and (17) of the B-boson are not modified in higher orders, because p_B has not changed. In contrast, the spinors for the fermions become more complicated than in lowest order:

$$\begin{aligned} \bar{u}_{+\frac{1}{2}}(p_t) &= (a_{1+}, 0, a_{1-}, 0) & \bar{u}_{-\frac{1}{2}}(p_t) &= (0, a_{1-}, 0, a_{1+}) \\ v_{+\frac{1}{2}}(p_{\bar{t}}) &= (a_{2+}s_2, -a_{2+}c_2, -a_{2-}s_2, a_{2-}c_2) & v_{-\frac{1}{2}}(p_{\bar{t}}) &= (a_{2-}c_2, a_{2-}s_2, -a_{2+}c_2, -a_{2+}s_2) \end{aligned}$$

where $s_2 = \sin \frac{\omega}{2}$, $c_2 = \cos \frac{\omega}{2}$ and $a_{i\pm}^2 = \frac{Q}{2}x_i(1 \pm \beta_i)$, $i = 1, 2$.

Using these parametrizations, the real gluon amplitudes $M_I(B^* \rightarrow t\bar{t}g)(H, h, \bar{h})$, $I = V, A$ and $h, \bar{h} = \pm \frac{1}{2}$, must be calculated. As in lowest order, it is sufficient to know the case $H = +1$. Before performing the phase space integrations, the density matrix must be formed. More precisely, we have calculated the normalized

density matrices $R_{IJ}(+1, h, \bar{h}, +1, h', \bar{h}')$, $IJ = VV, VAAVAA$ and AA , Eq. (12), corresponding to the finite combination Eq. (14). Numerical results for all the 30 independent matrix elements are shown in Figures 2–61 as a function of the e^+e^- energy Q and for a top quark mass of $m_t = 170$ GeV. The results are shown in the following form: each density matrix element has a decomposition of the form

$$R_{IJ}(+1, h, \bar{h}, +1, h', \bar{h}') = C_1 \frac{1}{2}(1 + c_t^2) + C_2 s_t^2 + C_3 c_t + C_4 s_t + C_5 c_t s_t \quad (28)$$

where $c_t = \cos \theta$, $s_t = \sin \theta$ and of course the coefficients C_j depend on the spin quantum numbers h, \bar{h}, h' and \bar{h}' . Each coefficient C_j has a lowest order contribution, which however vanishes in many cases, and a higher order correction, i.e.

$$C_j = \text{LO} + \alpha \text{ HO} \quad (29)$$

where $\alpha = C_F \frac{\alpha_s}{2\pi}$ as before. In Figures 2–61 there is always one figure displaying the lowest order term (LO) for each $j = 1, 2, 3, 4, 5$ followed by the corresponding figure for the higher order term (HO); and these pairs of figures are successively presented for each combination $(+1, h, \bar{h}, +1, h', \bar{h}')$. Note that only the following combinations of $(h, \bar{h}, h', \bar{h}')$ are shown: $(- - - -), (- - - +), (- - + -), (- - ++), (- + - +), (- + + -), (+ - + -), (+ + - +), (+ + + -), (+ + ++)$. The rest follows from the symmetry of the density matrix, i.e. $R_{IJ}(+1, h, \bar{h}, +1, h', \bar{h}') = R_{IJ}(+1, h', \bar{h}', +1, h, \bar{h})$. Some of the curves seem to increase rather strongly with increasing Q^2 . However, it can be shown that all HO corrections converge to a constant at $Q \rightarrow \infty$. Corrections are typically at the percent level. This is not astonishing, because by forming the *normalized* density matrix, the bulk of the higher order correction due to the known overall K-factors [14] drops out. The odd figure numbers 3–61 really contain the main results of our paper, from which higher order QCD corrections to any angular distribution of top quark spins or top quark decay products can in principle be determined (for the latter one needs in addition the QCD corrections to the top quark decay amplitudes calculated in [10]).

For convenience, we present in figures 62–91 the θ dependence of the matrix

elements $R_{IJ}(+1, h, \bar{h}, +1, h', \bar{h}')$. More precisely, the matrix elements are written as $R_{IJ}(+1, h, \bar{h}, +1, h', \bar{h}') = \text{LO} + \alpha \text{HO}$ and LO and HO are displayed as a function of θ for a fixed total energy $Q = 400 \text{ GeV}$. Again, the corrections are relatively small because the normalized density matrix is considered, in which the correction to the trace of the density matrix drops out.

7. Summary

In this article a complete decomposition into spin contributions of the production of top quarks in e^+e^- annihilation has been given including higher order QCD corrections. The corrections are relatively small (on the percent level) because the *normalized* density matrix was considered, in which the correction to the trace of the density matrix drops out. This means in turn that twoloop calculations are at most necessary for the trace of the density matrix (corrections of up to 10% [14]), but not for any of the normalized density matrix elements, because these $O(\alpha_s^2)$ corrections are most probably below the permille level.

Our results can be applied to calculate distributions for any decay product of top quarks at a future linear collider. I have not attempted to work out these applications, but have merely given in section 3 the necessary reduction formulae. To prove that the applications are rather straightforward, I would like to finish this work by making the QCD corrections to the e^+e^- cross section Eq. (10) explicit. Eq. (10) can be rewritten as

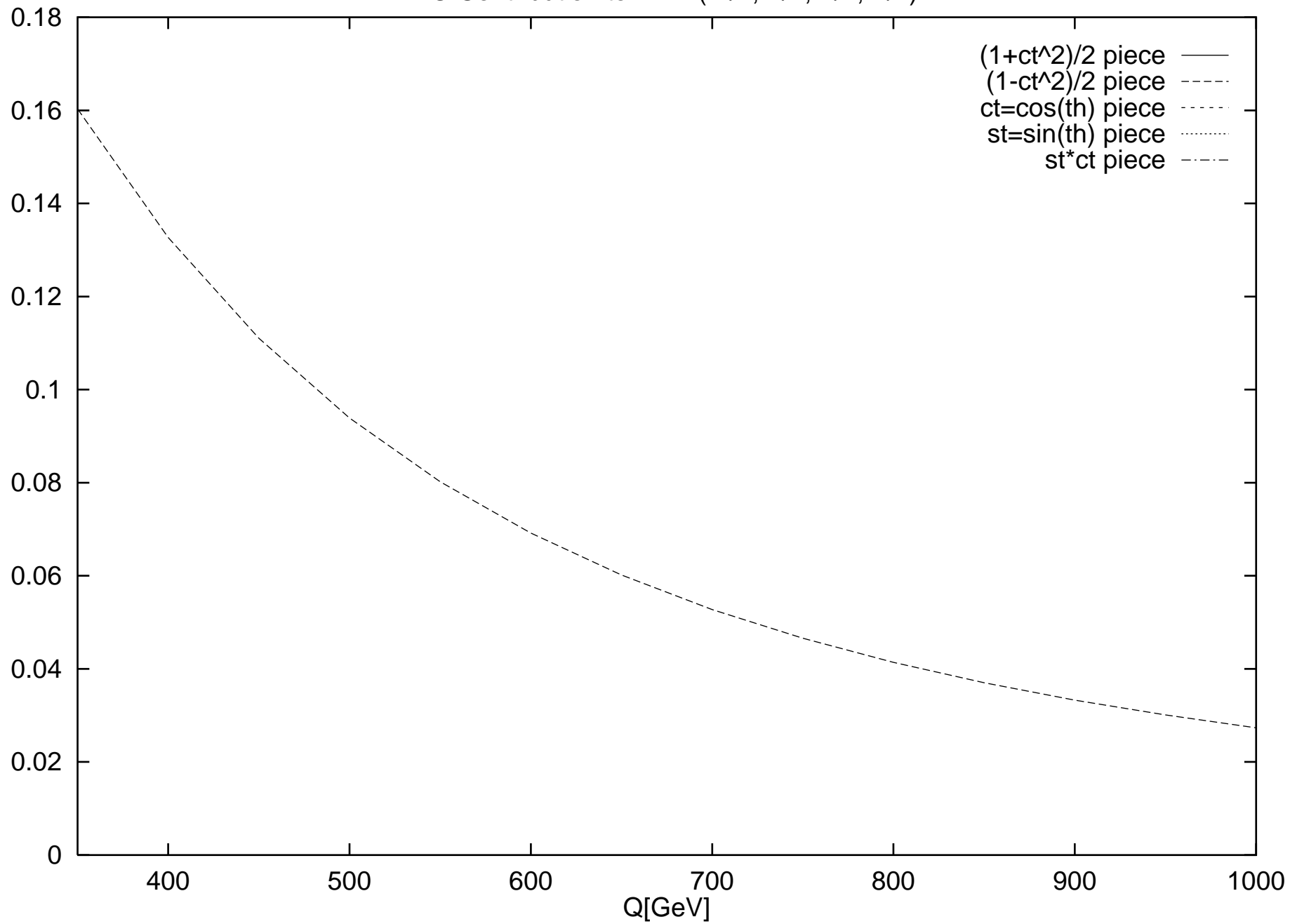
$$\begin{aligned} \sigma_{\pm} = & \sum_{h, \bar{h}, h', \bar{h}'} D(h, \bar{h}) D^*(h', \bar{h}') \\ & \left\{ v_{\pm}^2 R_{VV}(\pm 1, h, \bar{h}, \pm 1, h', \bar{h}') (4 + 8 \frac{m_t^2}{Q^2}) (1 + \alpha K_{VV}(\beta)) + 4\beta^2 (1 + \alpha K_{AA}(\beta)) \right. \\ & \left. [v_{\pm} a_{\pm} R_{VA AV AA}(\pm 1, h, \bar{h}, \pm 1, h', \bar{h}') + a_{\pm} (a_{\pm} - v_{\pm}) R_{AA}(\pm 1, h, \bar{h}, \pm 1, h', \bar{h}')] \right\} \end{aligned}$$

where $K_{VV}(\beta)$ and $K_{AA}(\beta)$ are the known corrections to the trace of the density matrix [14], cf. Eq. (19). Note that $K_{VA} = K_{AV} = 0$, so that there is an overall factor of $1 + \alpha K_{AA}$ in the second line of Eq. (31). Using Eq. (31) one can directly insert the corrections (figures 2–61) to obtain the cross sections including higher order QCD.

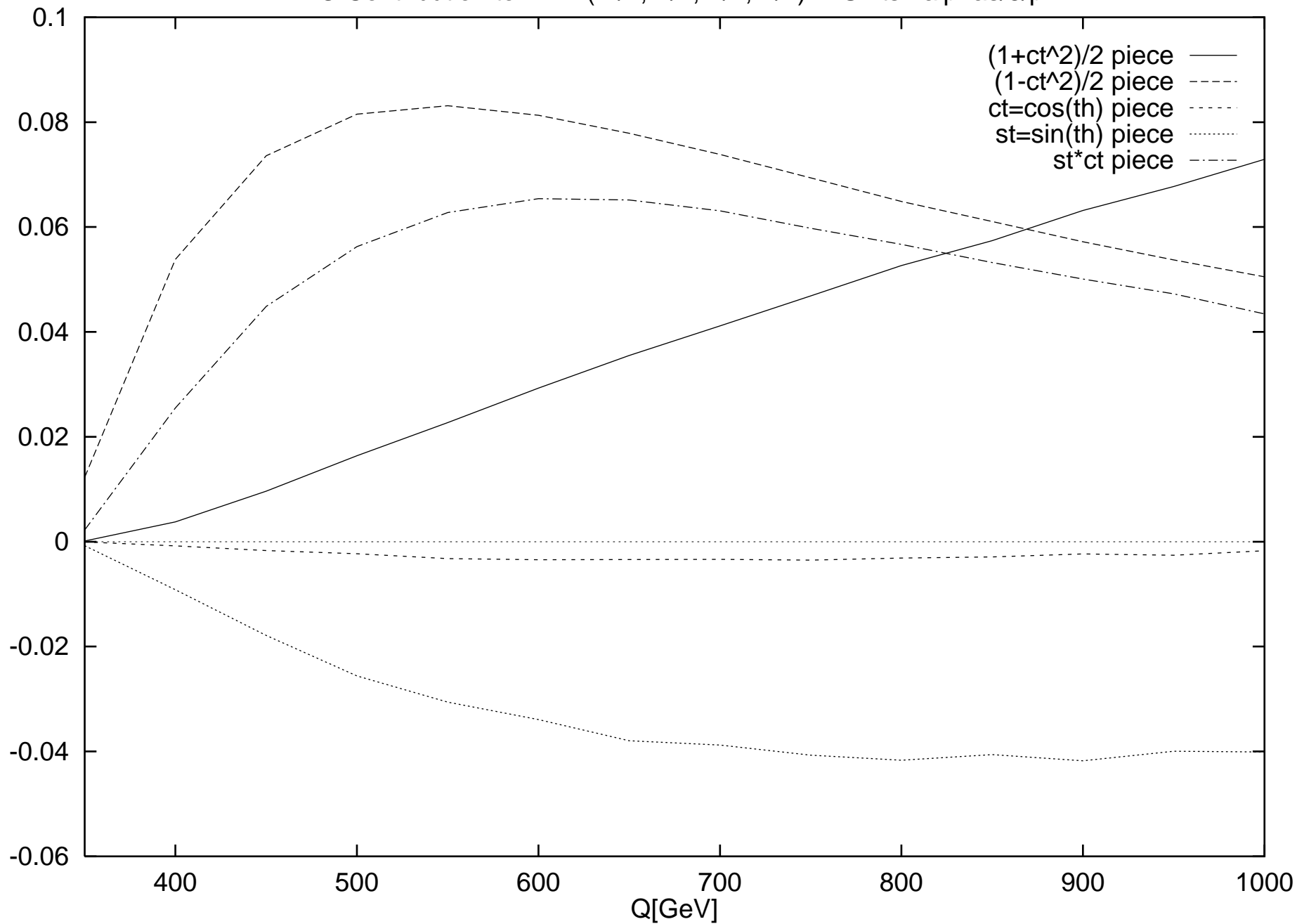
References

- [1] B.L. Combridge, Nucl. Phys. **B151** (1979) 429
- [2] J.H. Kühn, P. Zerwas and A. Reiter , Nucl. Phys. **B272** (1986) 560
- [3] S. Dawson, R.K. Ellis and P. Nason , Nucl. Phys. **303** (1988) 607
- [4] E. Laenen, W.L. van Neerven and J. Smith , Phys. Lett. **B321** (1994) 254
- [5] J. Jersak, E. Laermann and P.M. Zerwas, Phys. Rev. D **25** (1982) 1218
- [6] S. Jadach and Z. Was, Acta Polonica **15** (1984) 1151
- [7] G. Mahlon and S. Parke , Phys. Rev. **D53** (1996) 4886
- [8] T. Arens and L.M. Sehgal, Nucl. Phys. **B393** (1993) 46
- [9] S. Groote and J.G. Körner , Z. Phys. **C72** (1996) 255
- [10] B. Lampe, in Proc. of the International Workshop on QCD and New Physics, Hiroshima, 1997, hep-ph/9801346
- [11] L. Dixon and A. Signer, Phys. Rev. **D56** (1997) 4031
- [12] G.L. Kane, G.A. Ladinsky, and C.-P. Yuan, Phys. Rev. **D45** (1992) 124
- [13] C. Schmidt, Phys. Rev. **D54** (1996) 4031
- [14] J.H. Kühn and P. Zerwas, MPI-PAE/PTh 49/89
- [15] B. Lampe, Nucl. Phys. **B458** (1996) 23
B. Lampe, Nucl. Phys. **B454** (1995) 506
B. Lampe, Phys. Lett. **B301** (1993) 435
B. Lampe, G. Altarelli, Nucl. Phys. **B391** (1993) 3

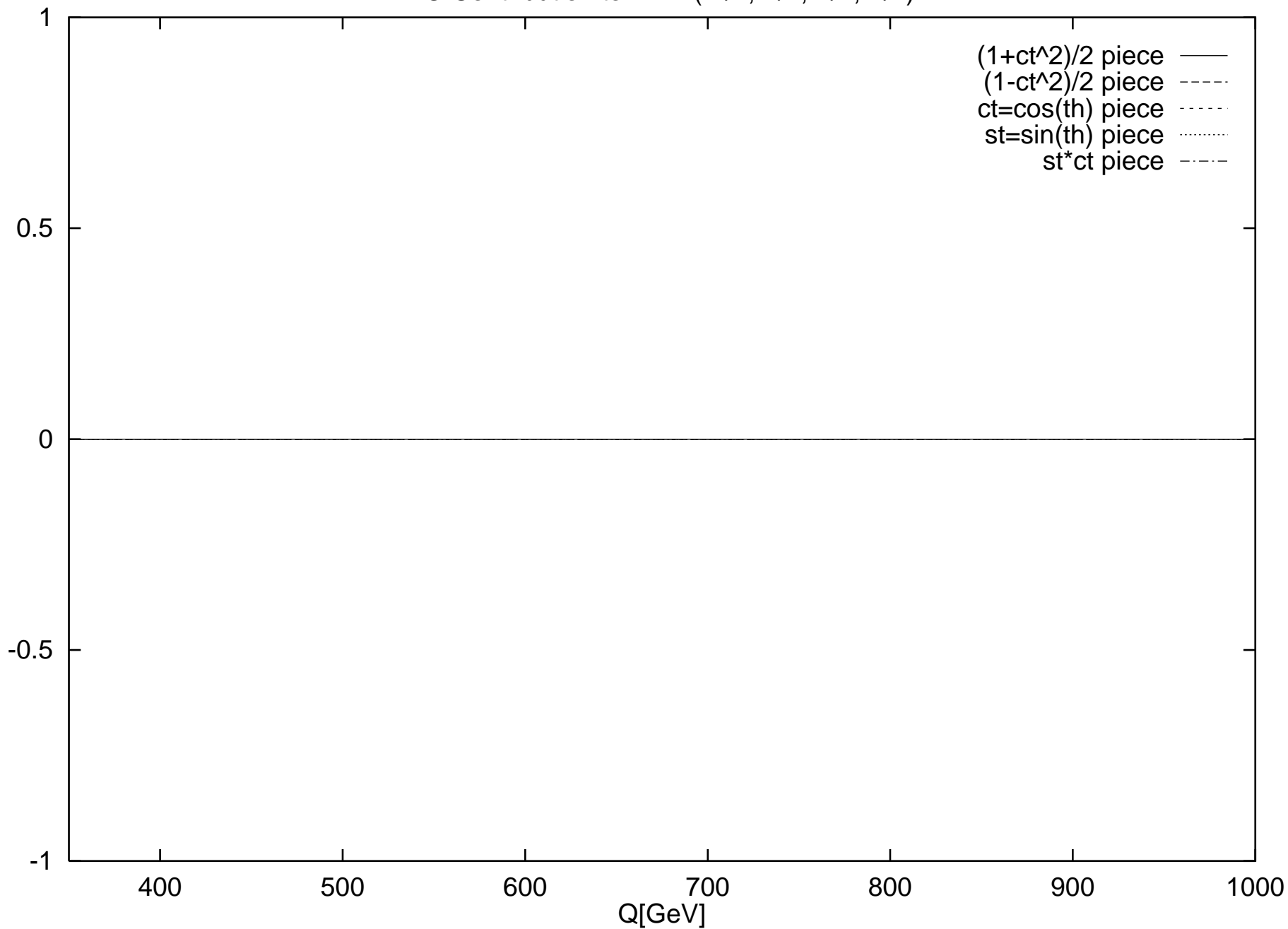
LO Contribution to R-VV(-1/2,-1/2,-1/2,-1/2)



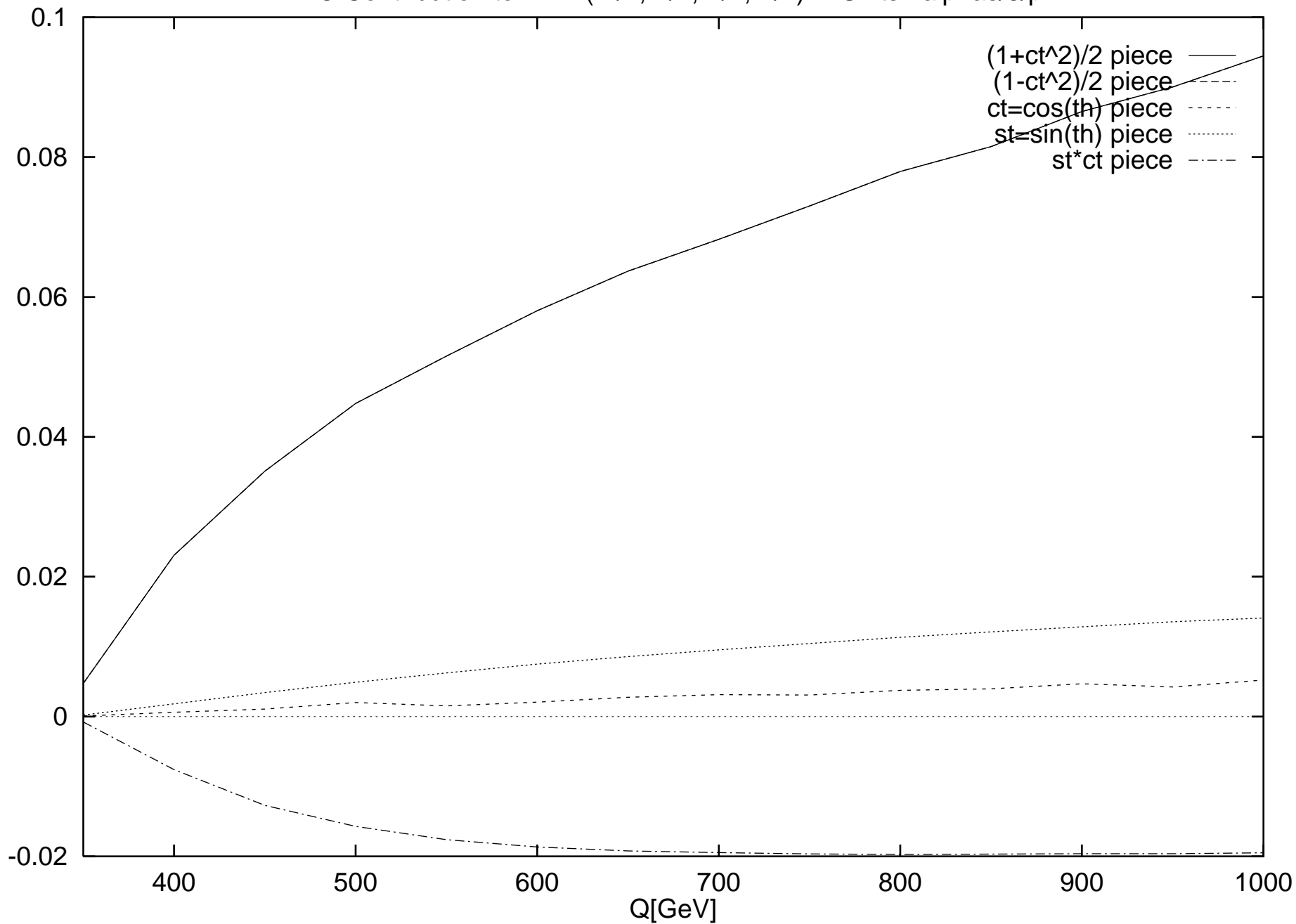
HO Contribution to R-VV(-1/2,-1/2,-1/2,-1/2) in Units $2\alpha/3\pi$



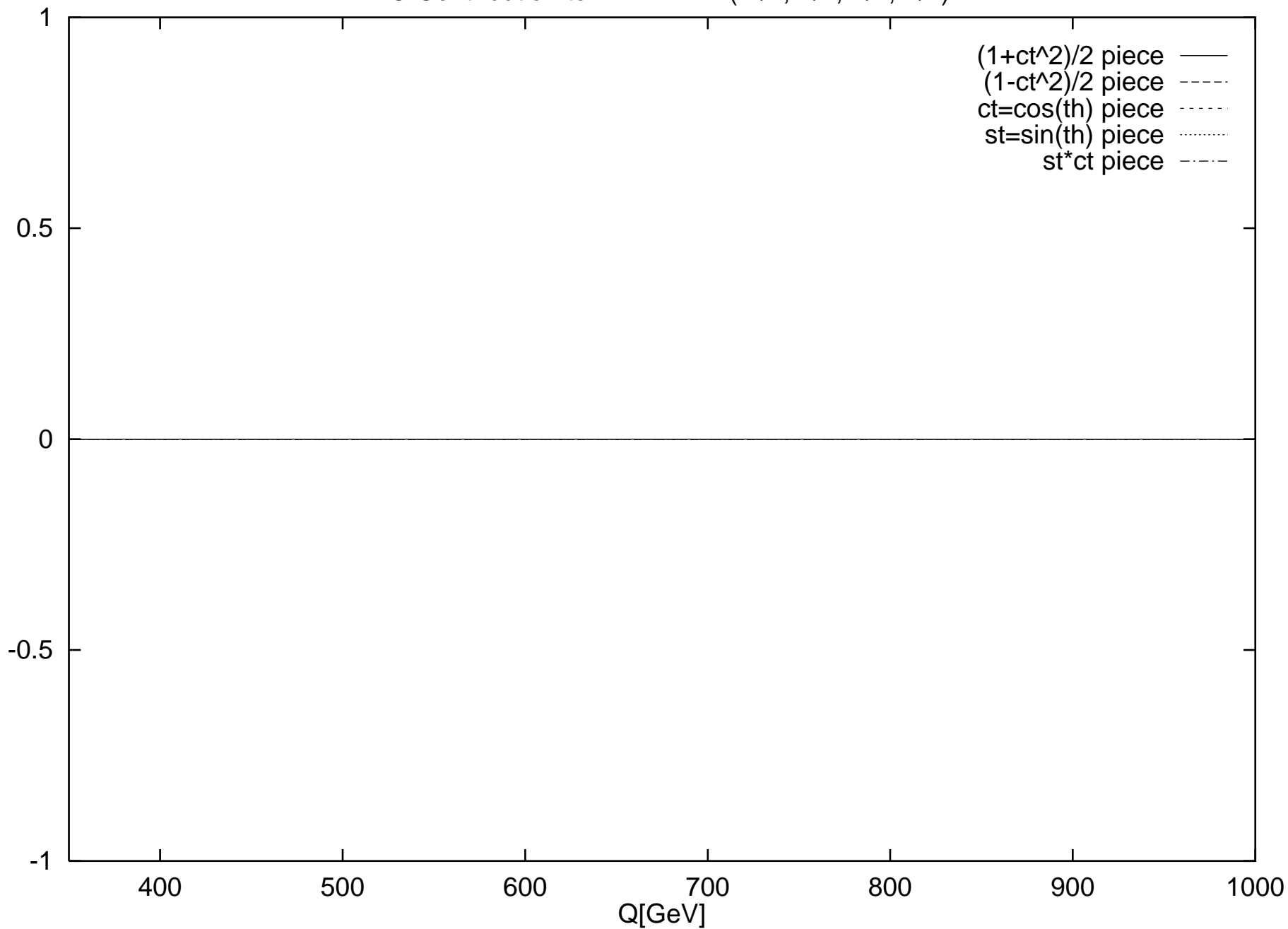
LO Contribution to R-AA(-1/2,-1/2,-1/2,-1/2)



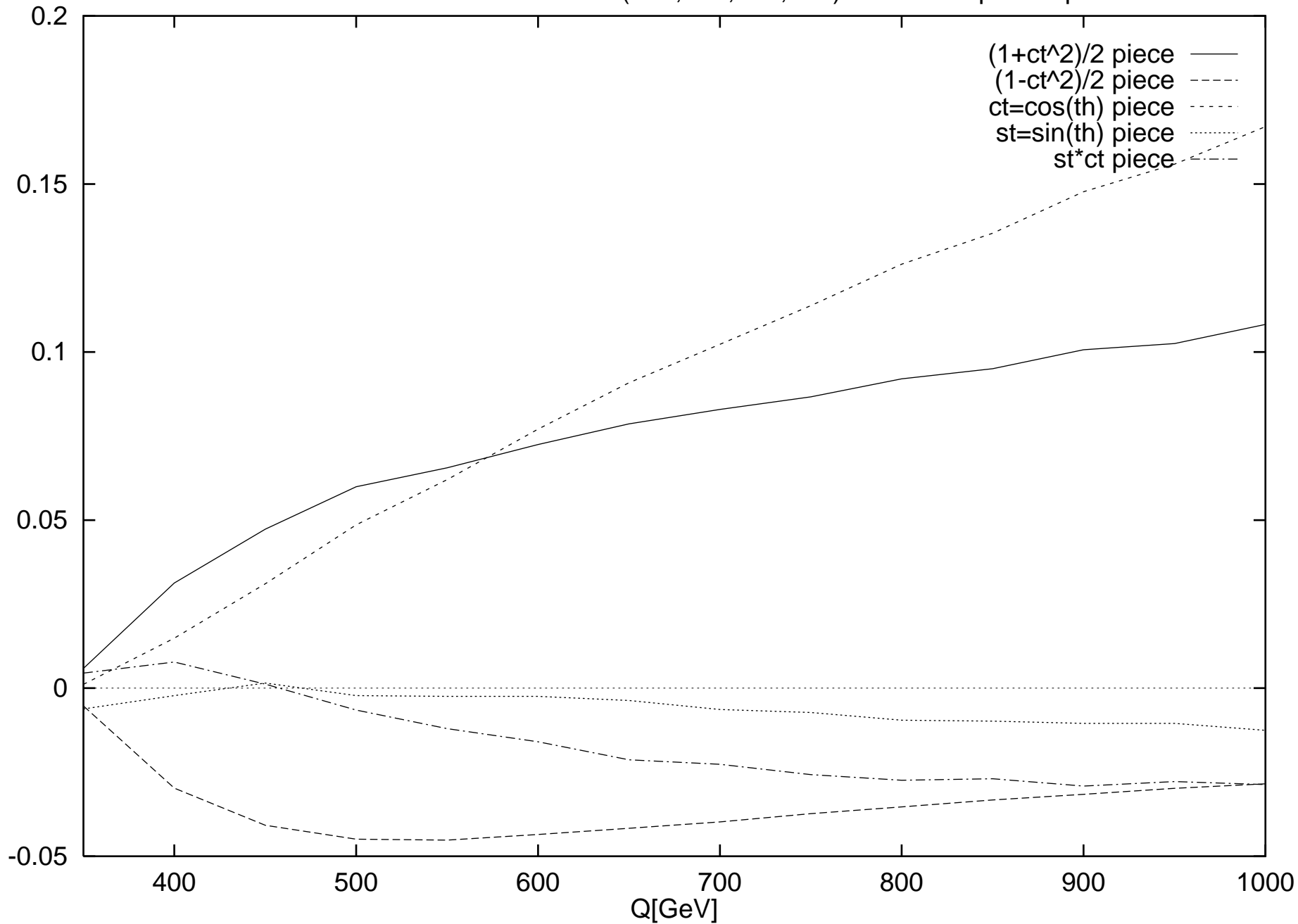
HO Contribution to R-AA(-1/2,-1/2,-1/2,-1/2) in Units $2\alpha_s/3\pi$



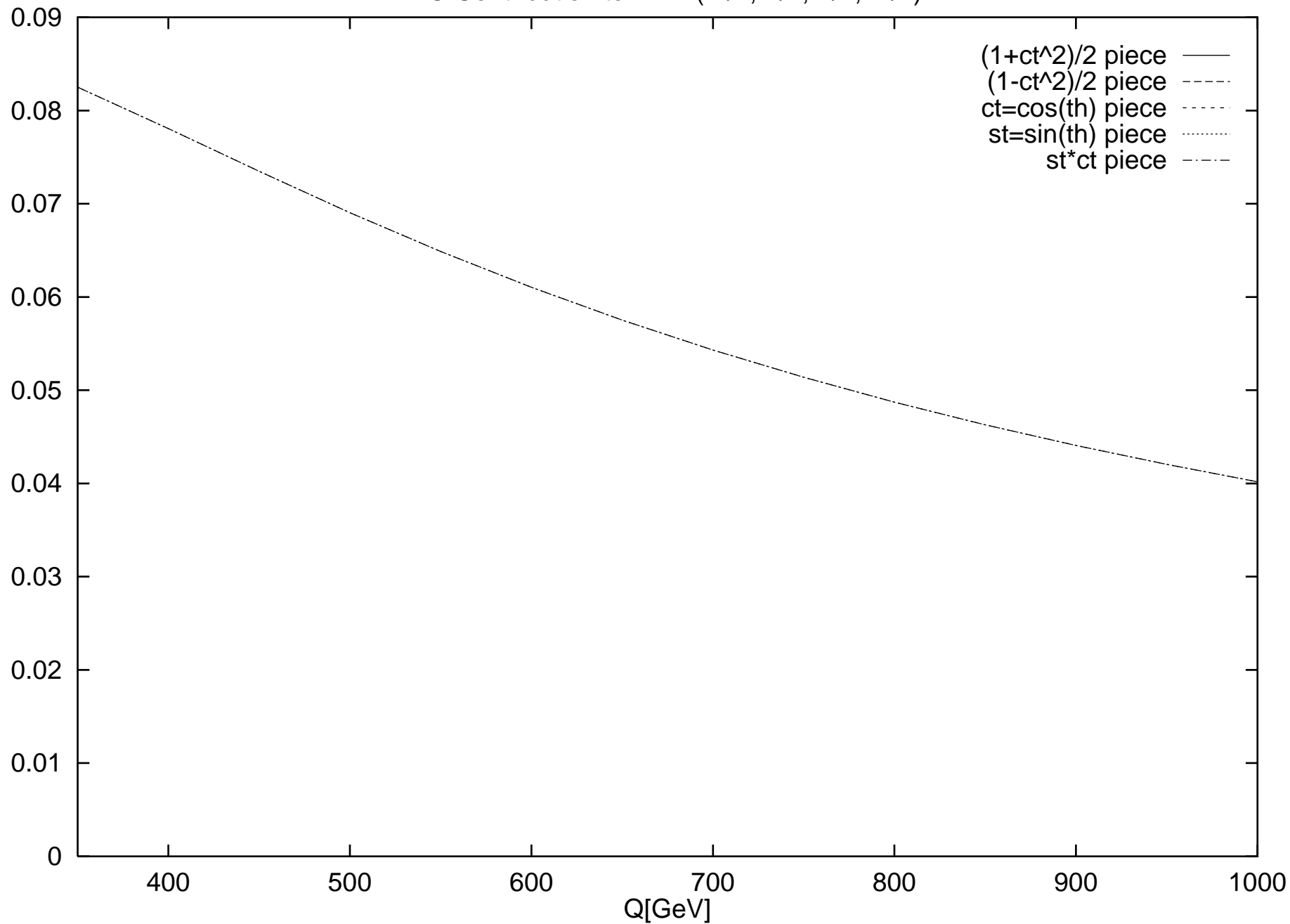
LO Contribution to R-VAAVAA(-1/2,-1/2,-1/2,-1/2)



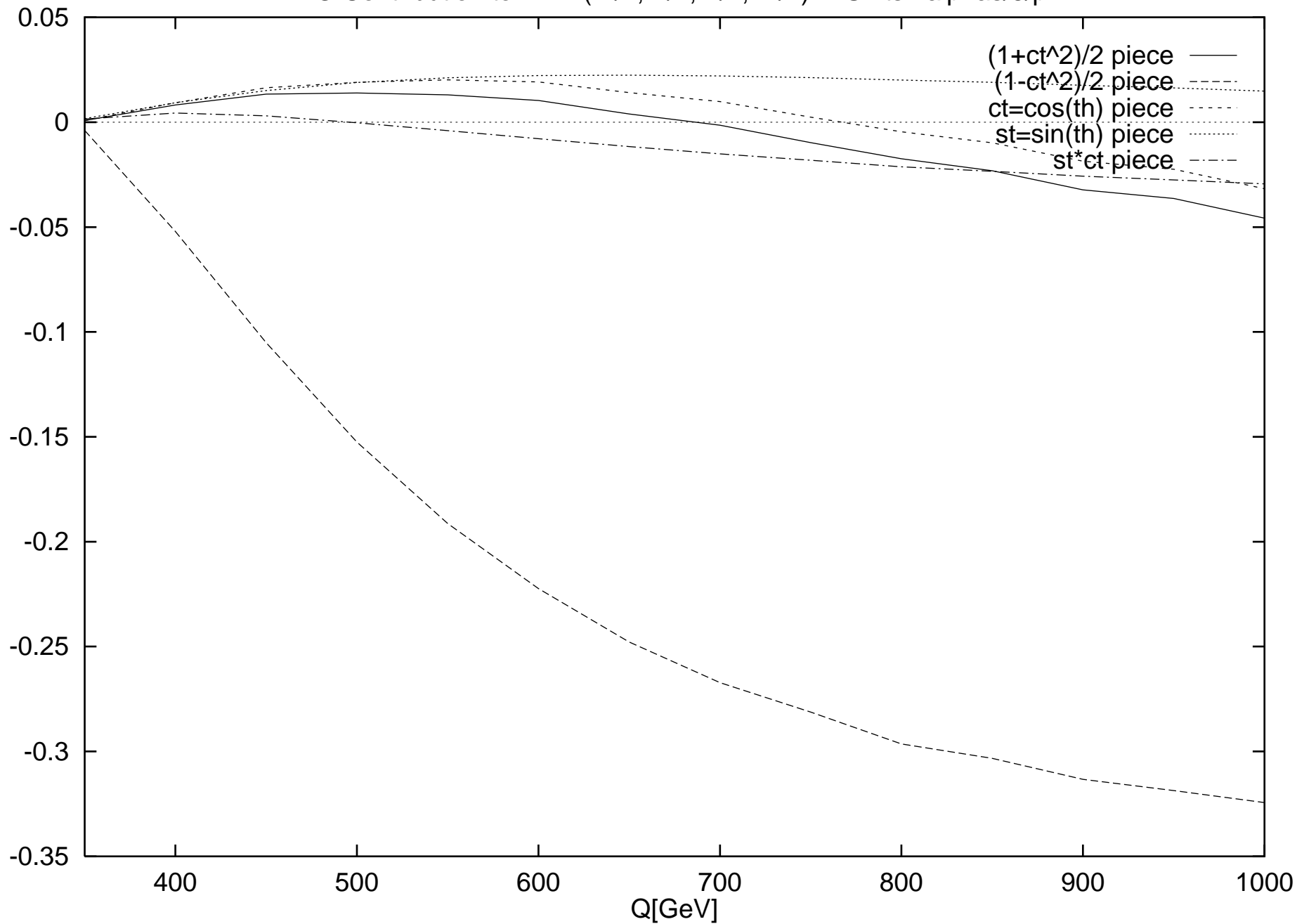
HO Contribution to R-VAAVAA(-1/2,-1/2,-1/2,-1/2) in Units $2\alpha/3\pi$



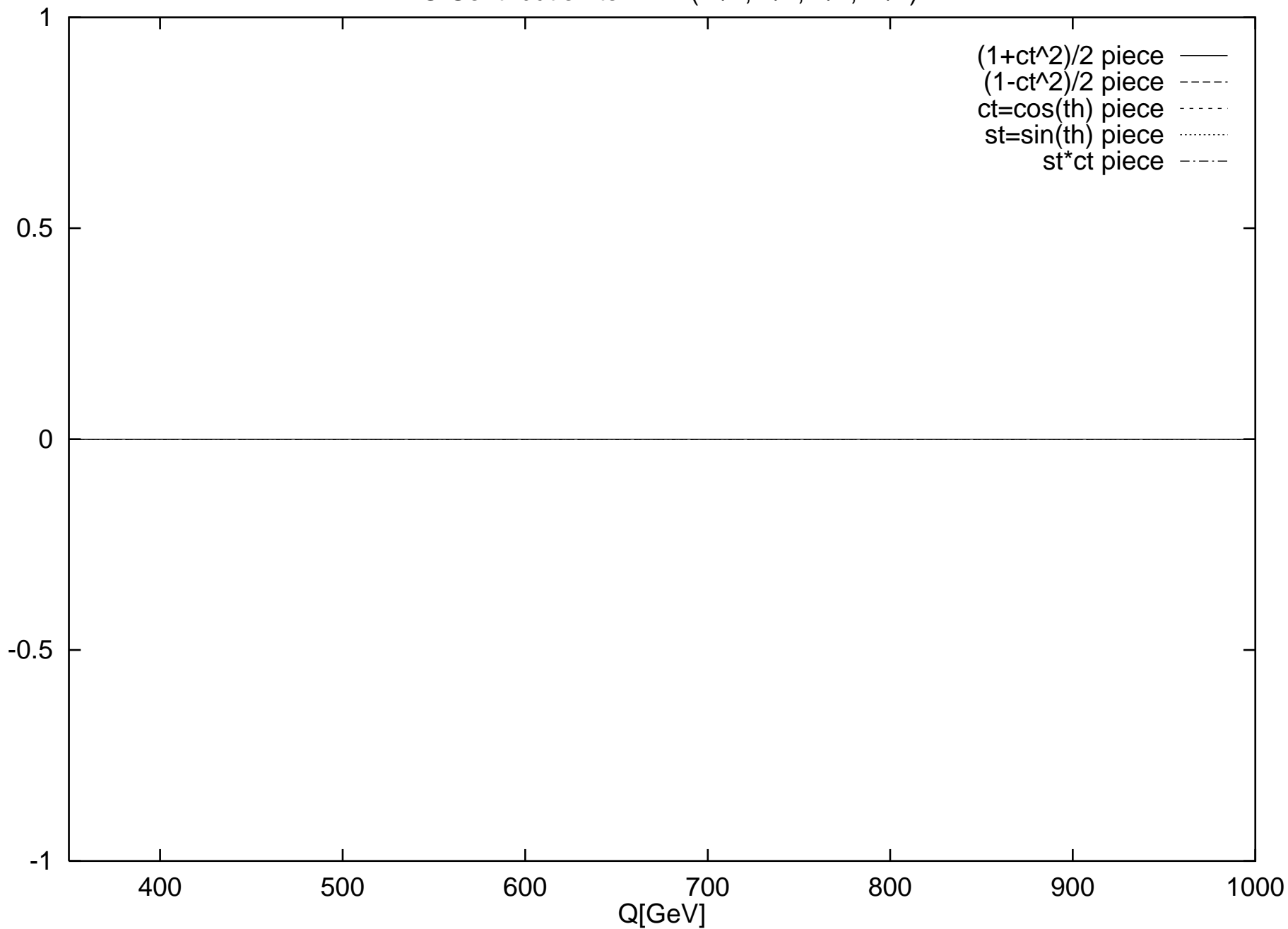
LO Contribution to R-VV(-1/2,-1/2,-1/2,+1/2)



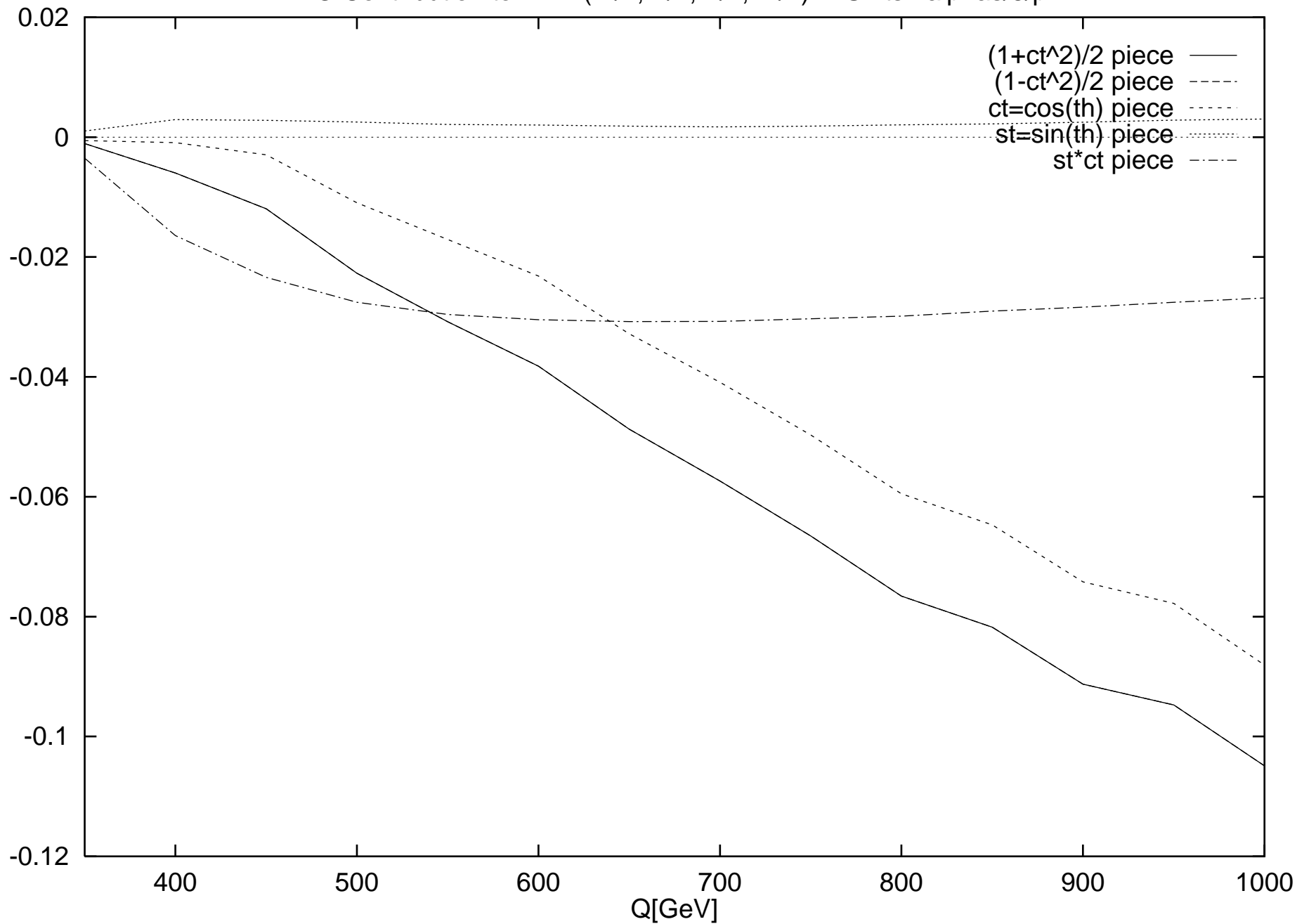
HO Contribution to R-VV(-1/2,-1/2,-1/2,+1/2) in Units $2\alpha_s/3\pi$



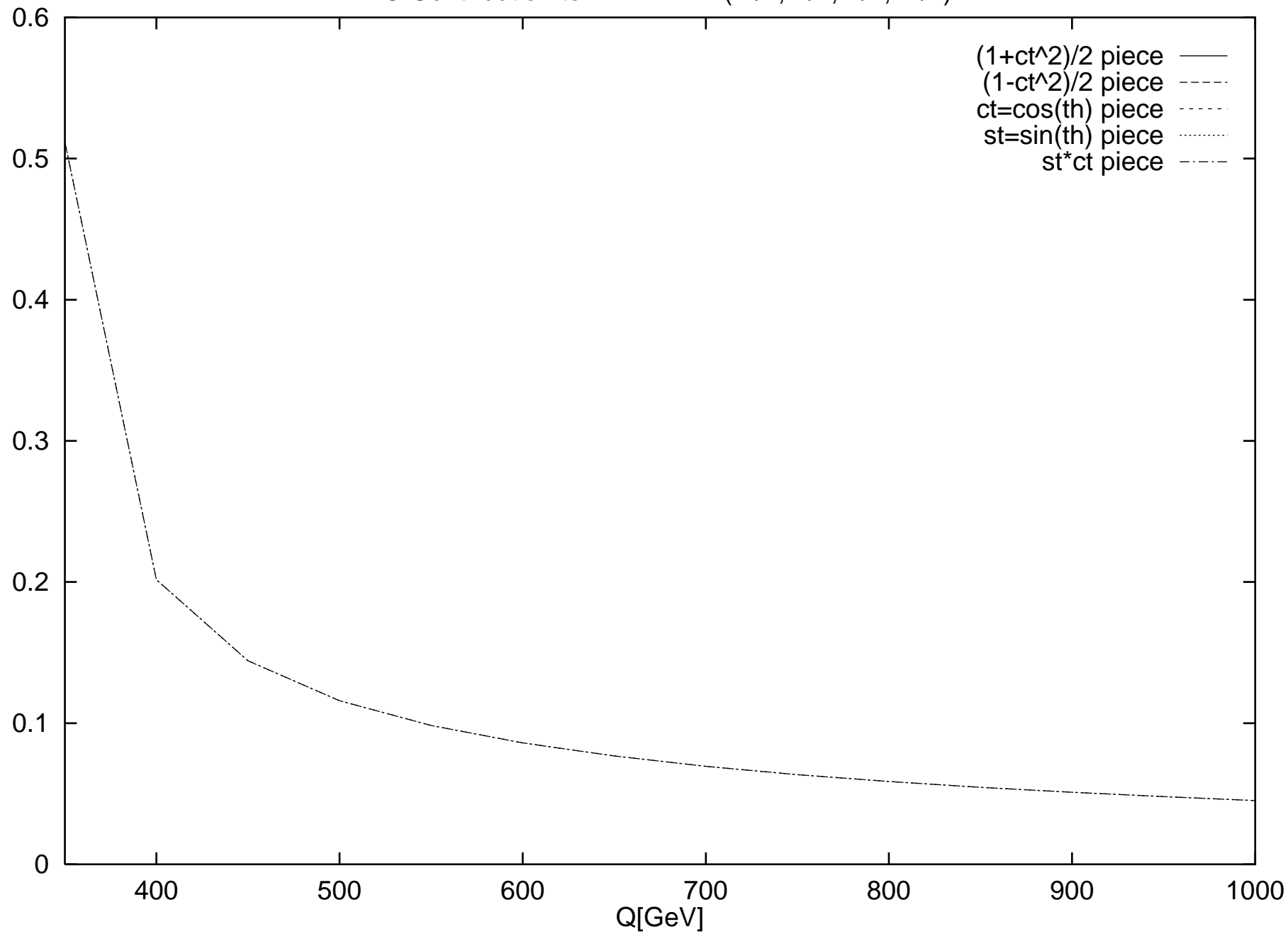
LO Contribution to R-AA(-1/2,-1/2,-1/2,+1/2)



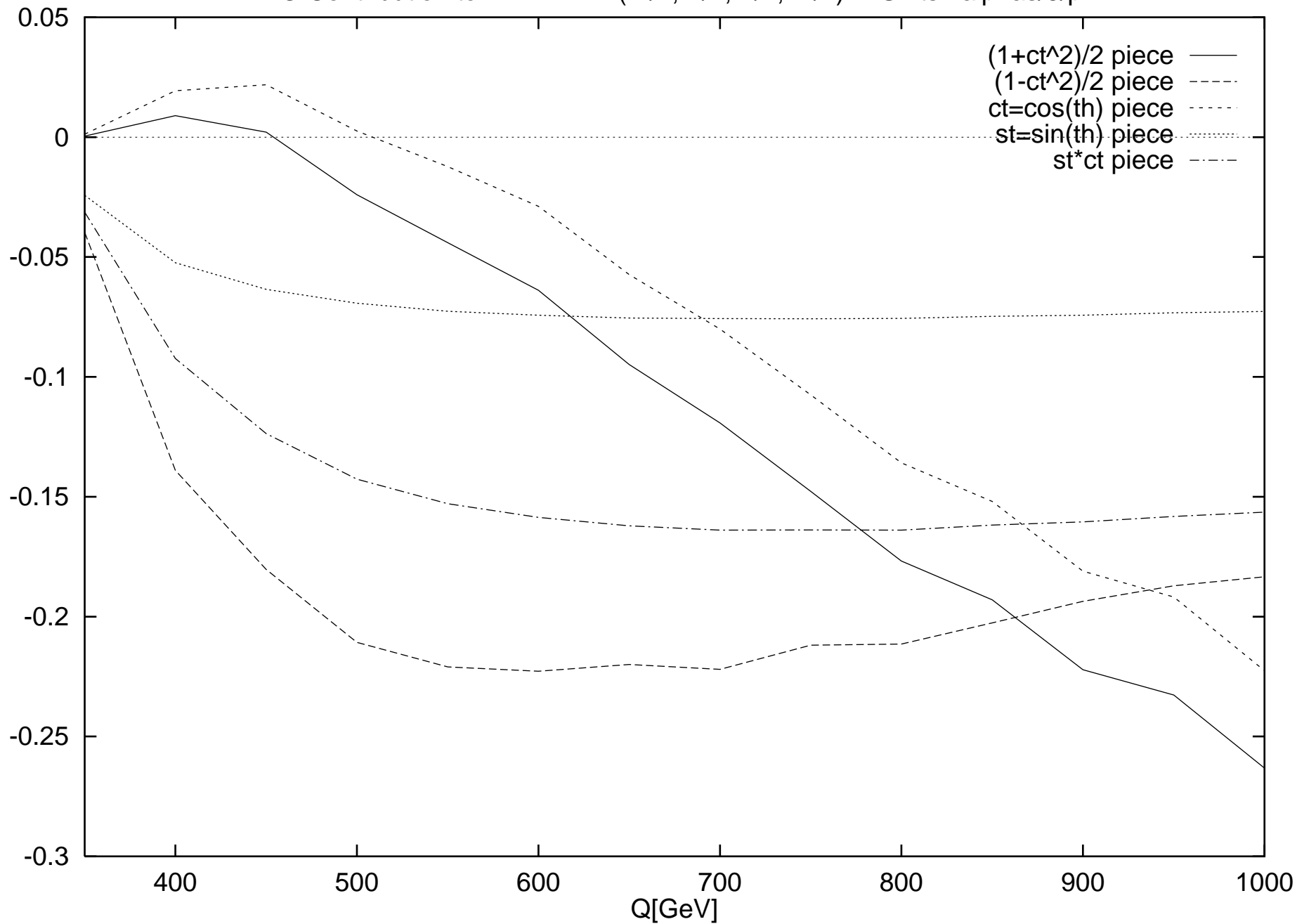
HO Contribution to R-AA(-1/2,-1/2,-1/2,+1/2) in Units $2\alpha_s/3\pi$



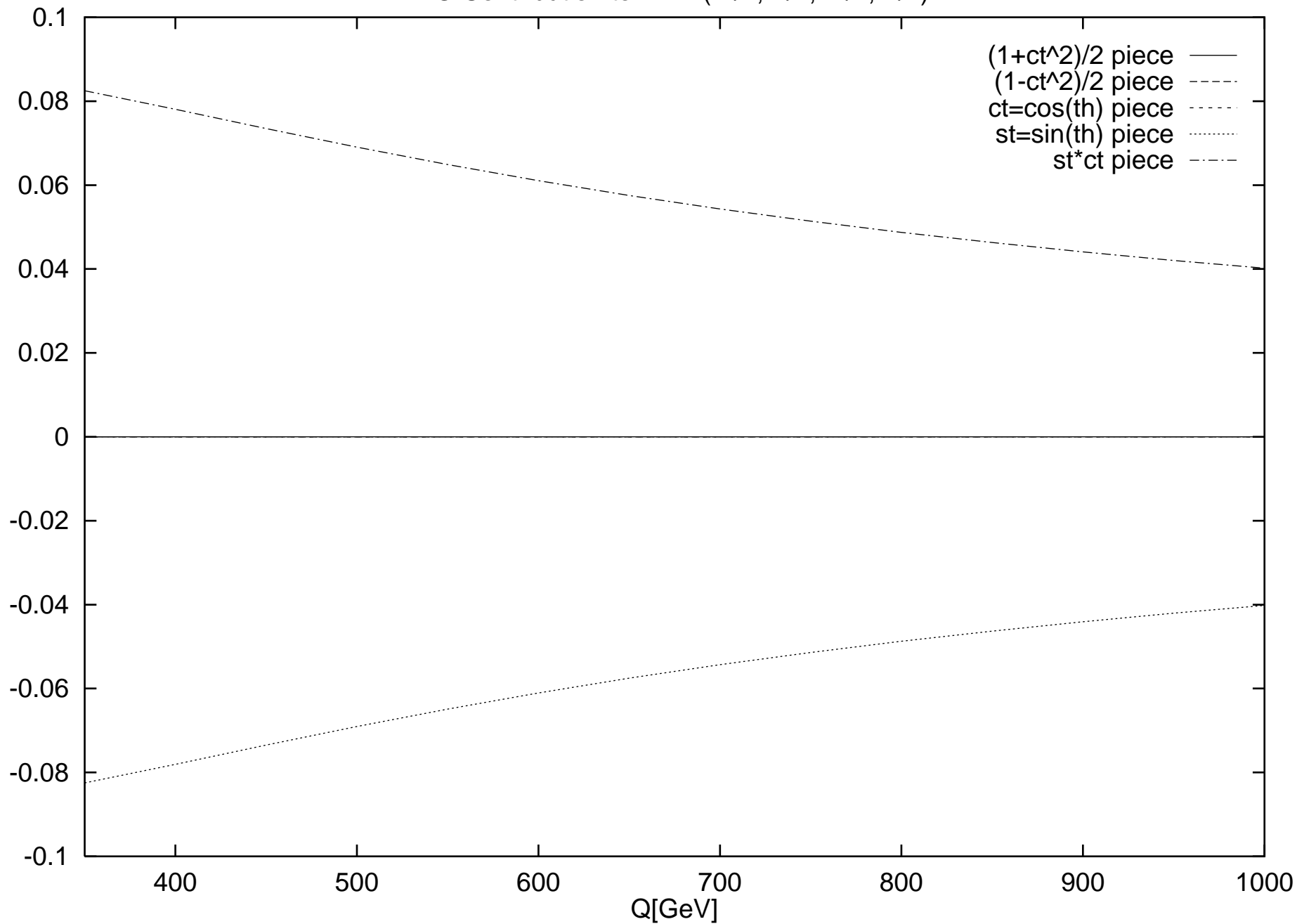
LO Contribution to R-VAAVAA(-1/2,-1/2,-1/2,+1/2)



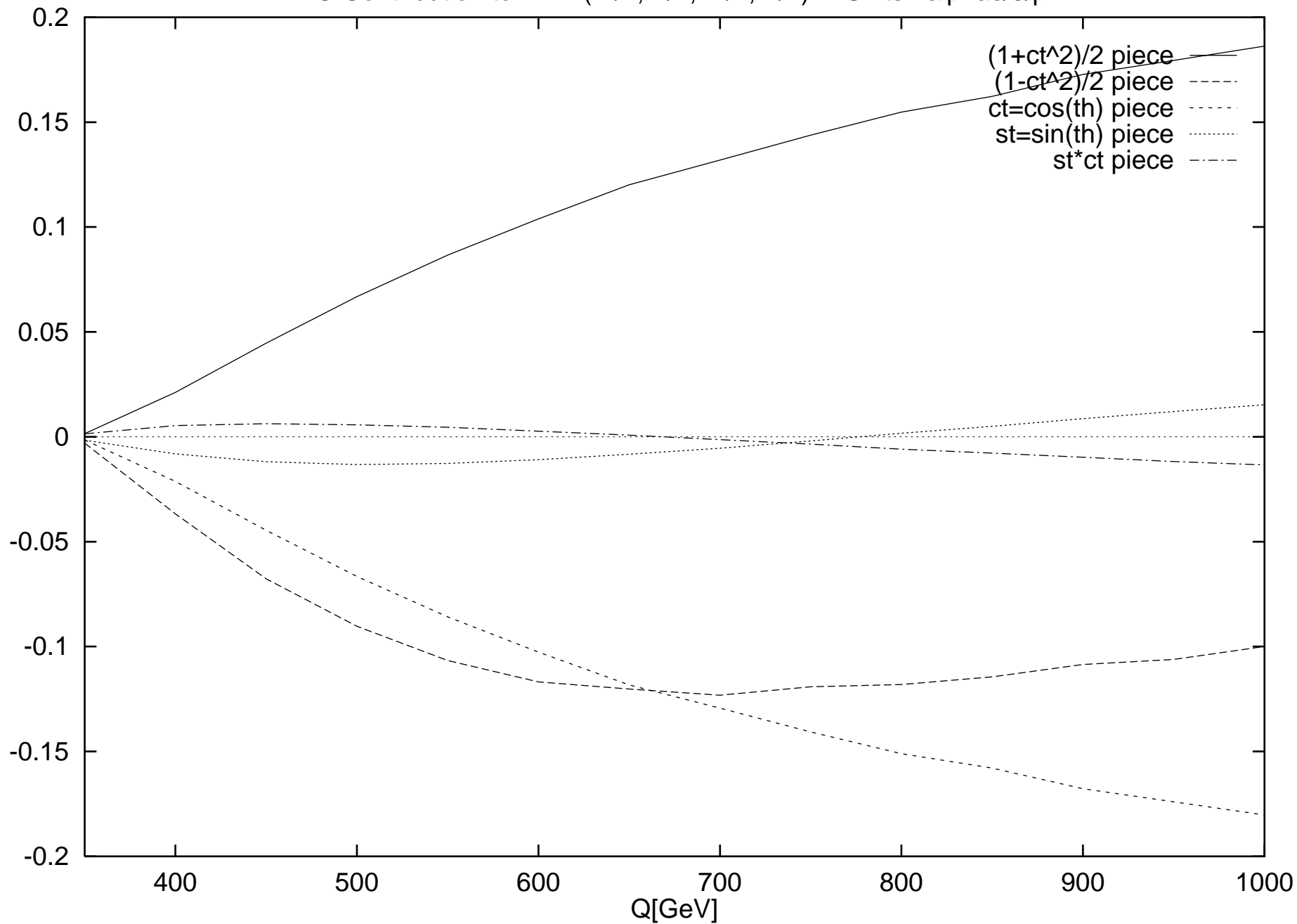
HO Contribution to R-VAAVAA(-1/2,-1/2,-1/2,+1/2) in Units $2\alpha/3\pi$

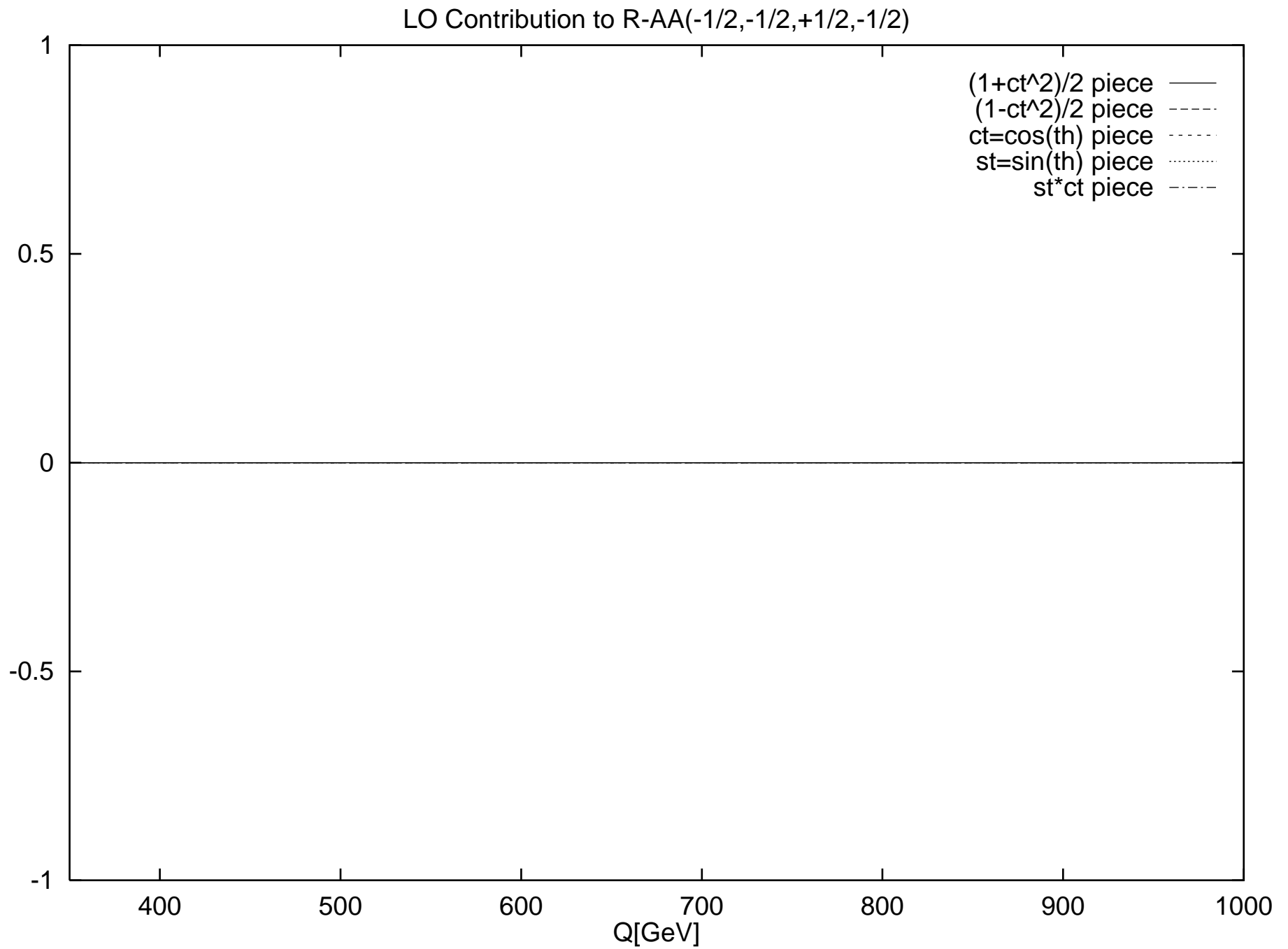


LO Contribution to R-VV(-1/2,-1/2,+1/2,-1/2)

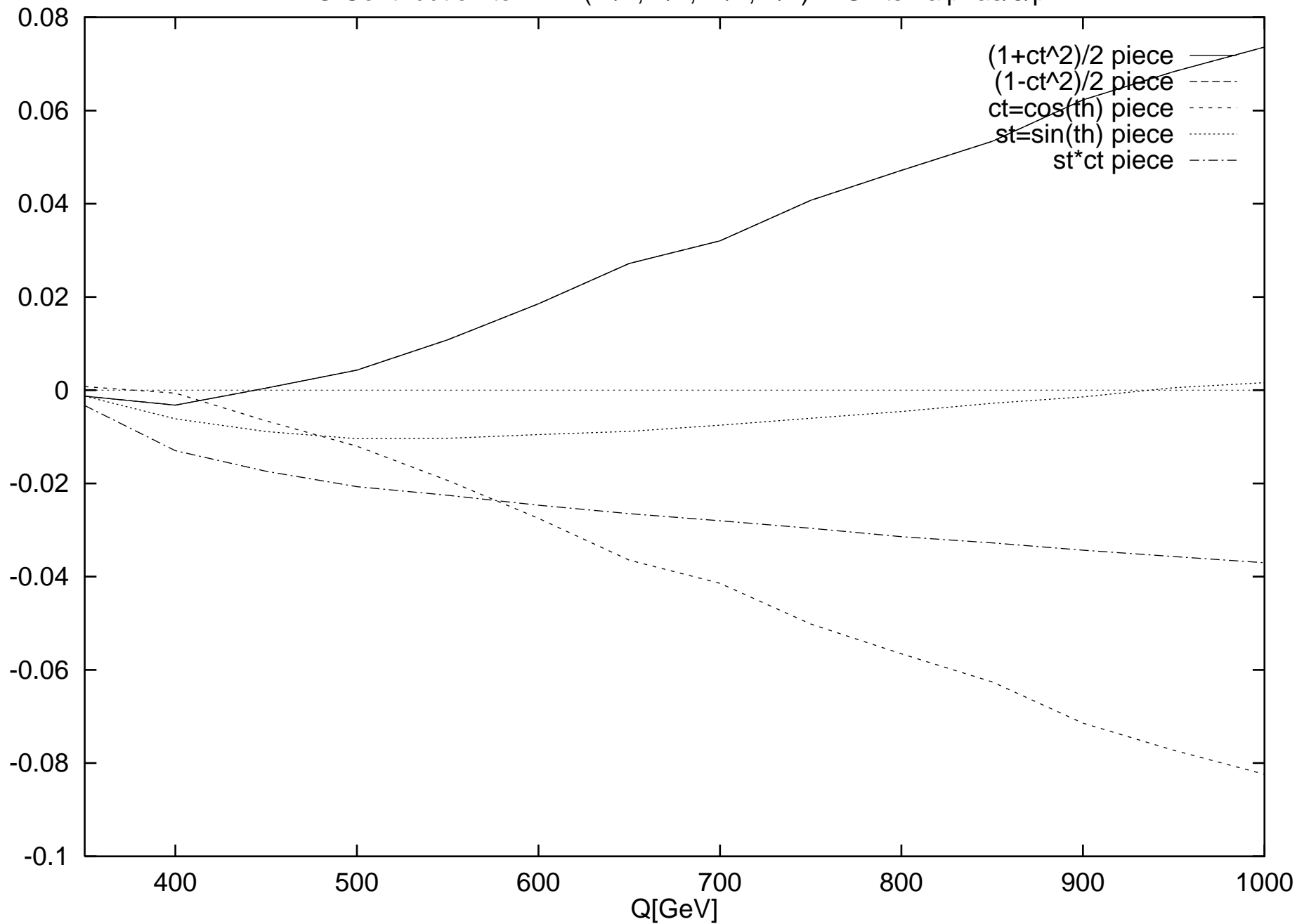


HO Contribution to R-VV(-1/2,-1/2,+1/2,-1/2) in Units $2\alpha_s/3\pi$

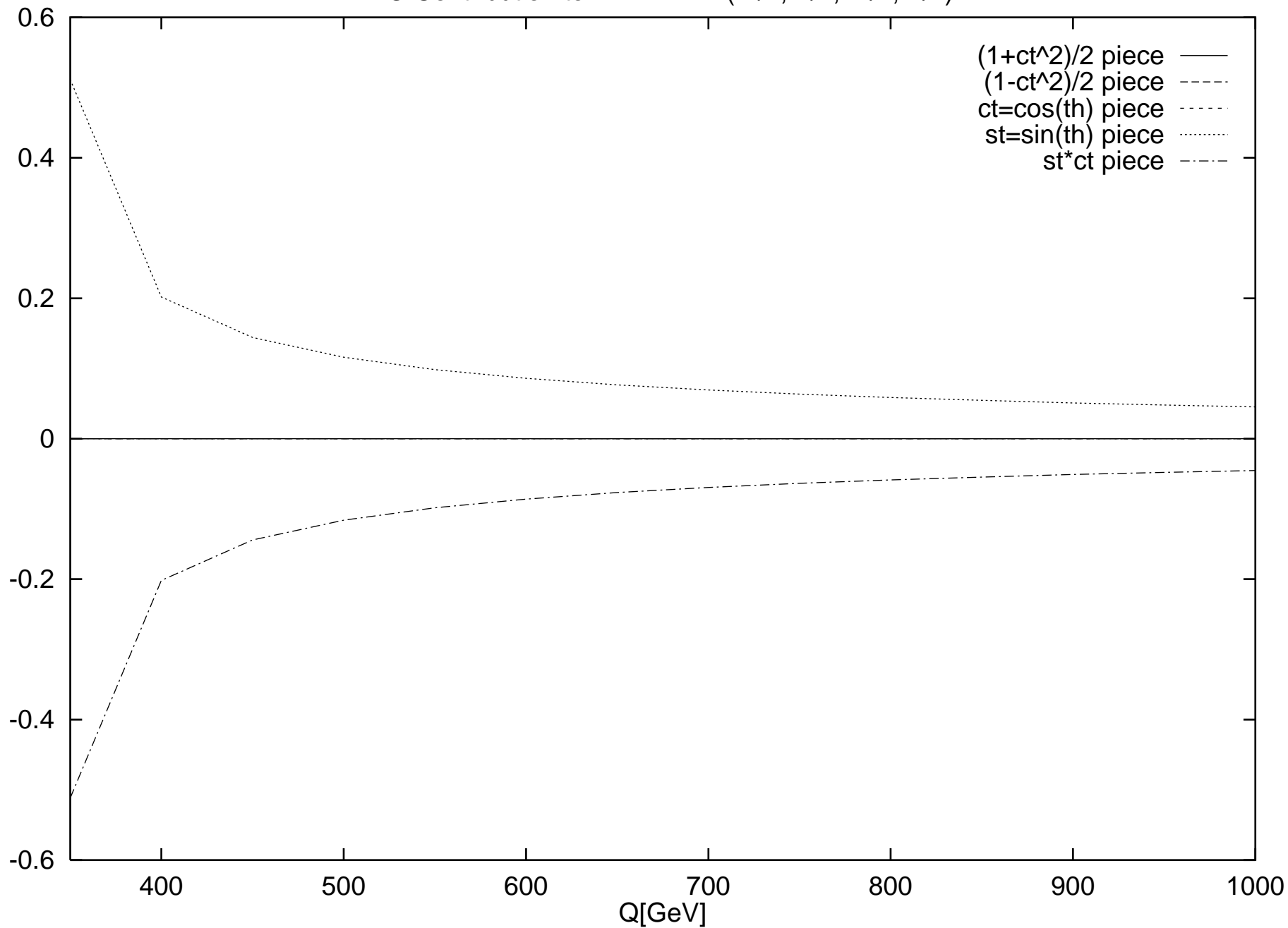




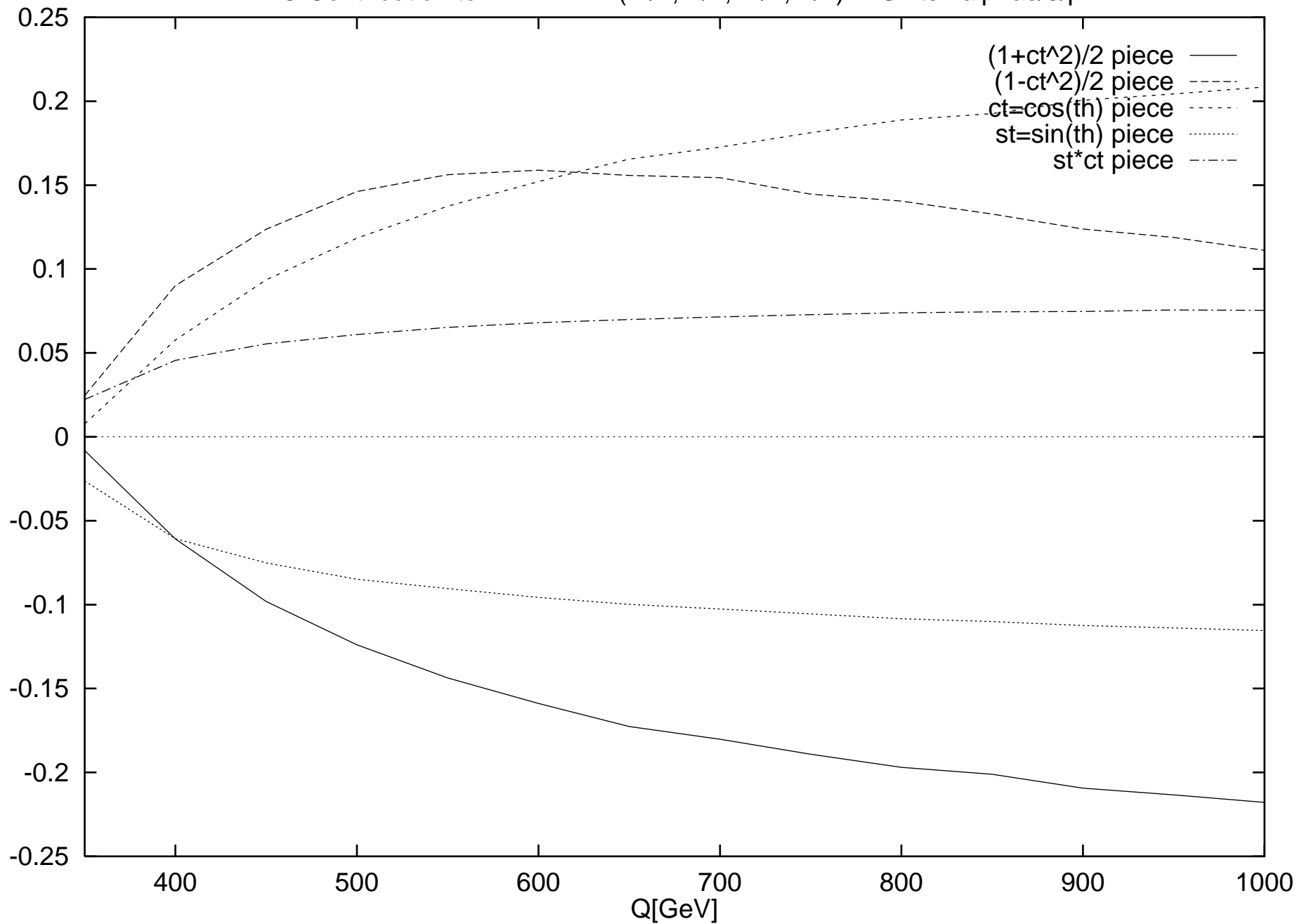
HO Contribution to R-AA(-1/2,-1/2,+1/2,-1/2) in Units $2\alpha_s/3\pi$



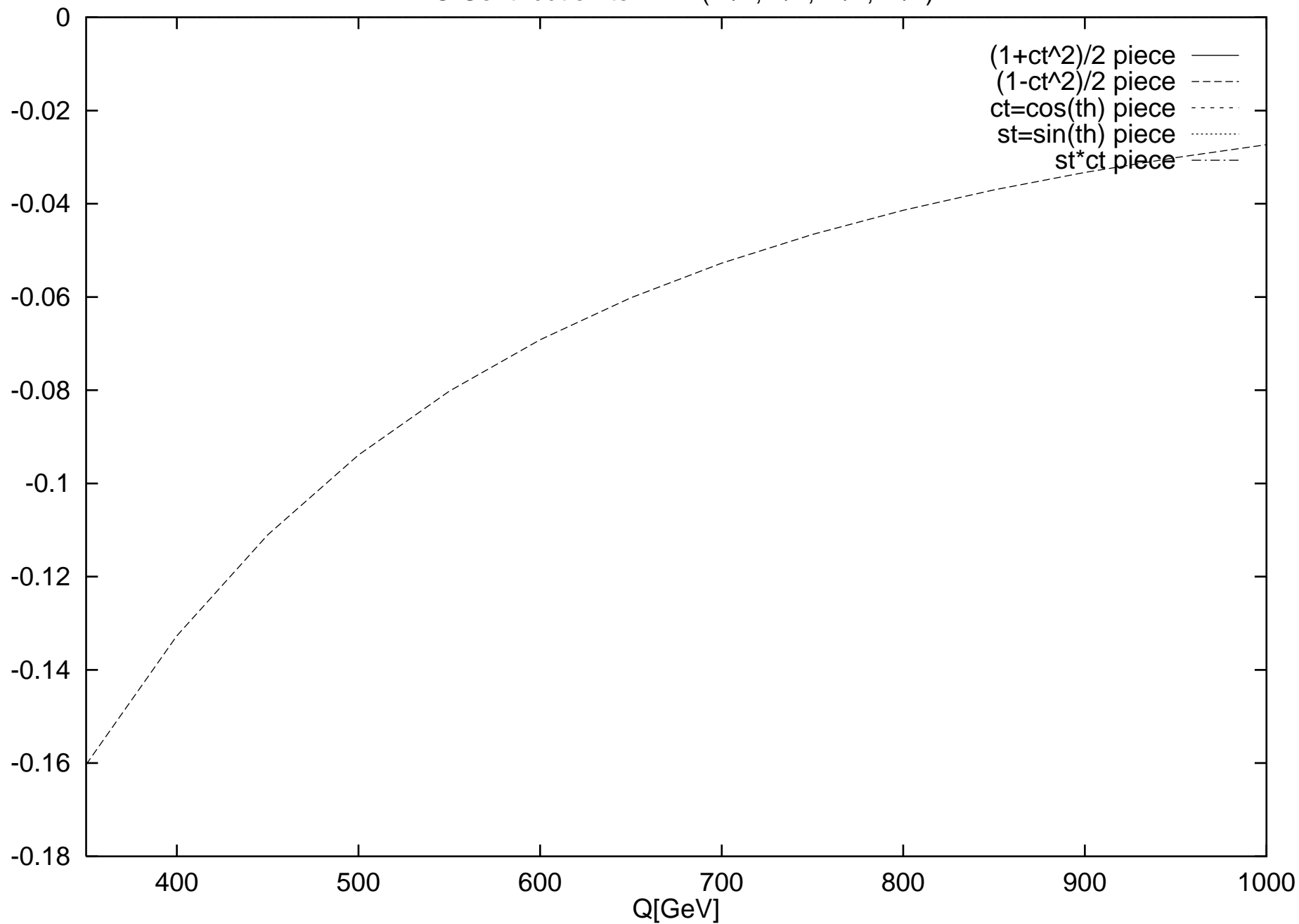
LO Contribution to R-VAAVAA(-1/2,-1/2,+1/2,-1/2)



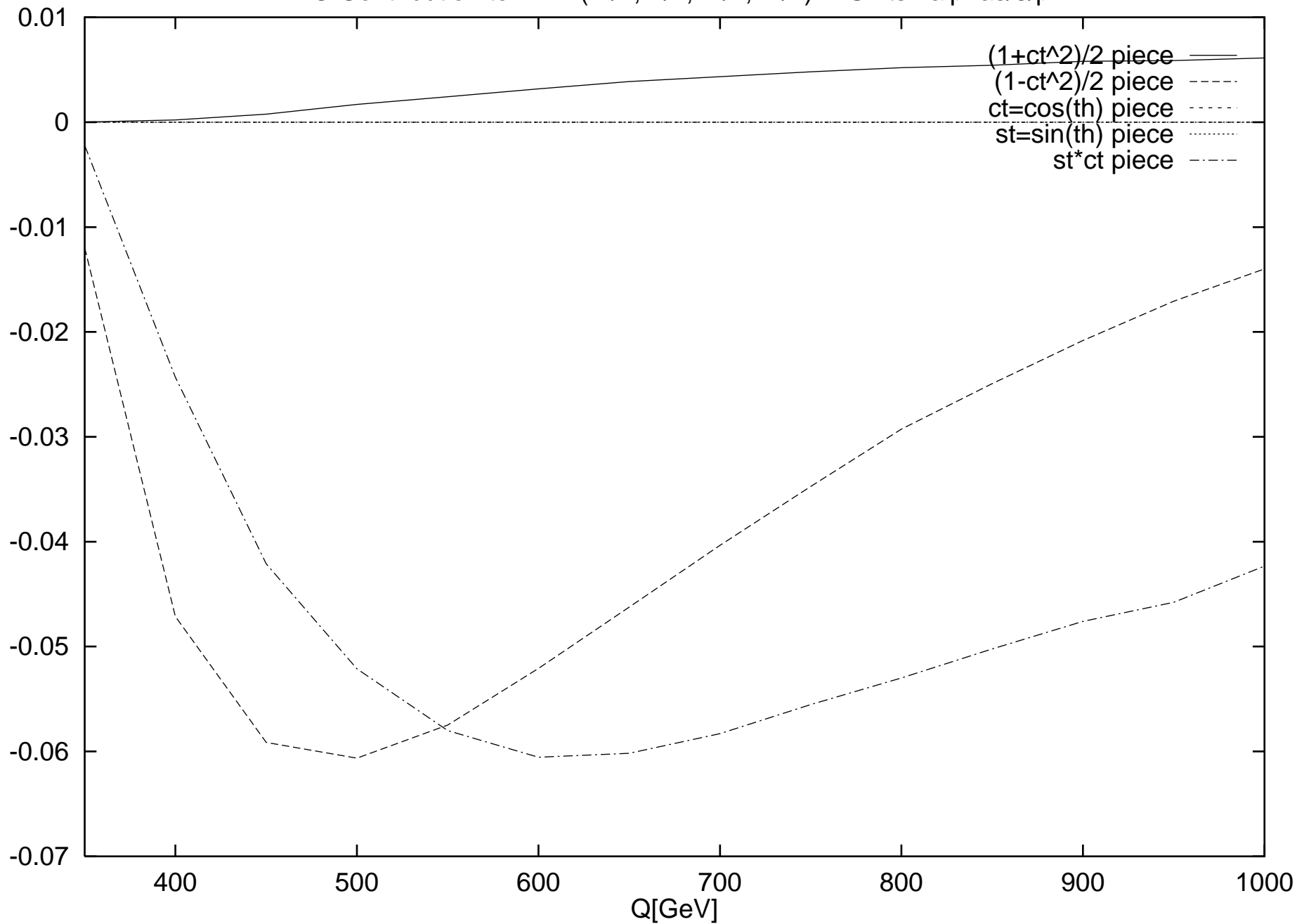
HO Contribution to R-VAAVAA(-1/2,-1/2,+1/2,-1/2) in Units $2\alpha/3\pi$

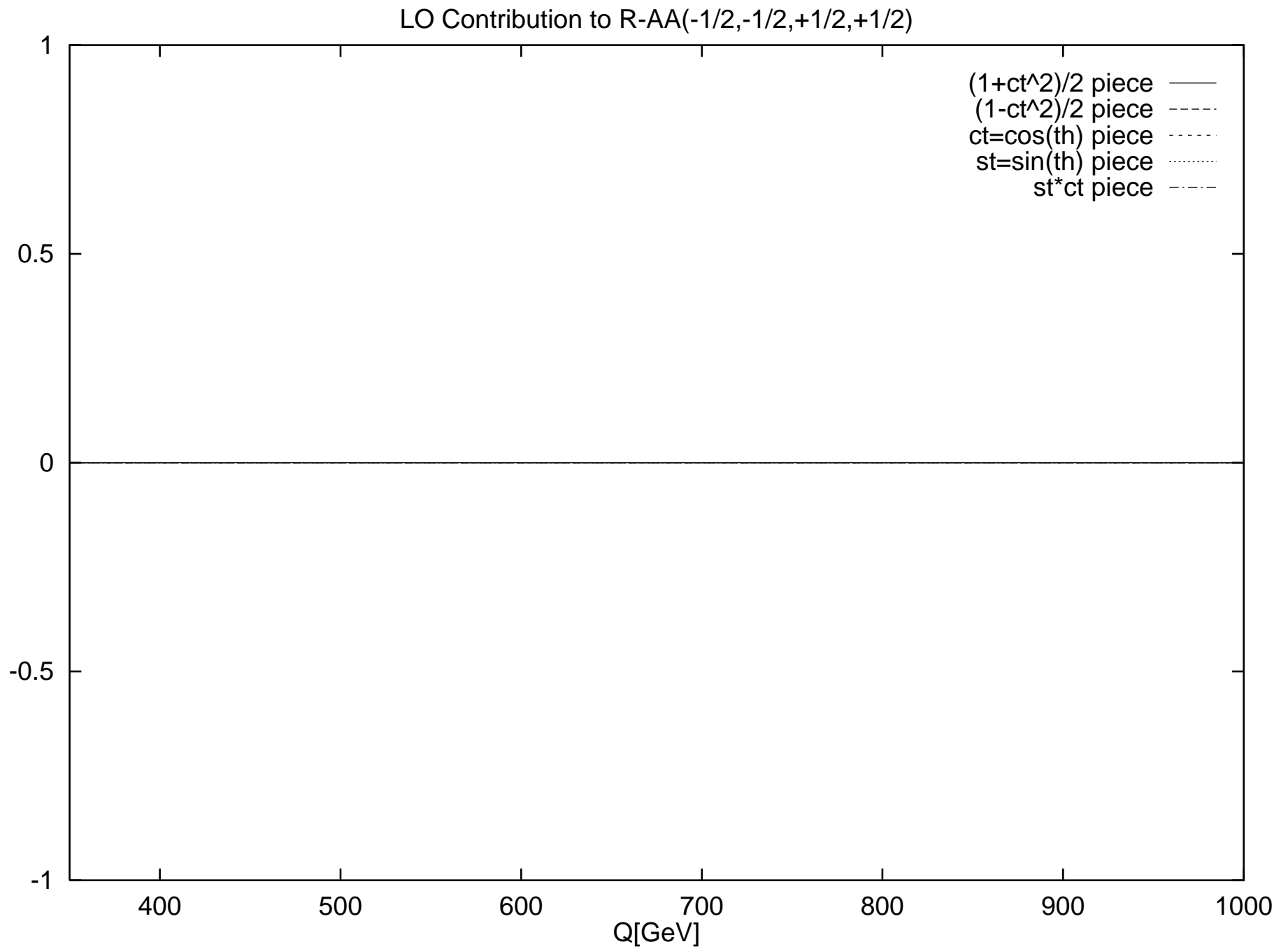


LO Contribution to R-VV(-1/2,-1/2,+1/2,+1/2)

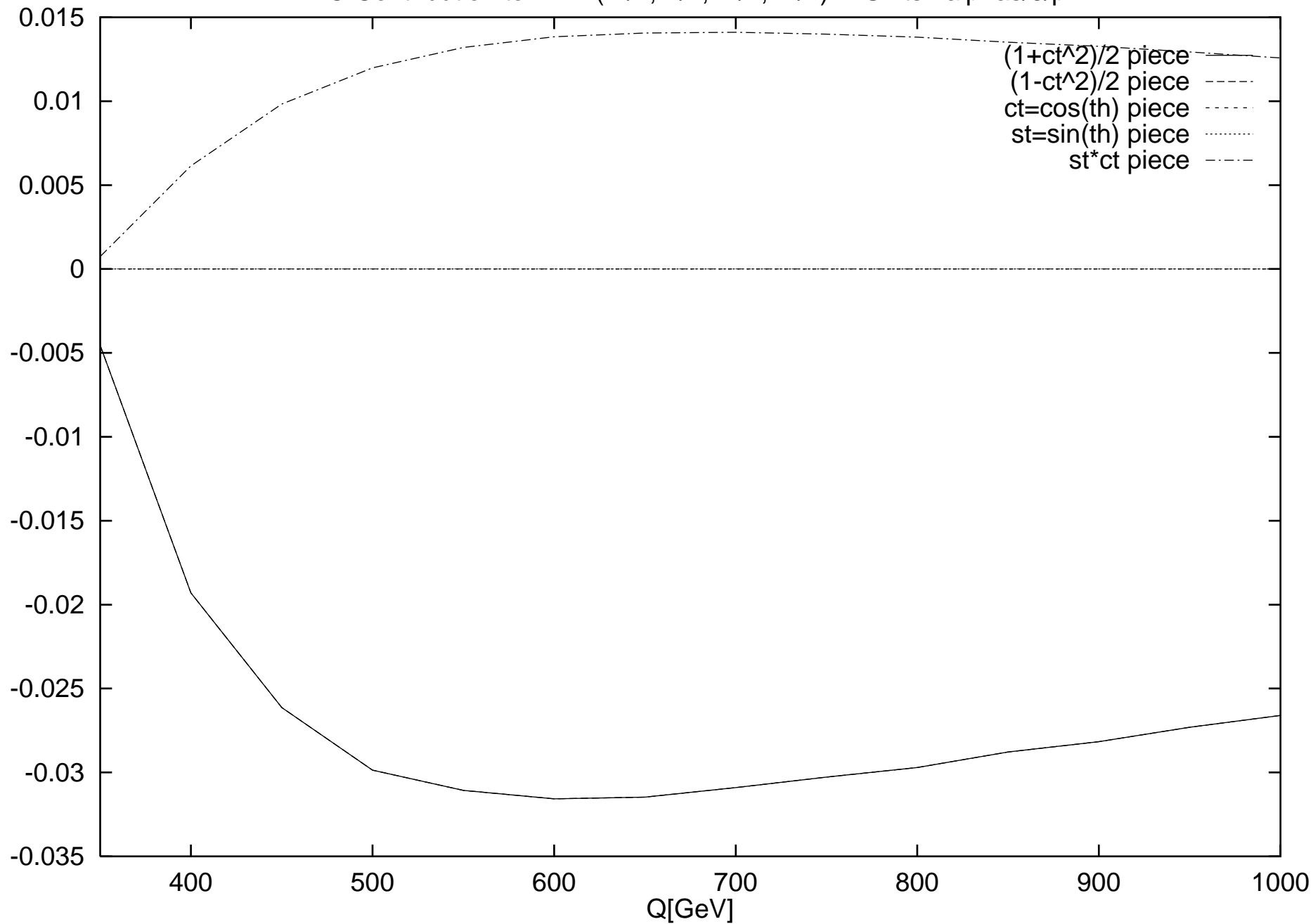


HO Contribution to R-VV(-1/2,-1/2,+1/2,+1/2) in Units $2\alpha/3\pi$

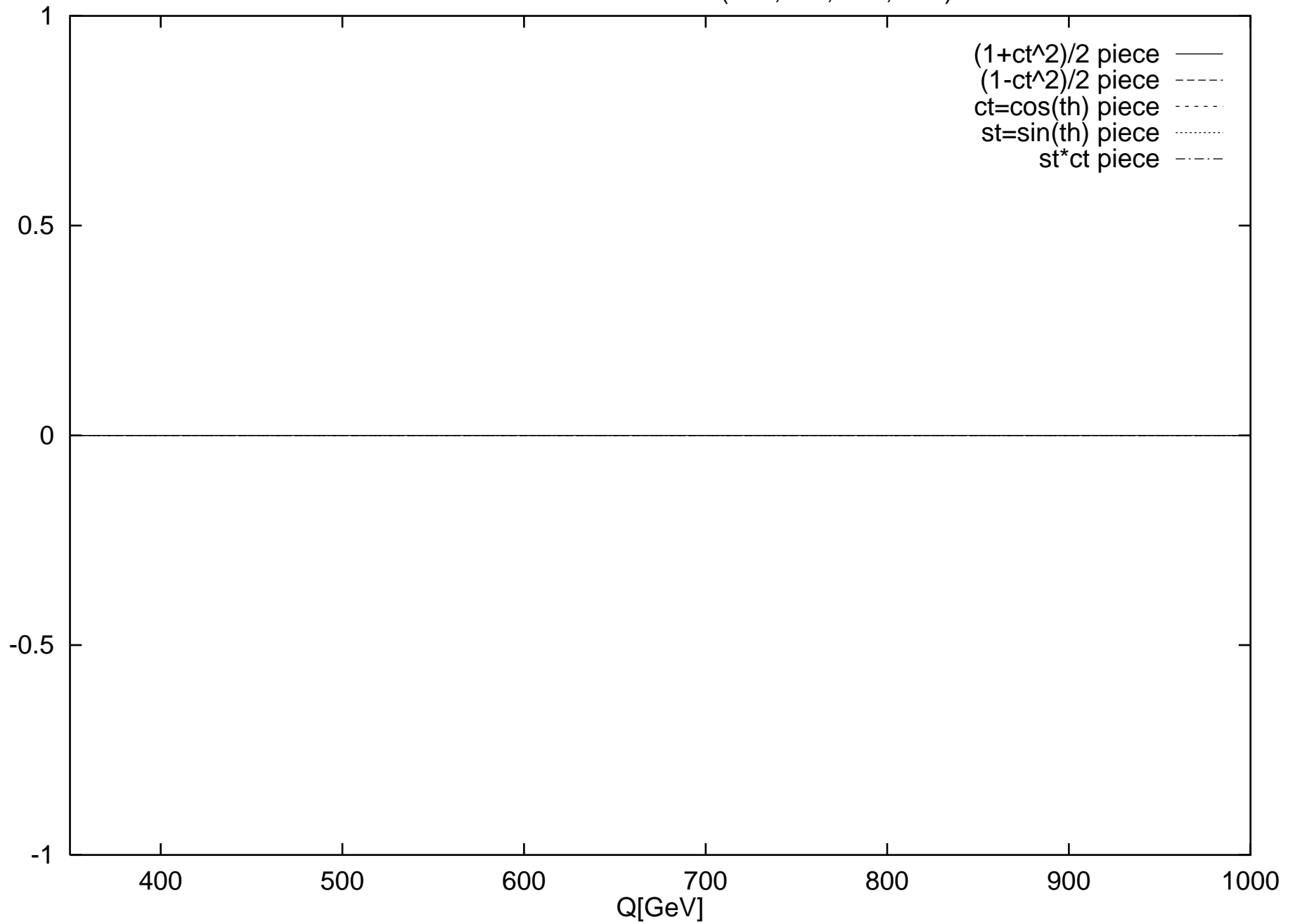




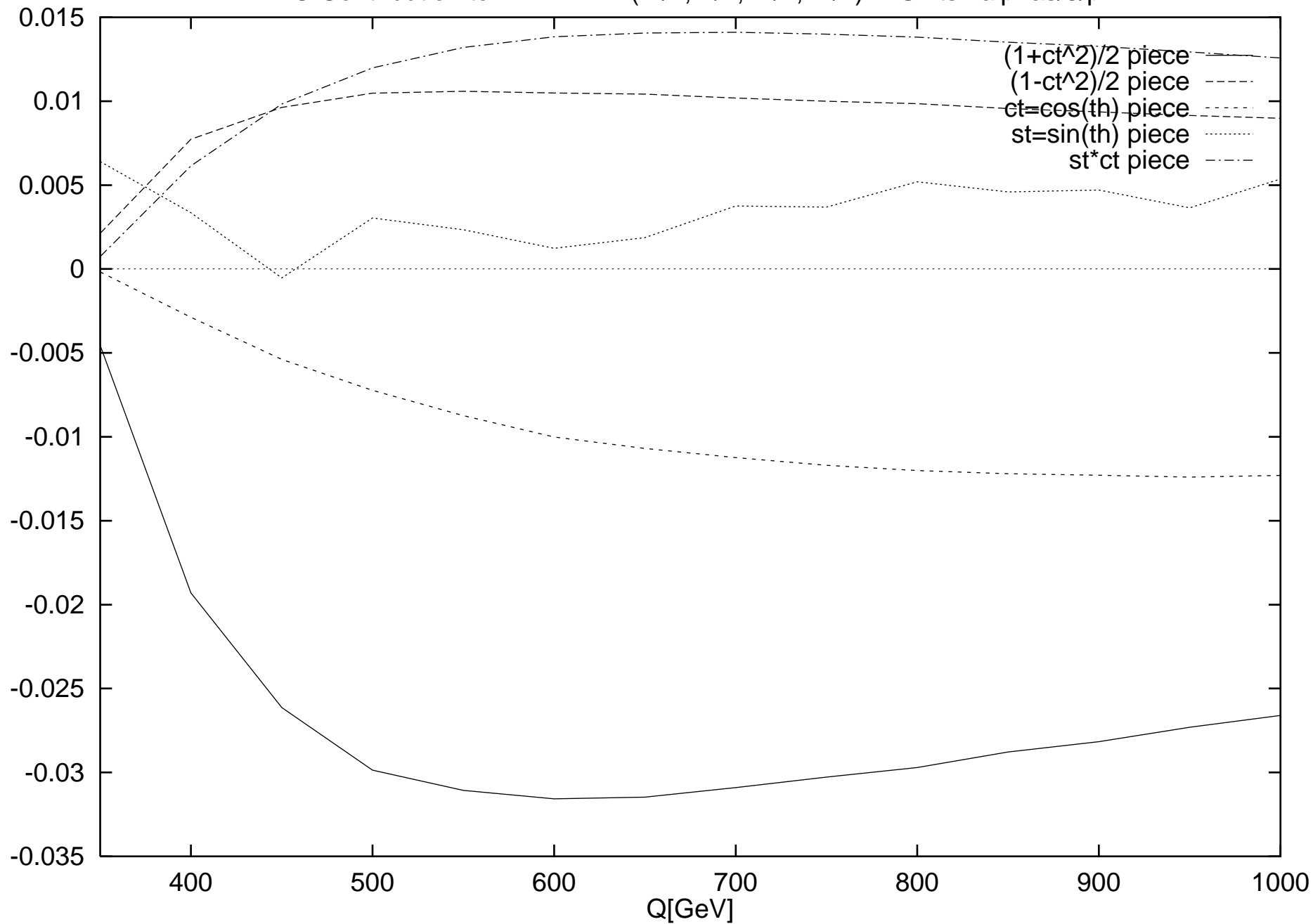
HO Contribution to R-AA(-1/2,-1/2,+1/2,+1/2) in Units $2\alpha_s/3\pi$



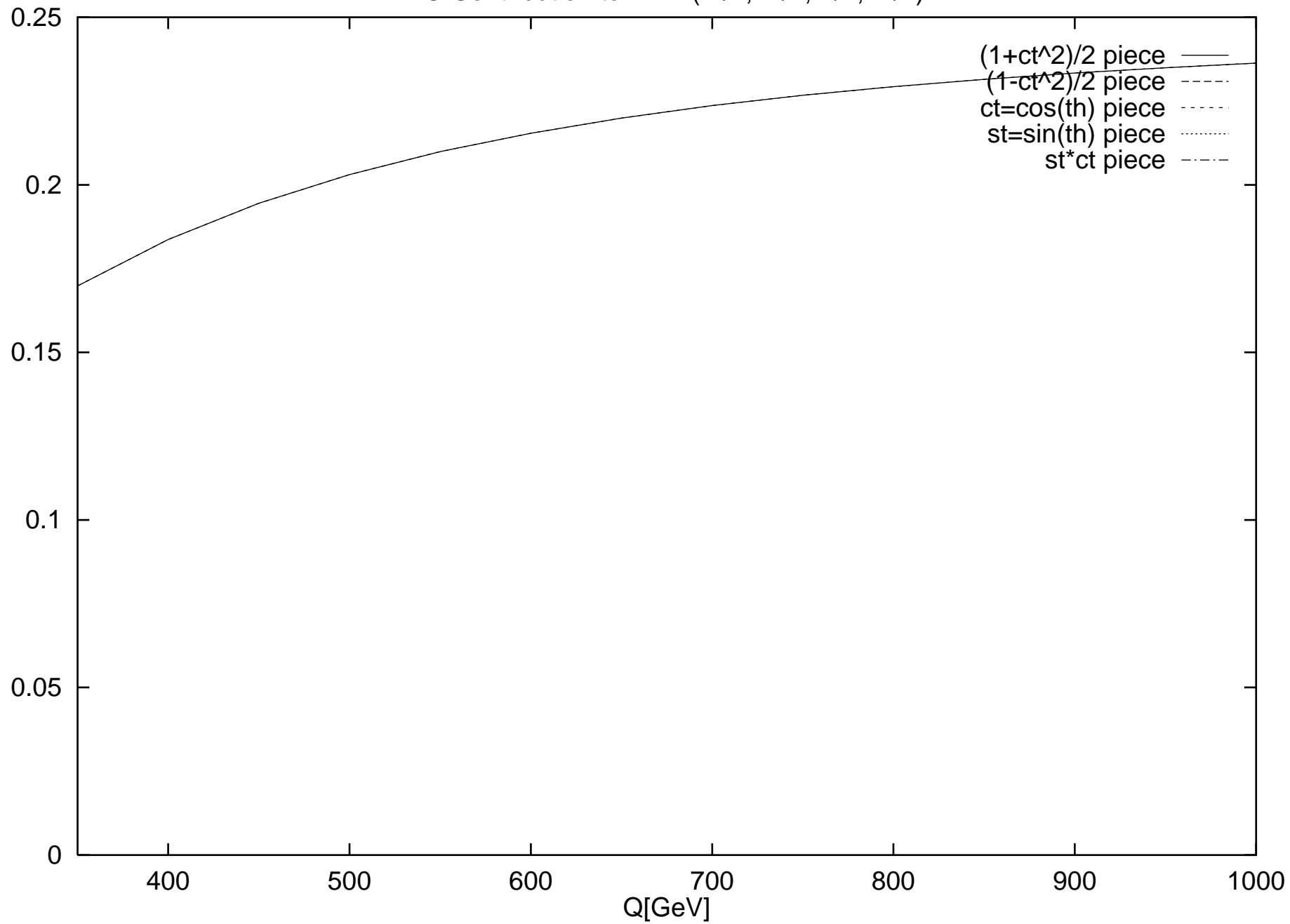
LO Contribution to R-VAAVAA(-1/2,-1/2,+1/2,+1/2)



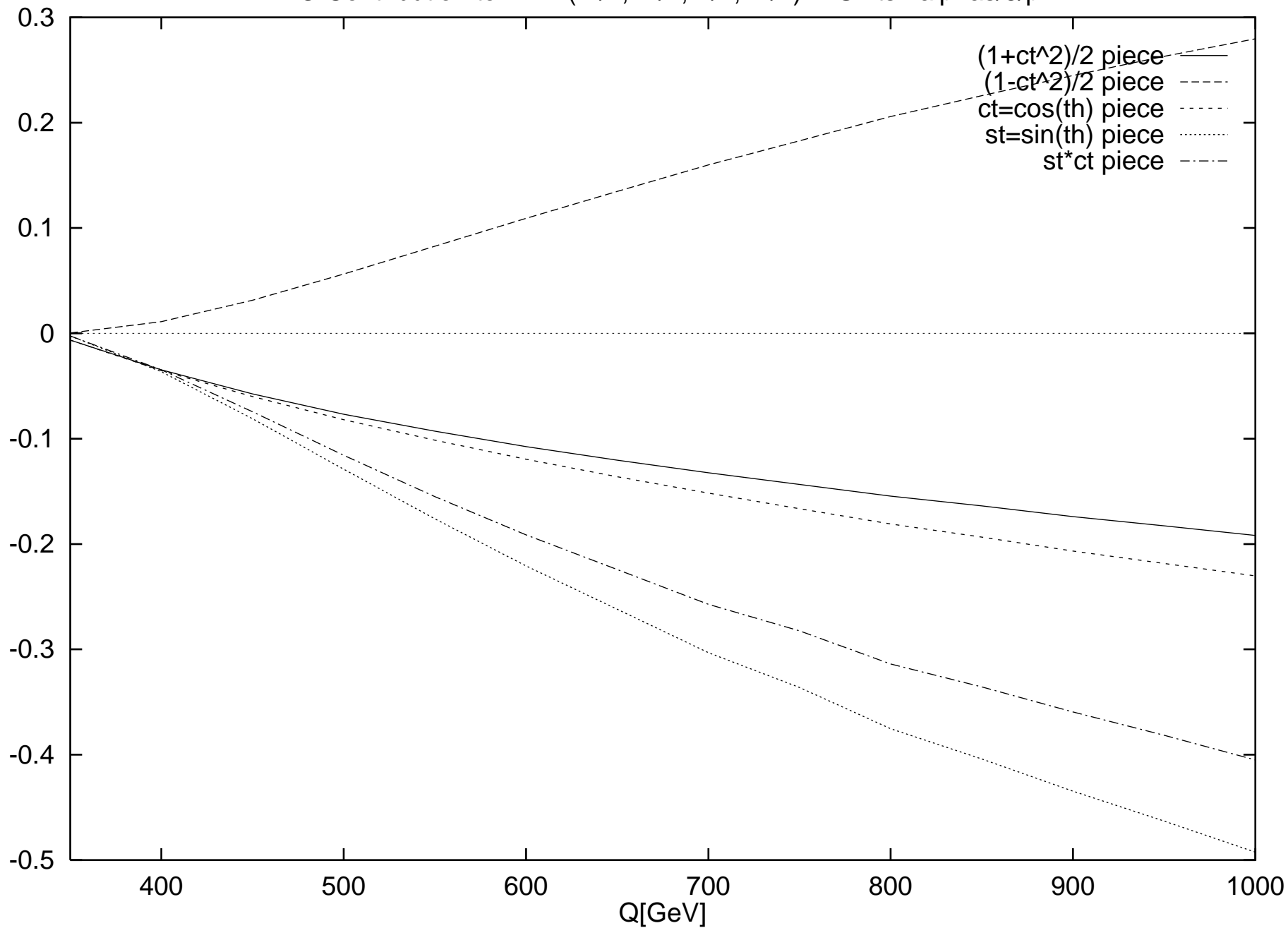
HO Contribution to R-VA AVAA(-1/2,-1/2,+1/2,+1/2) in Units $2\alpha/3\pi$

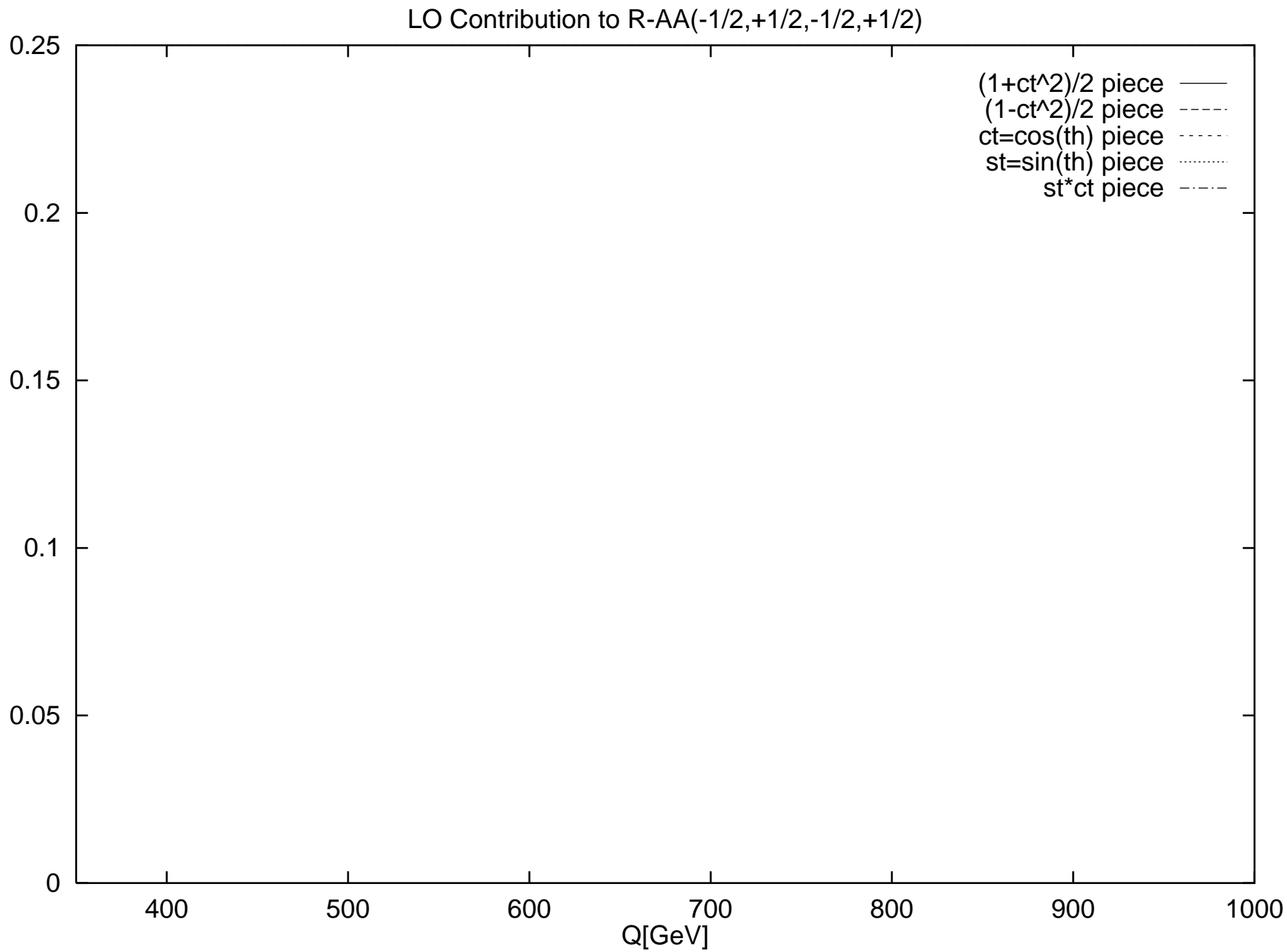


LO Contribution to R-VV(-1/2,+1/2,-1/2,+1/2)

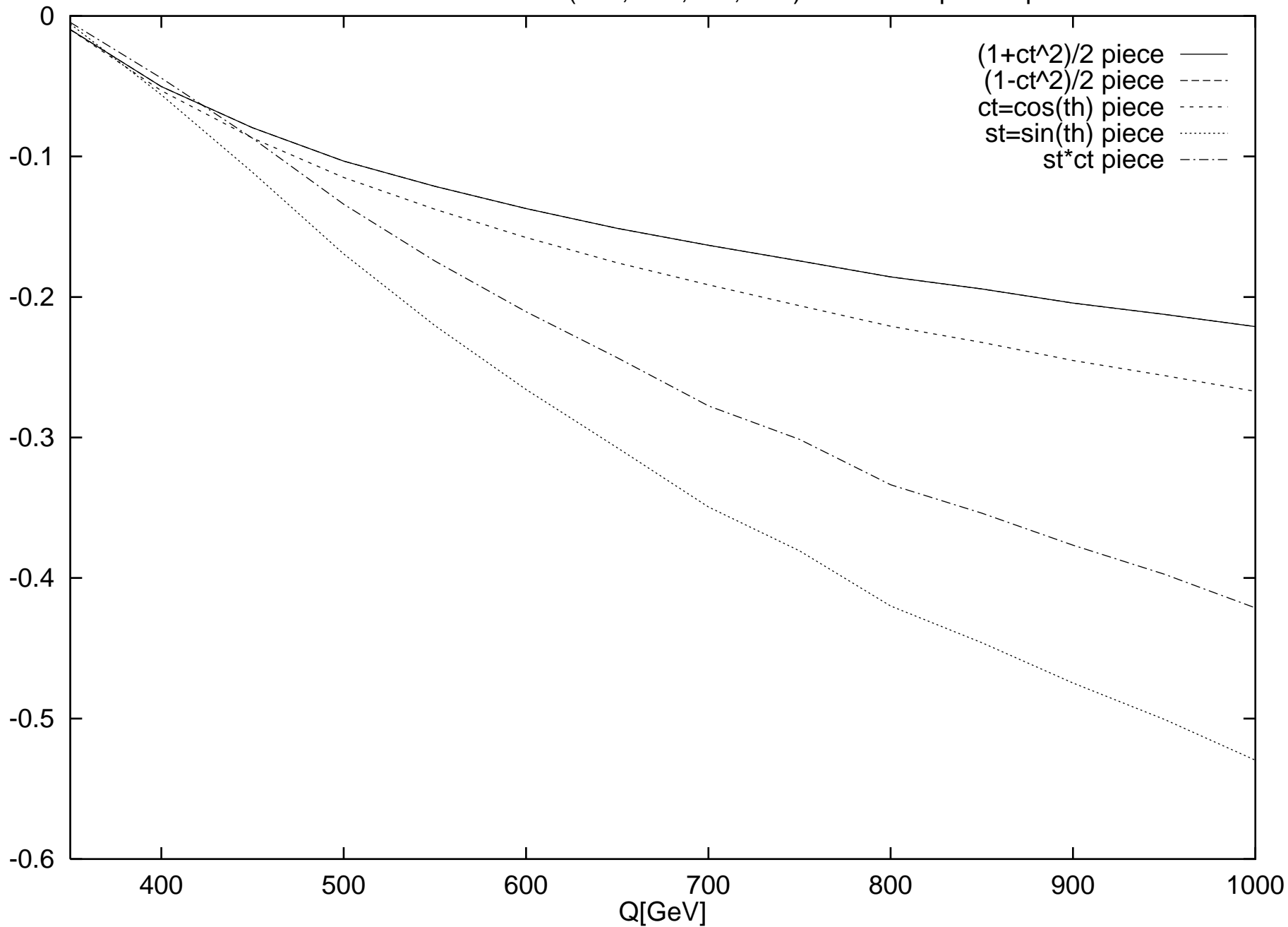


HO Contribution to R-VV(-1/2,+1/2,-1/2,+1/2) in Units $2\alpha/3\pi$

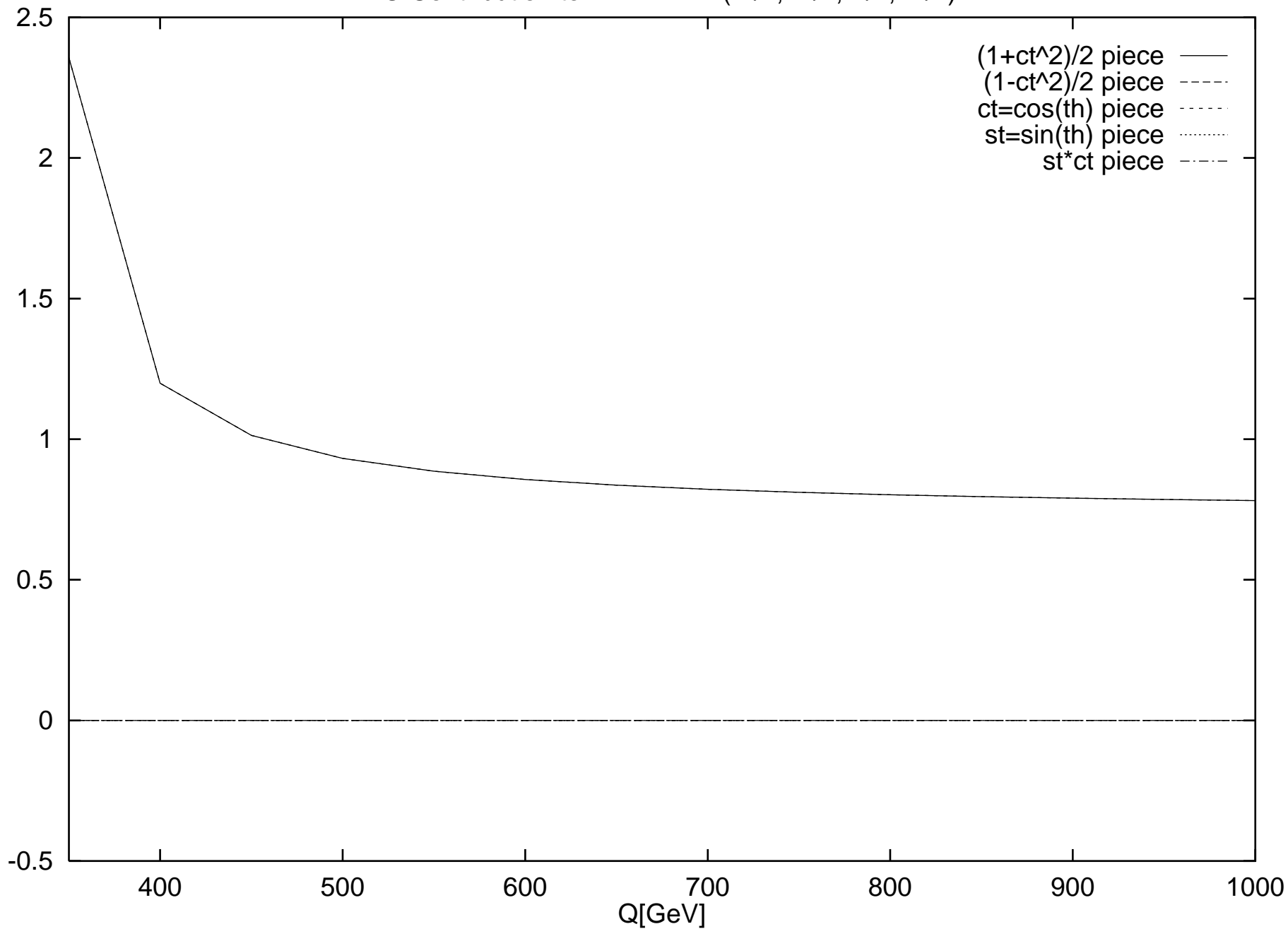




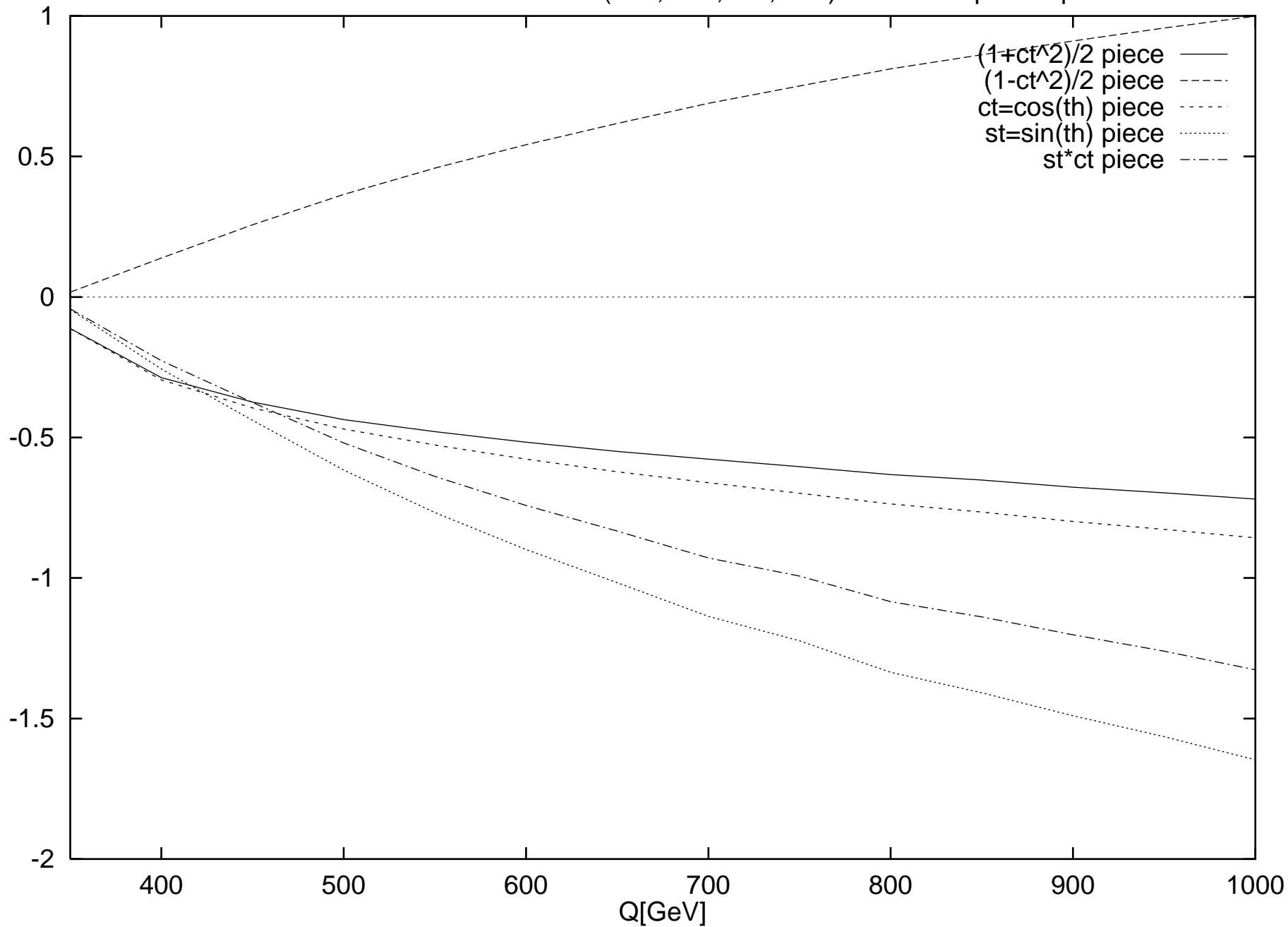
HO Contribution to R-AA(-1/2,+1/2,-1/2,+1/2) in Units $2\alpha_s/3\pi$



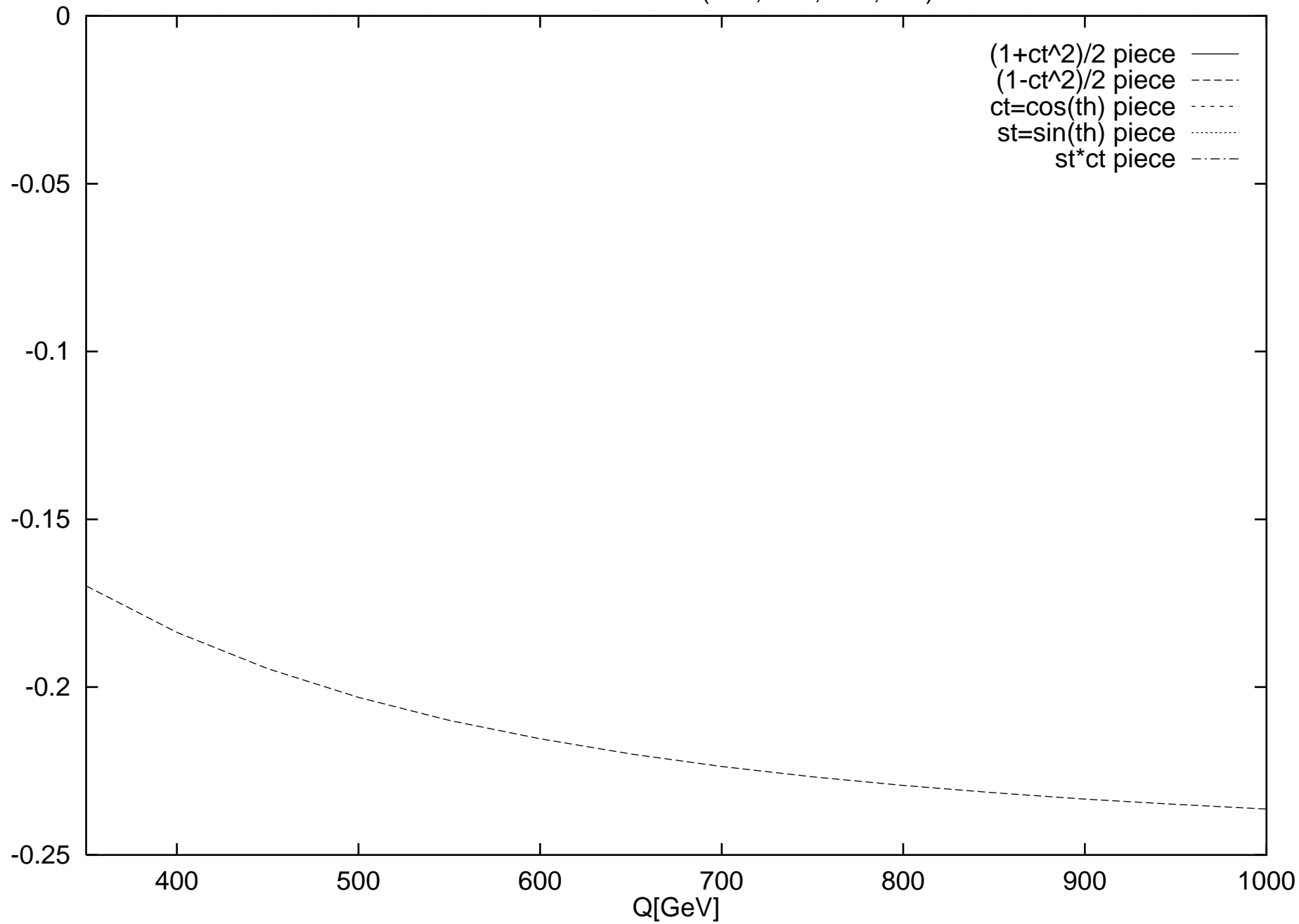
LO Contribution to R-VAAVAA(-1/2,+1/2,-1/2,+1/2)



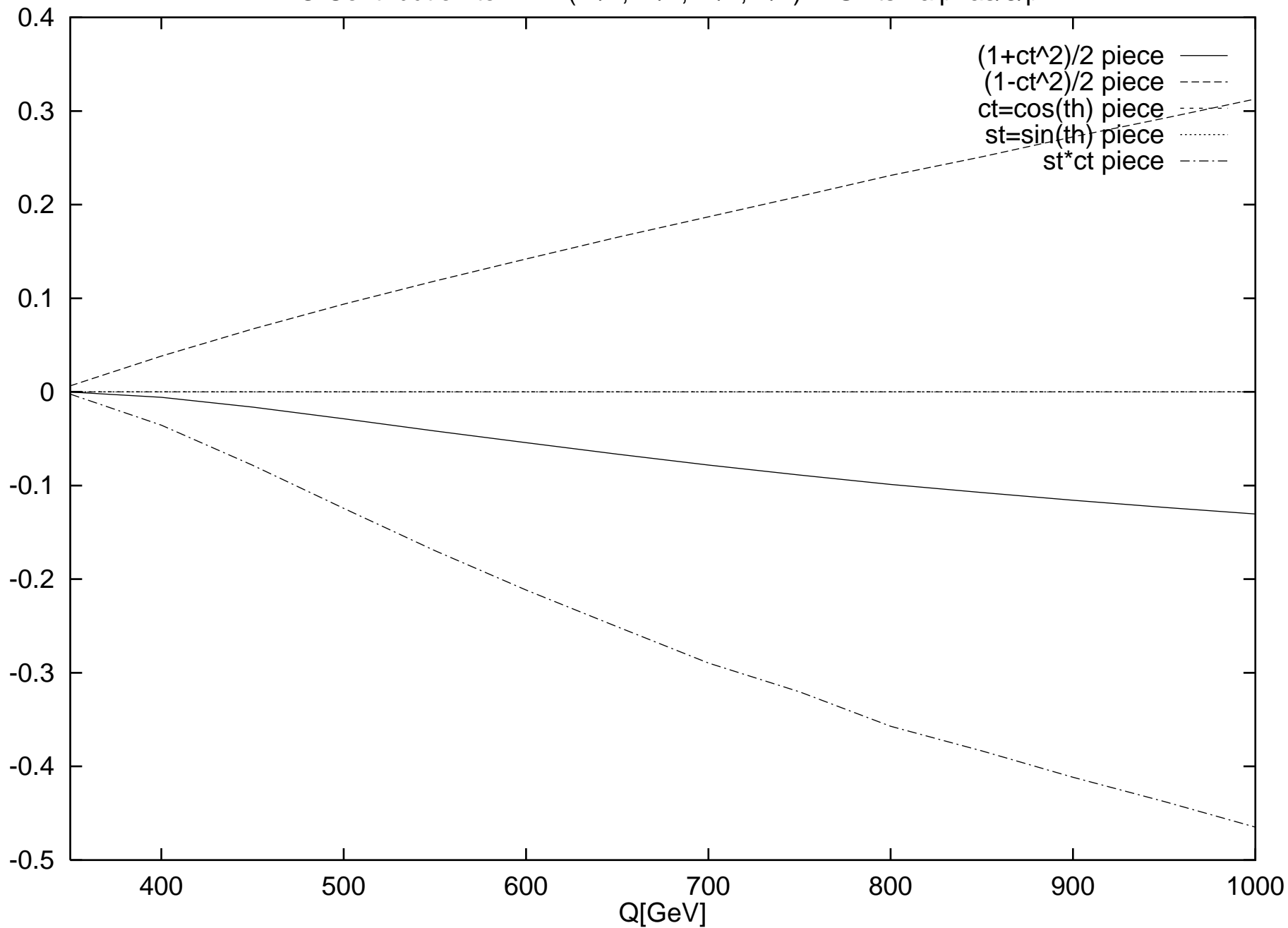
HO Contribution to R-VAAVAA(-1/2,+1/2,-1/2,+1/2) in Units $2\alpha/3\pi$

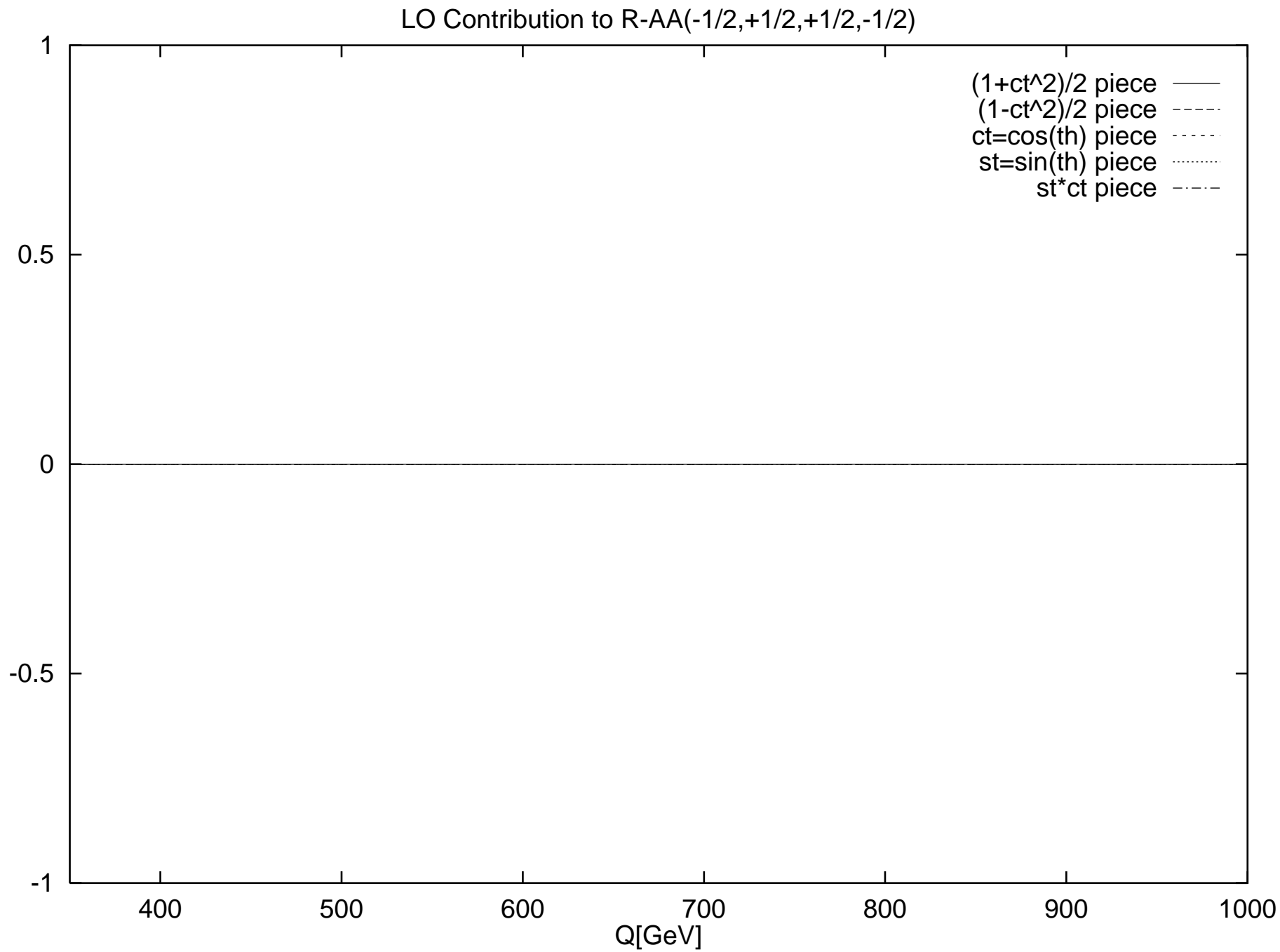


LO Contribution to R-VV(-1/2,+1/2,+1/2,-1/2)

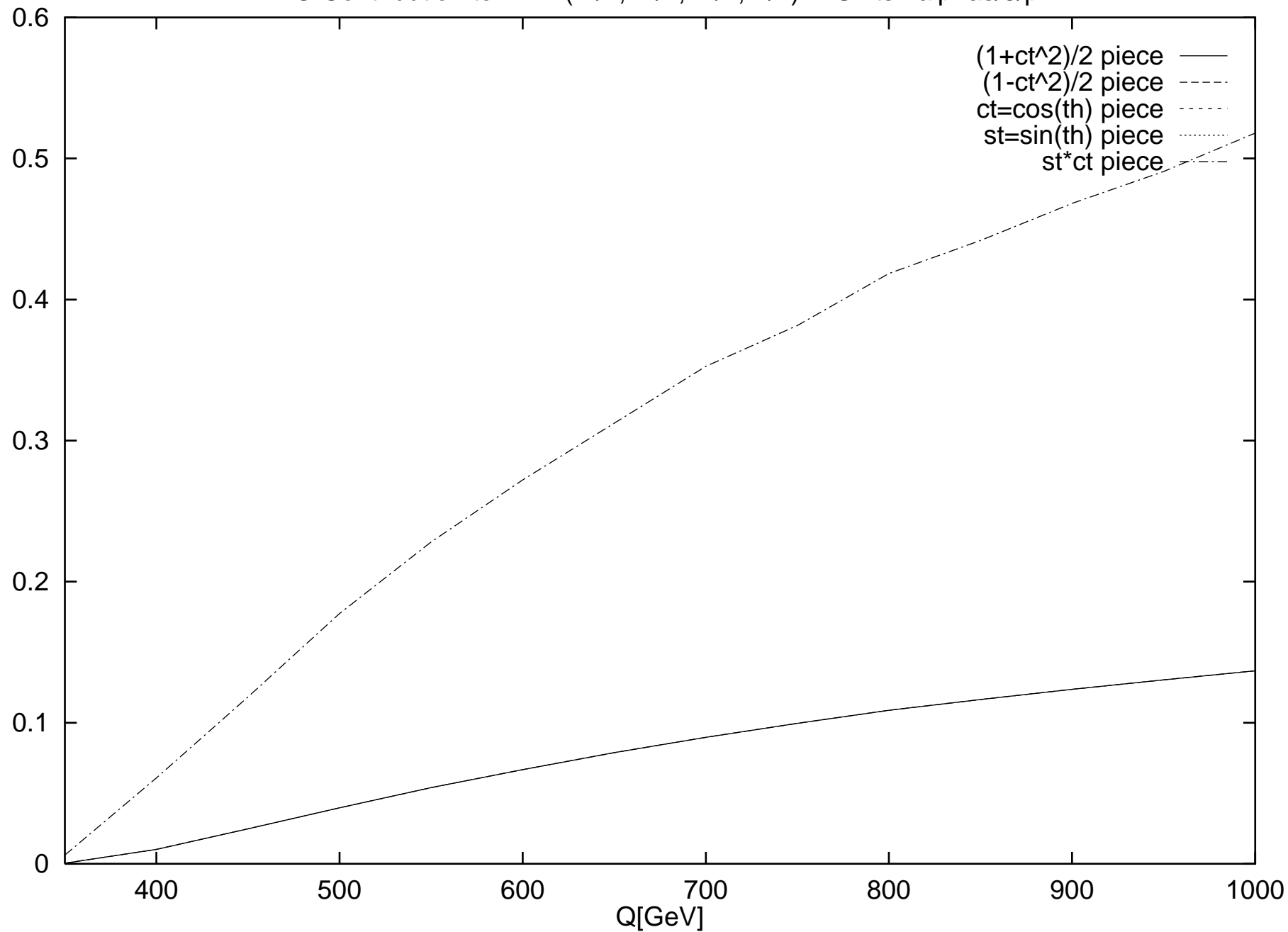


HO Contribution to R-VV(-1/2,+1/2,+1/2,-1/2) in Units $2\alpha/3\pi$

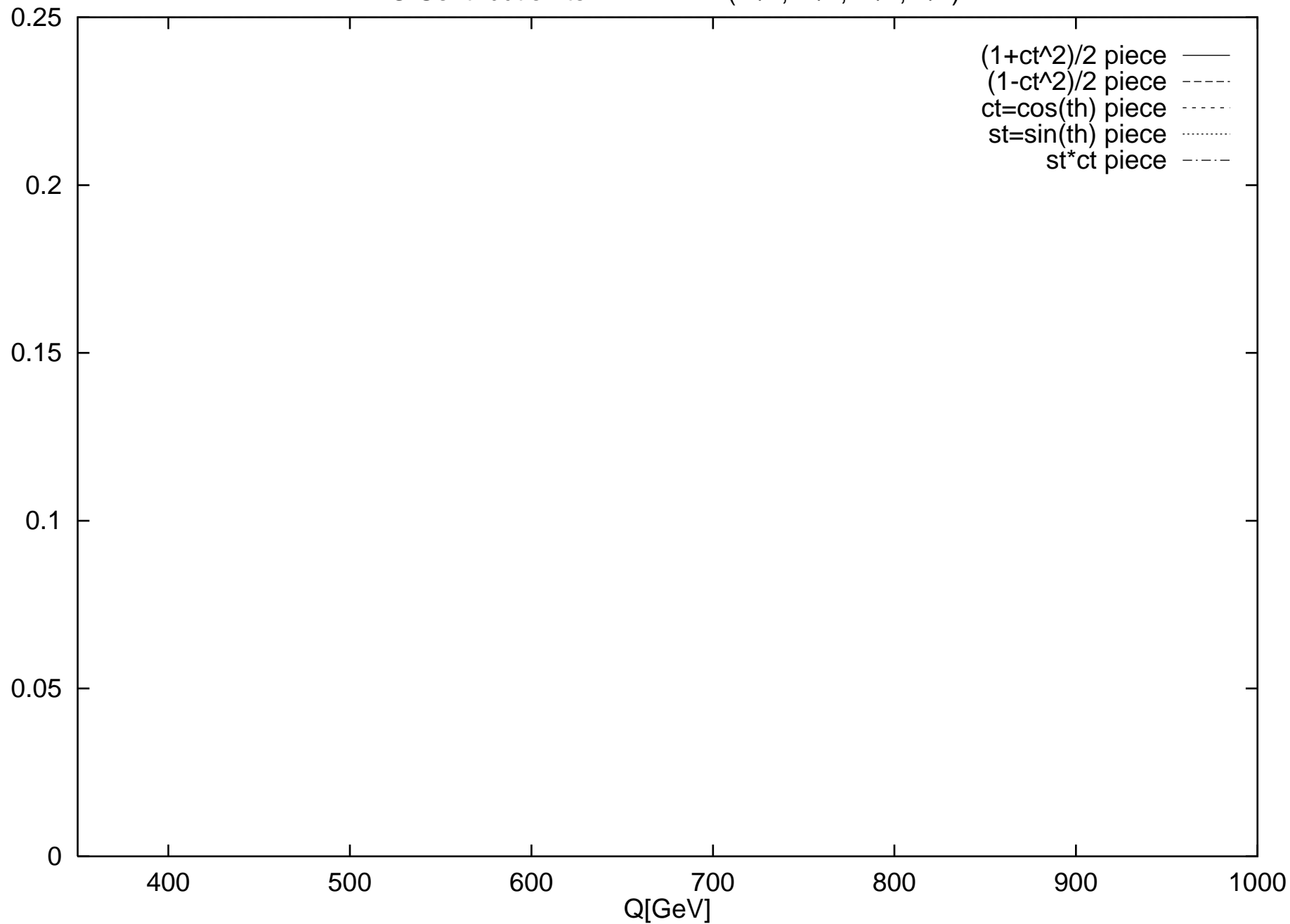




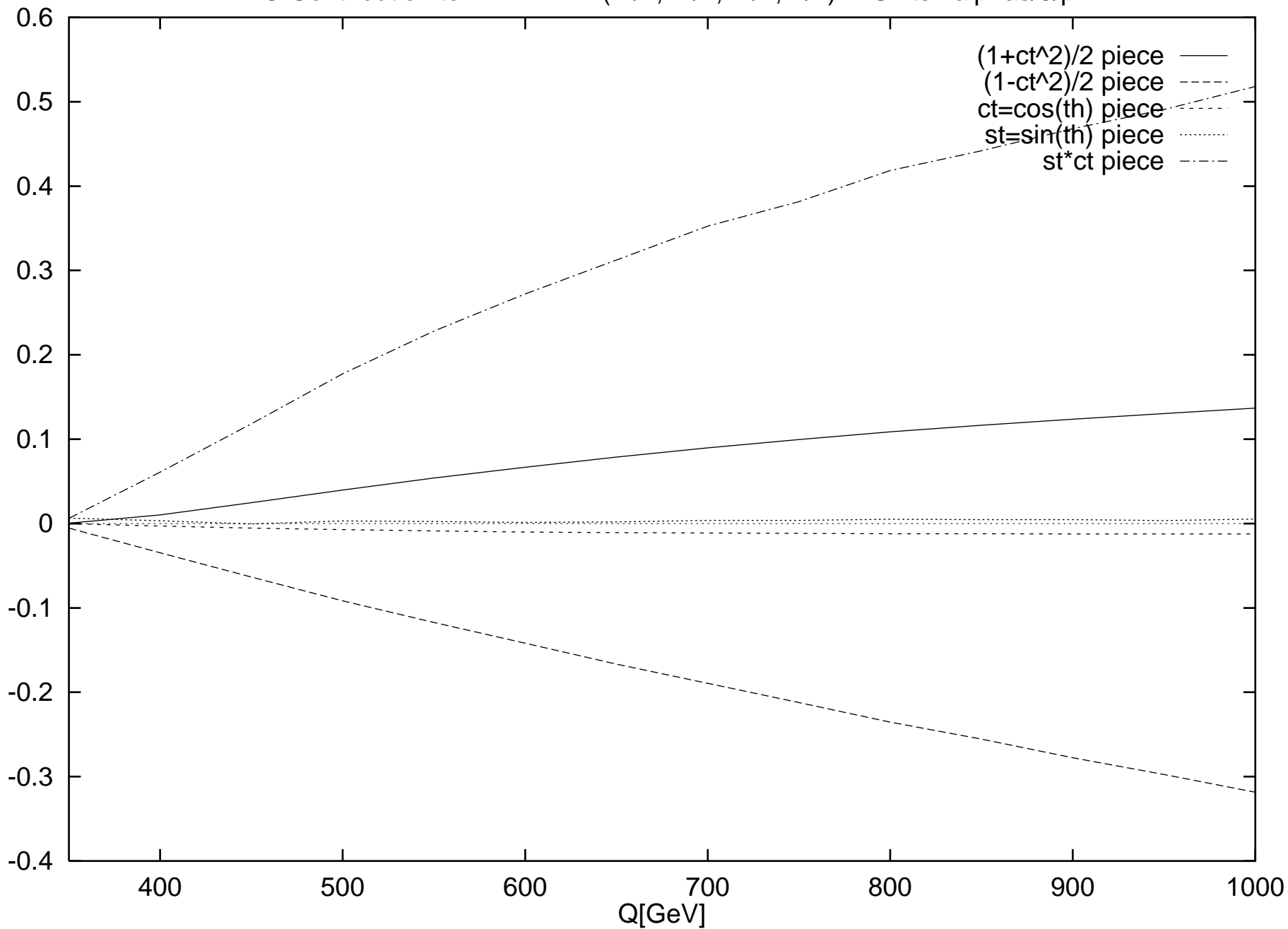
HO Contribution to R-AA(-1/2,+1/2,+1/2,-1/2) in Units $2\alpha_s/3\pi$



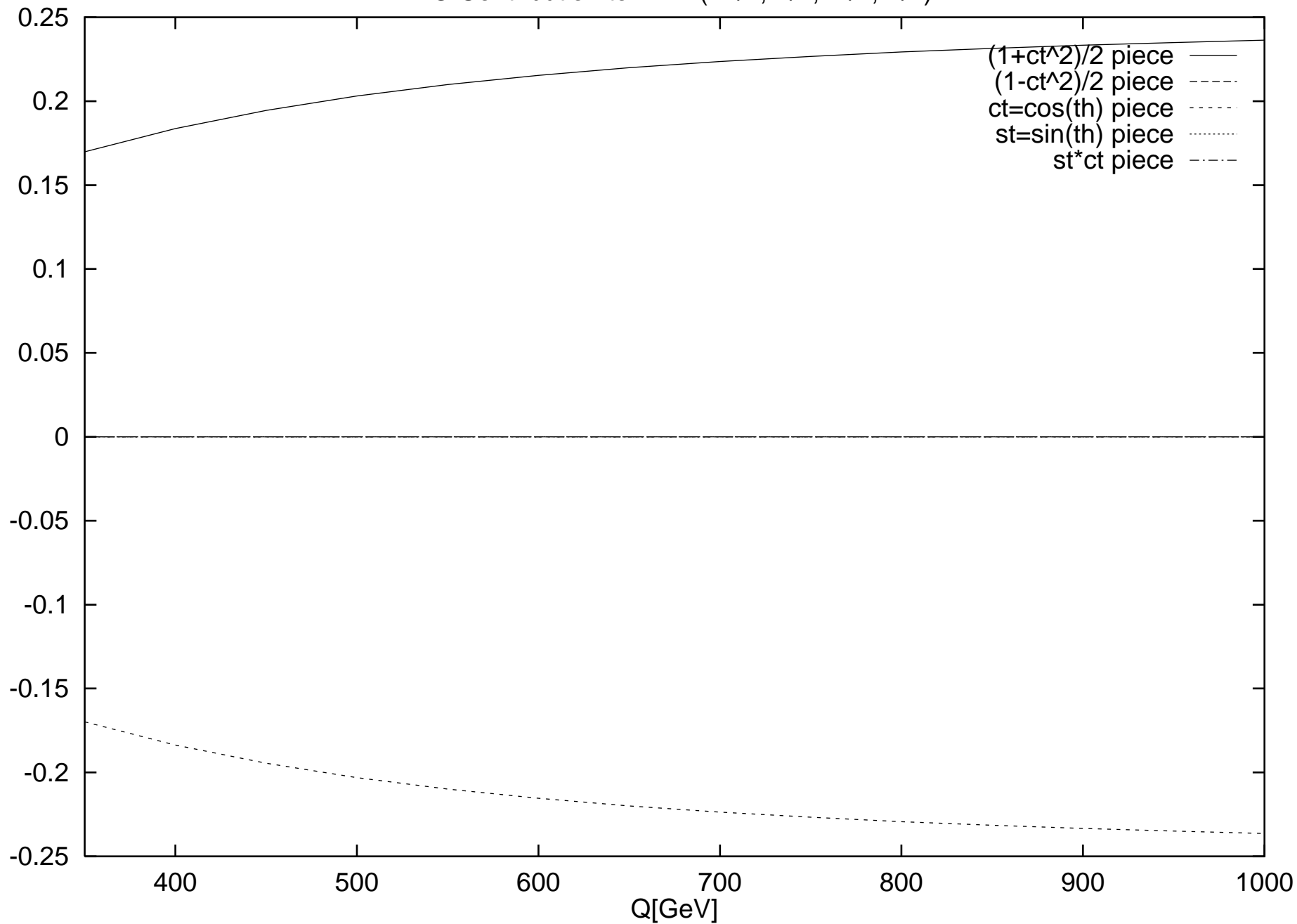
LO Contribution to R-VAAVAA(-1/2,+1/2,+1/2,-1/2)



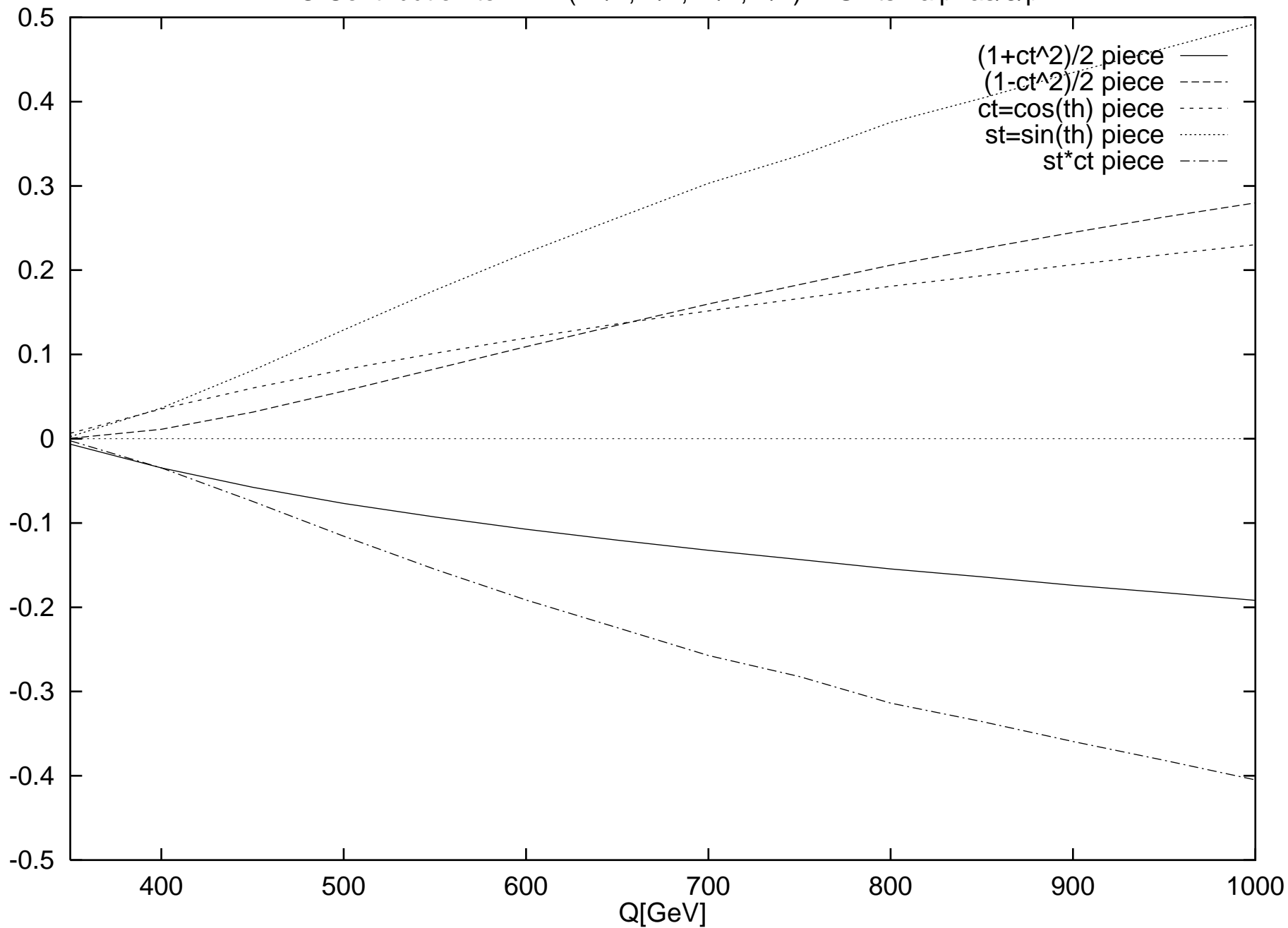
HO Contribution to R-VAAVAA(-1/2,+1/2,+1/2,-1/2) in Units $2\alpha/3\pi$

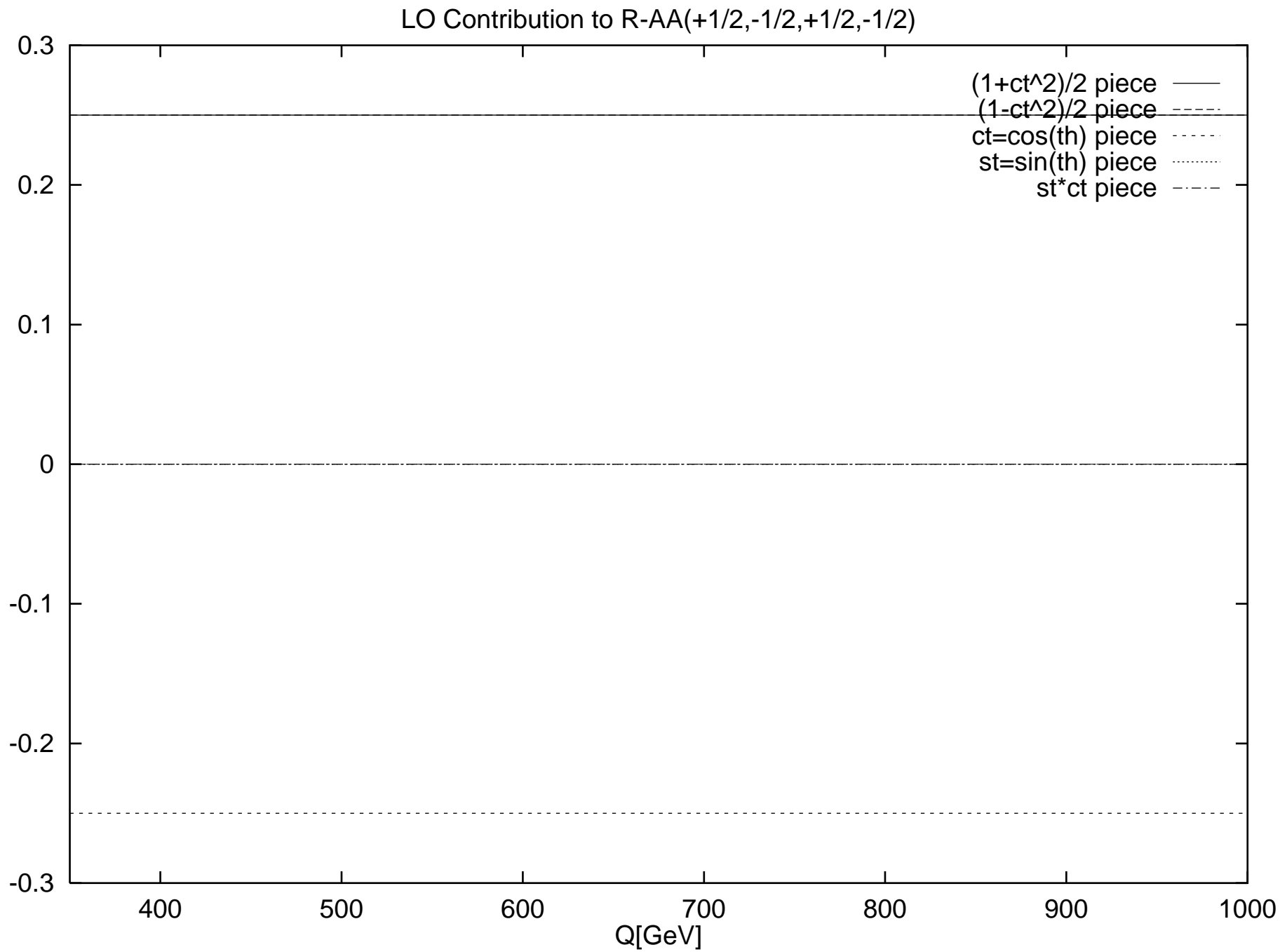


LO Contribution to R-VV(+1/2,-1/2,+1/2,-1/2)

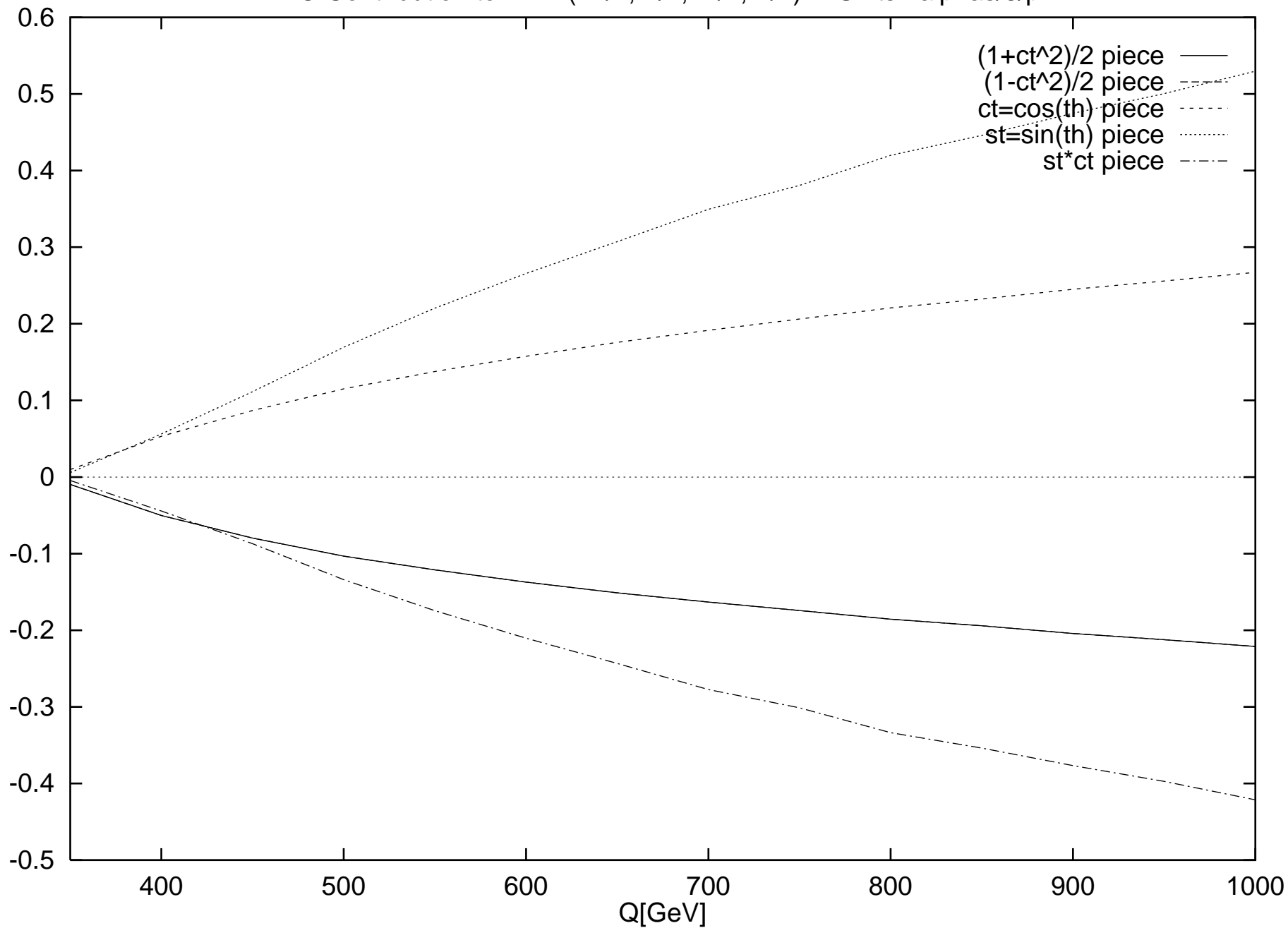


HO Contribution to R-VV(+1/2,-1/2,+1/2,-1/2) in Units $2\alpha/3\pi$

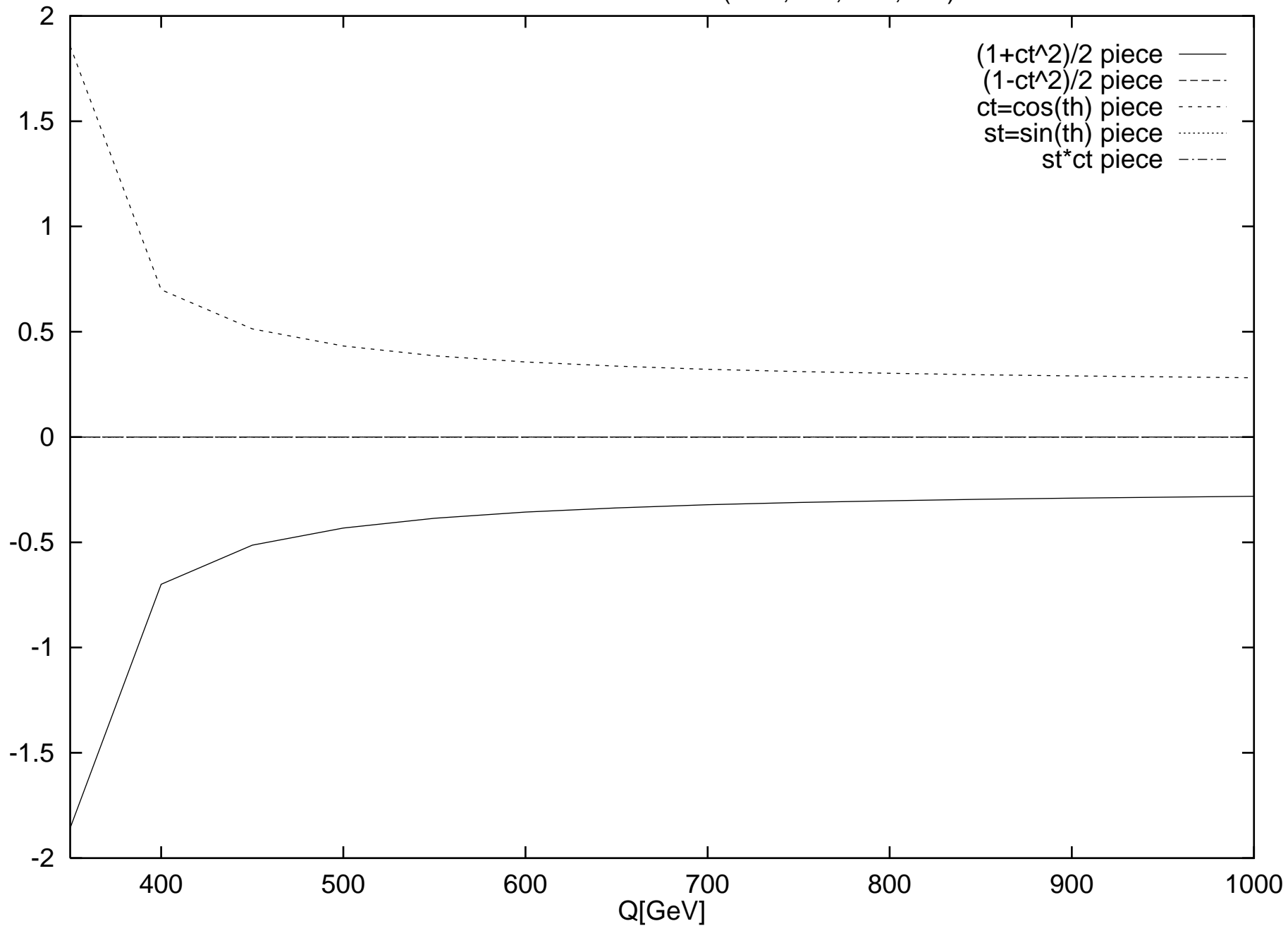




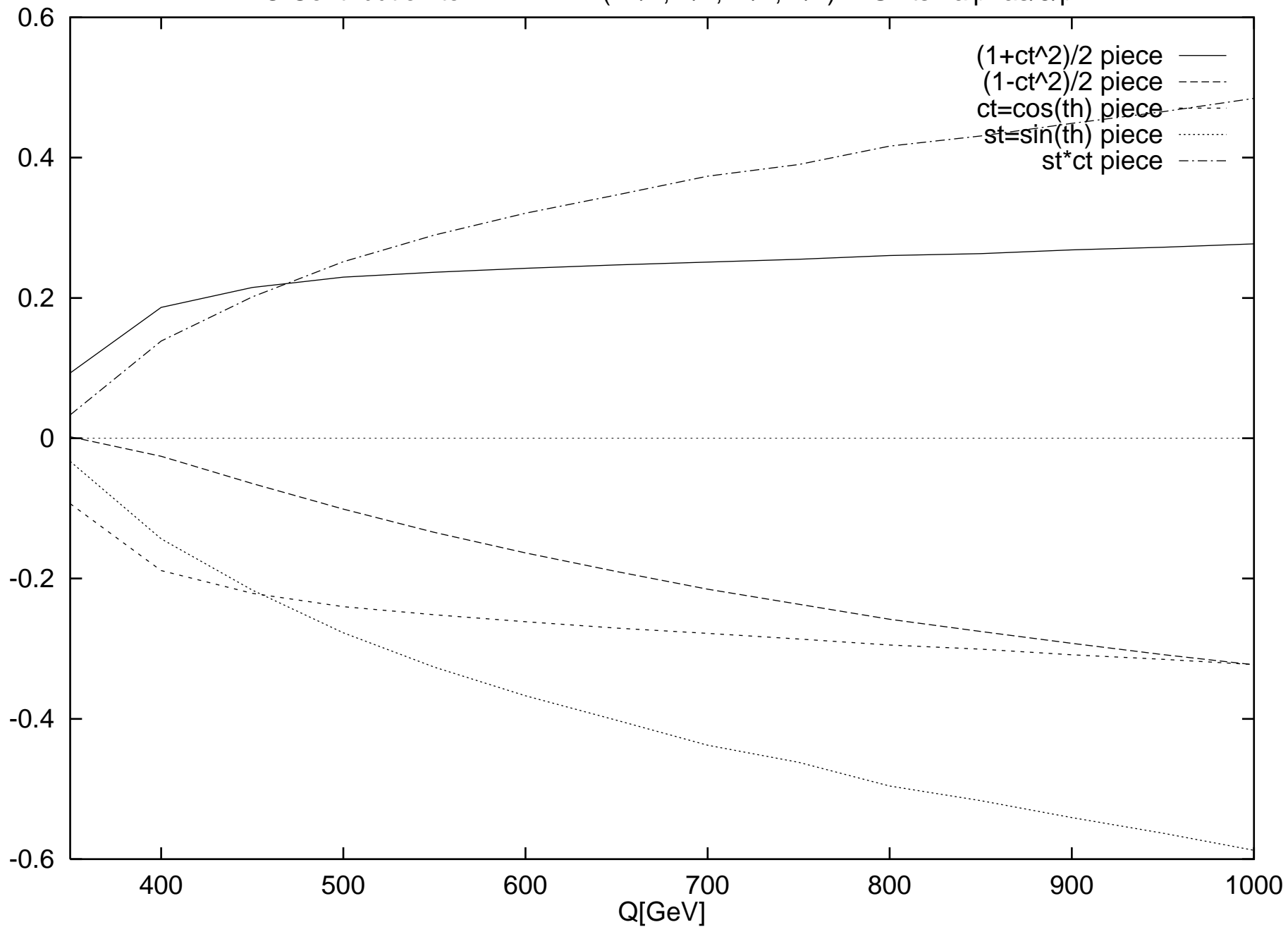
HO Contribution to R-AA(+1/2,-1/2,+1/2,-1/2) in Units $2\alpha/3\pi$



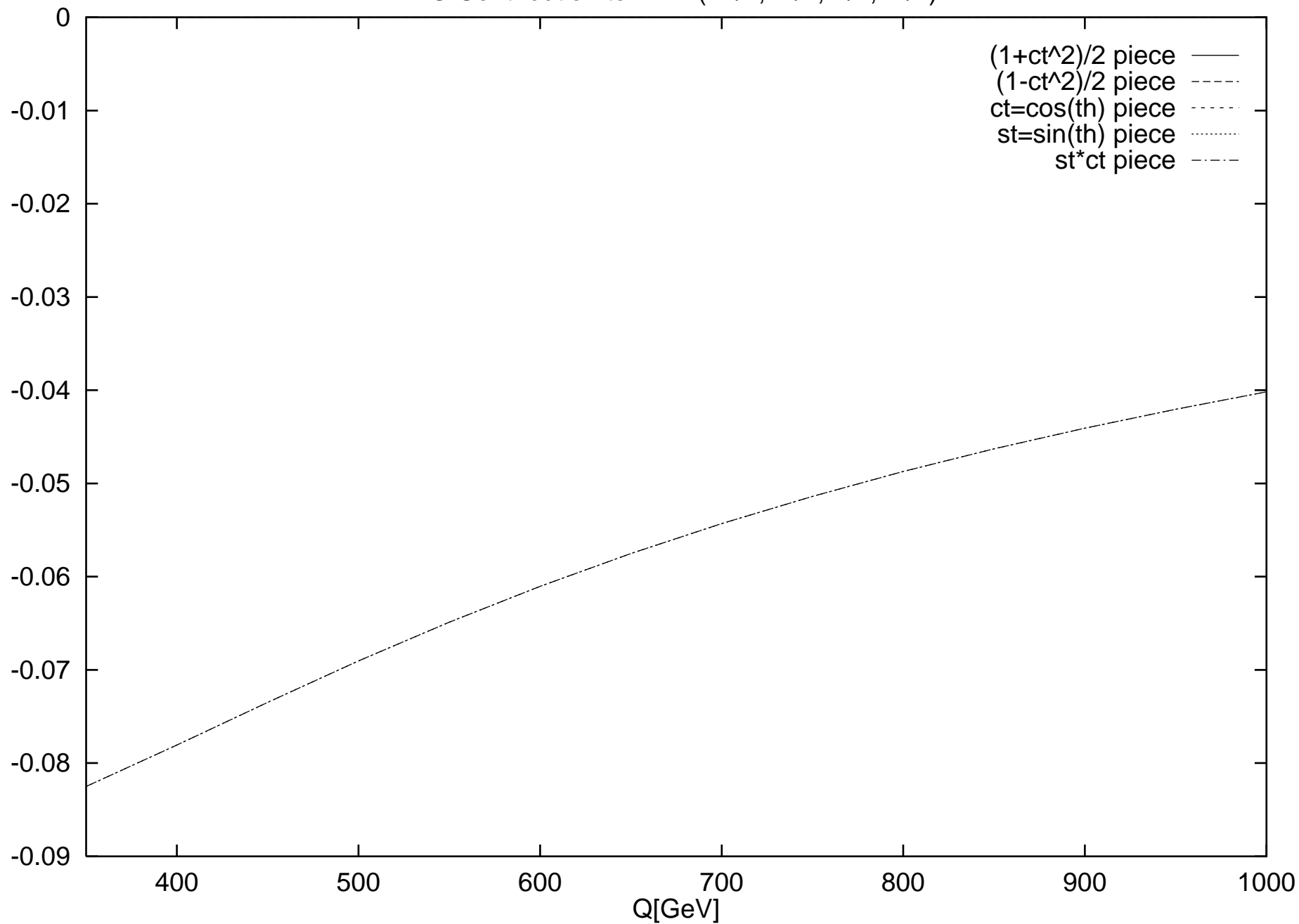
LO Contribution to R-VA AVAA(+1/2,-1/2,+1/2,-1/2)



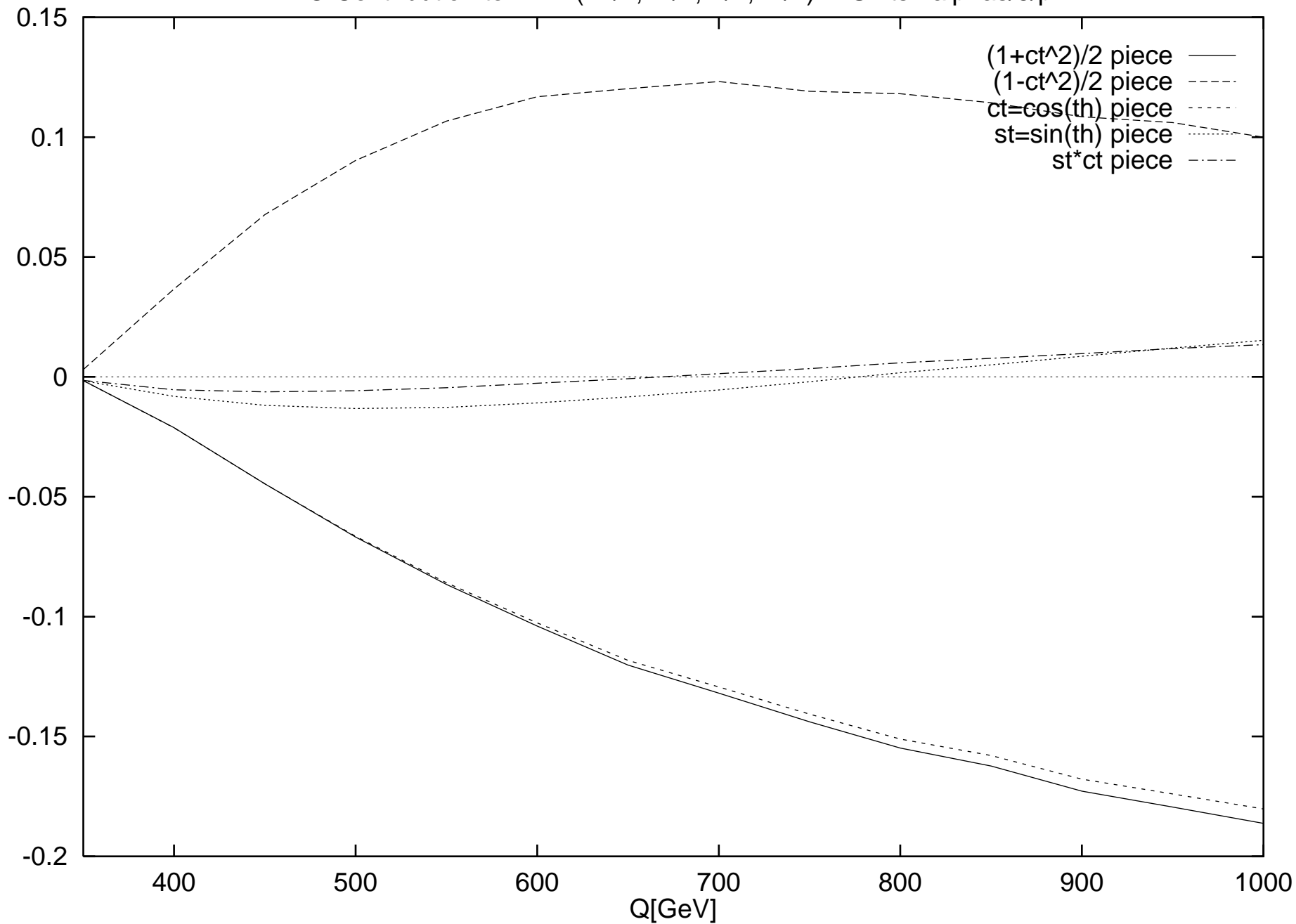
HO Contribution to R-VAAVAA(+1/2,-1/2,+1/2,-1/2) in Units $2\alpha/3\pi$



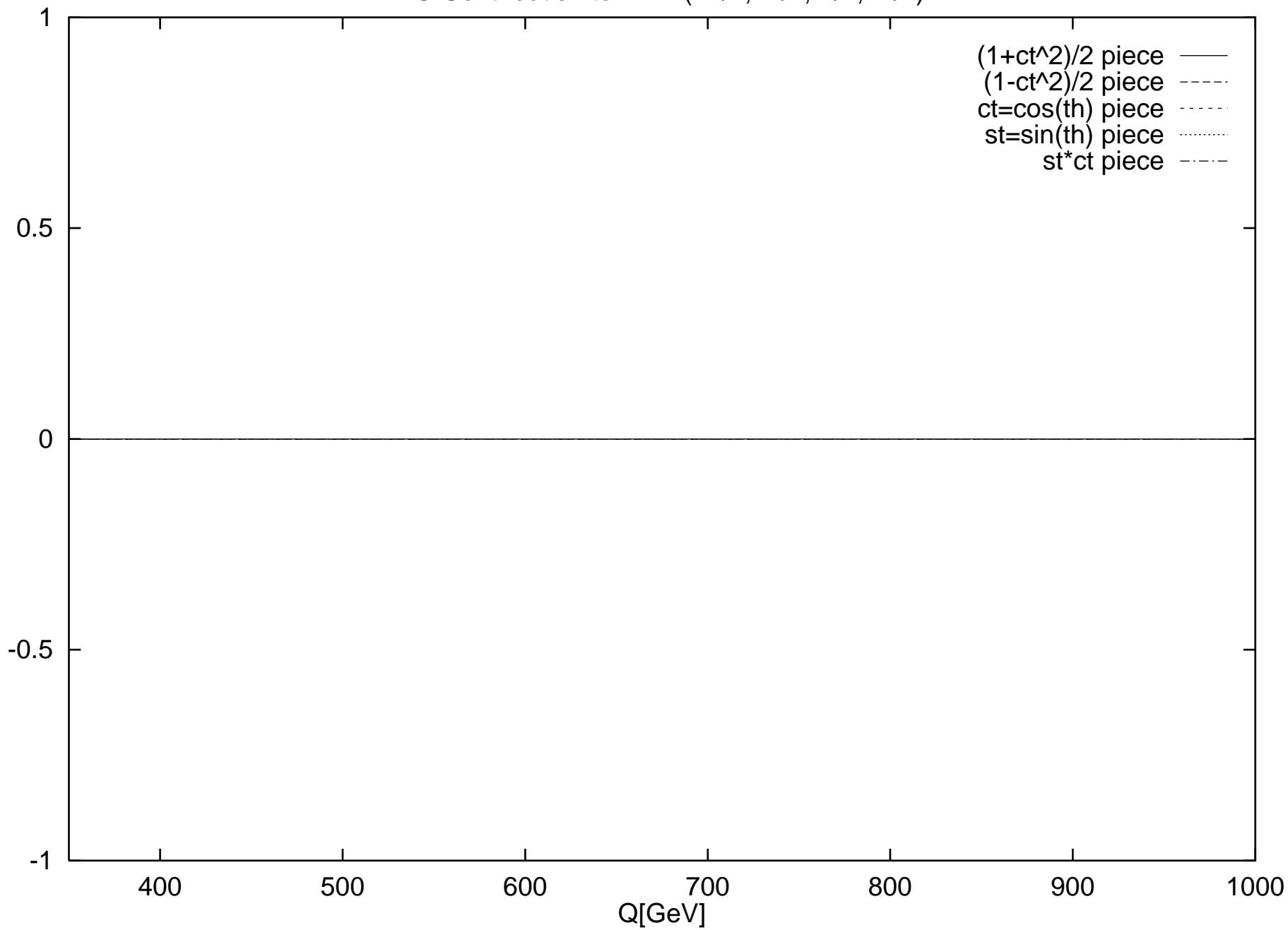
LO Contribution to R-VV(+1/2,+1/2,-1/2,+1/2)



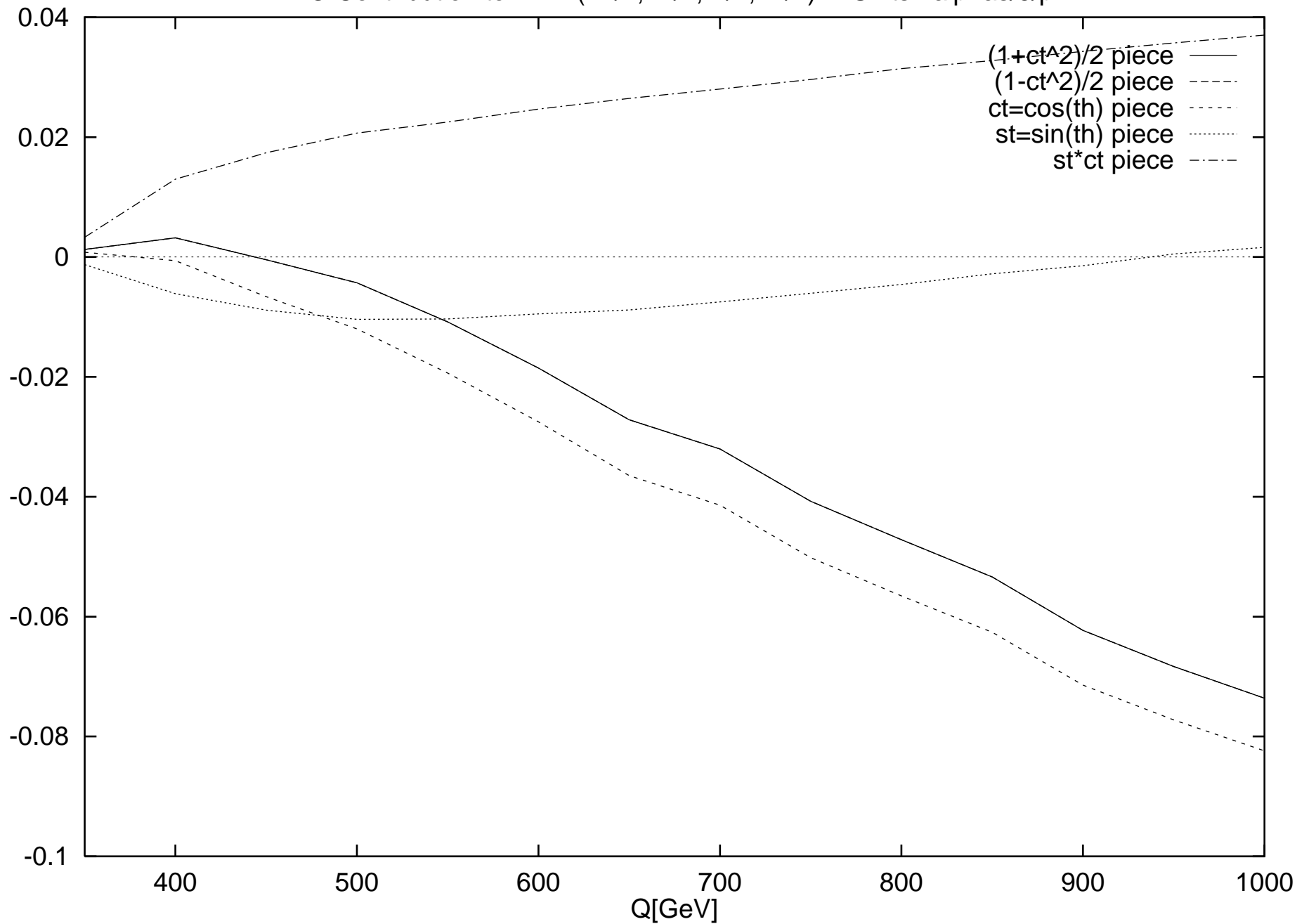
HO Contribution to R-VV(+1/2,+1/2,-1/2,+1/2) in Units $2\alpha/3\pi$



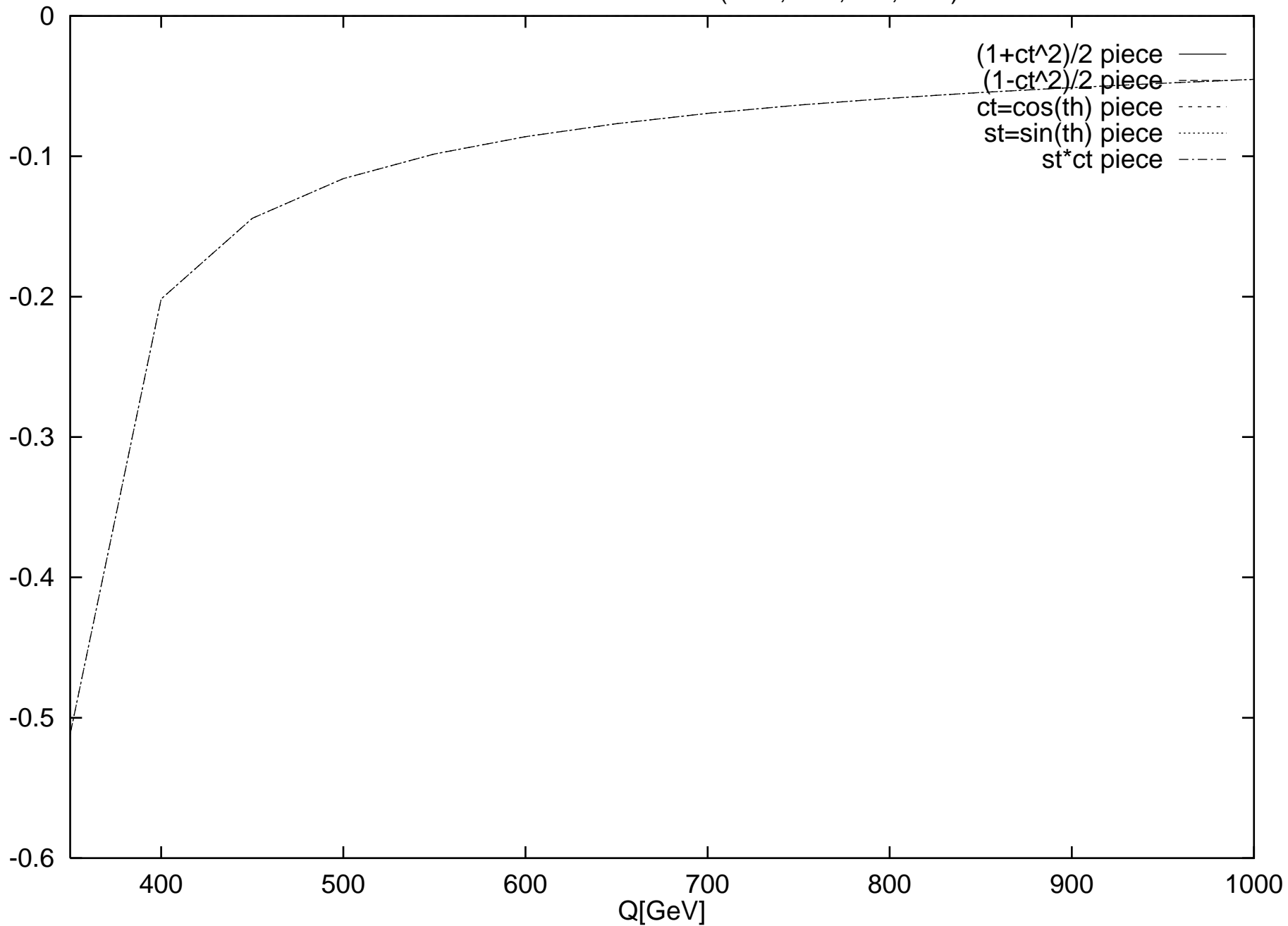
LO Contribution to R-AA(+1/2,+1/2,-1/2,+1/2)



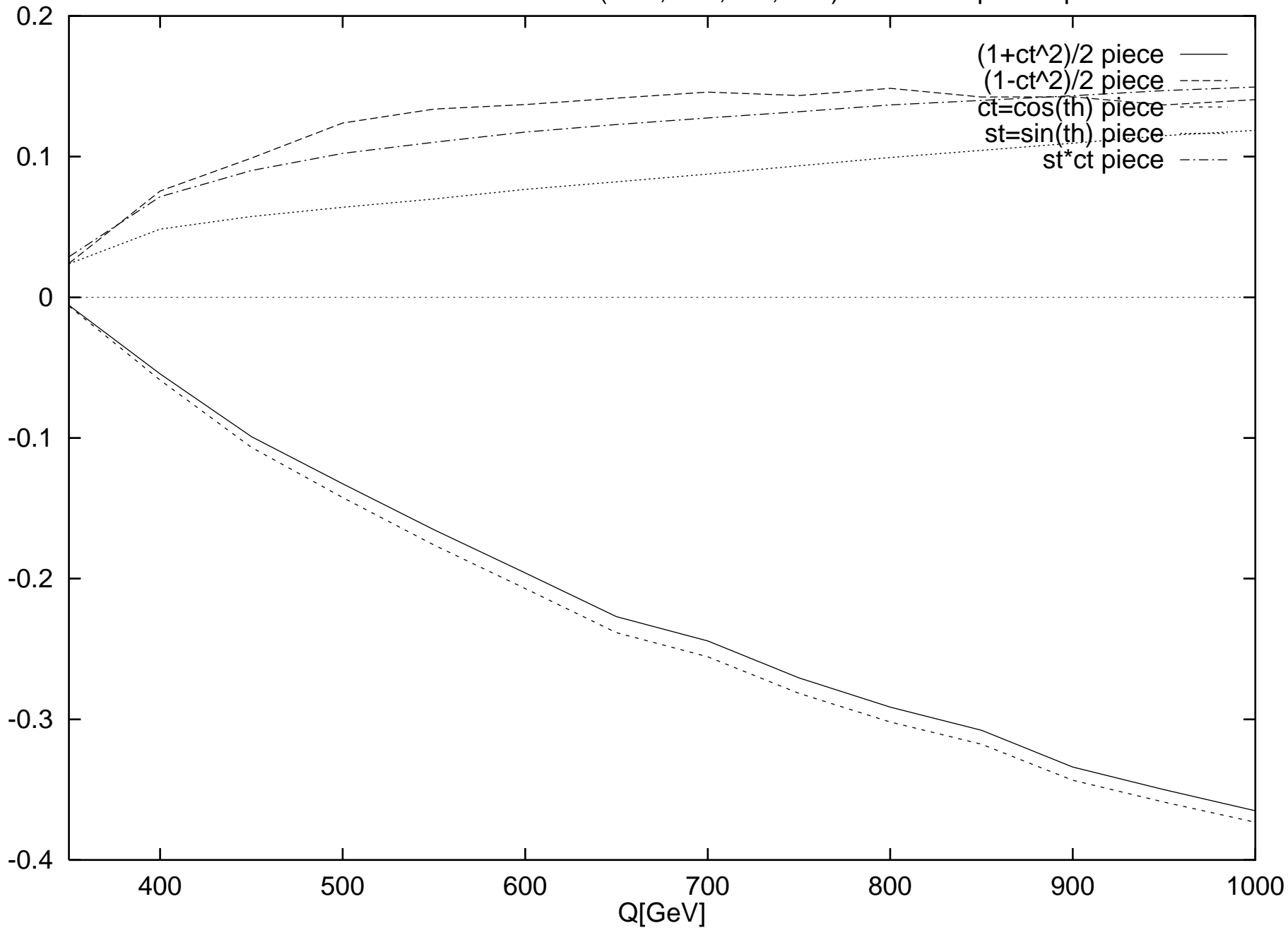
HO Contribution to R-AA(+1/2,+1/2,-1/2,+1/2) in Units $2\alpha_s/3\pi$



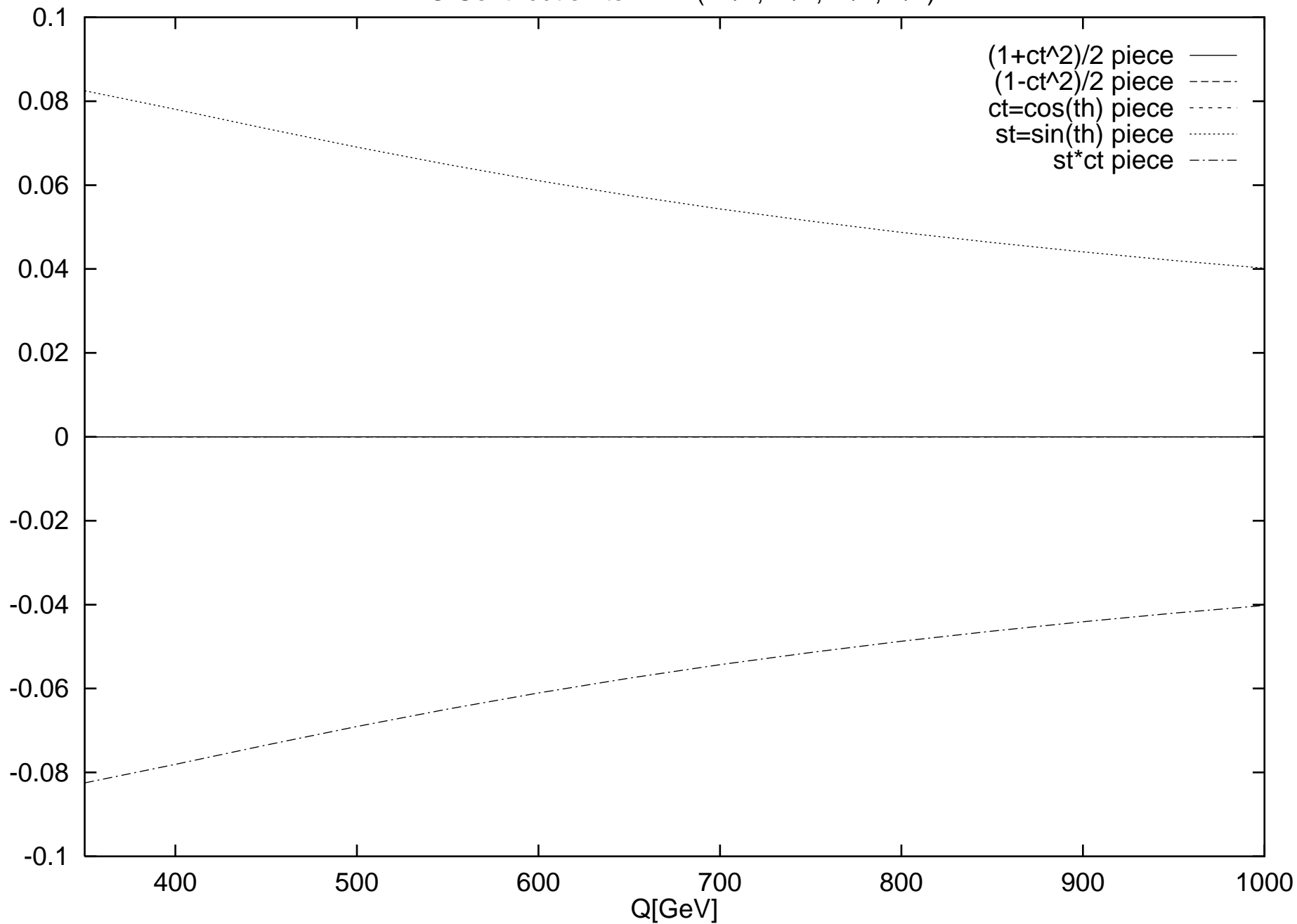
LO Contribution to R-VAAVAA(+1/2,+1/2,-1/2,+1/2)



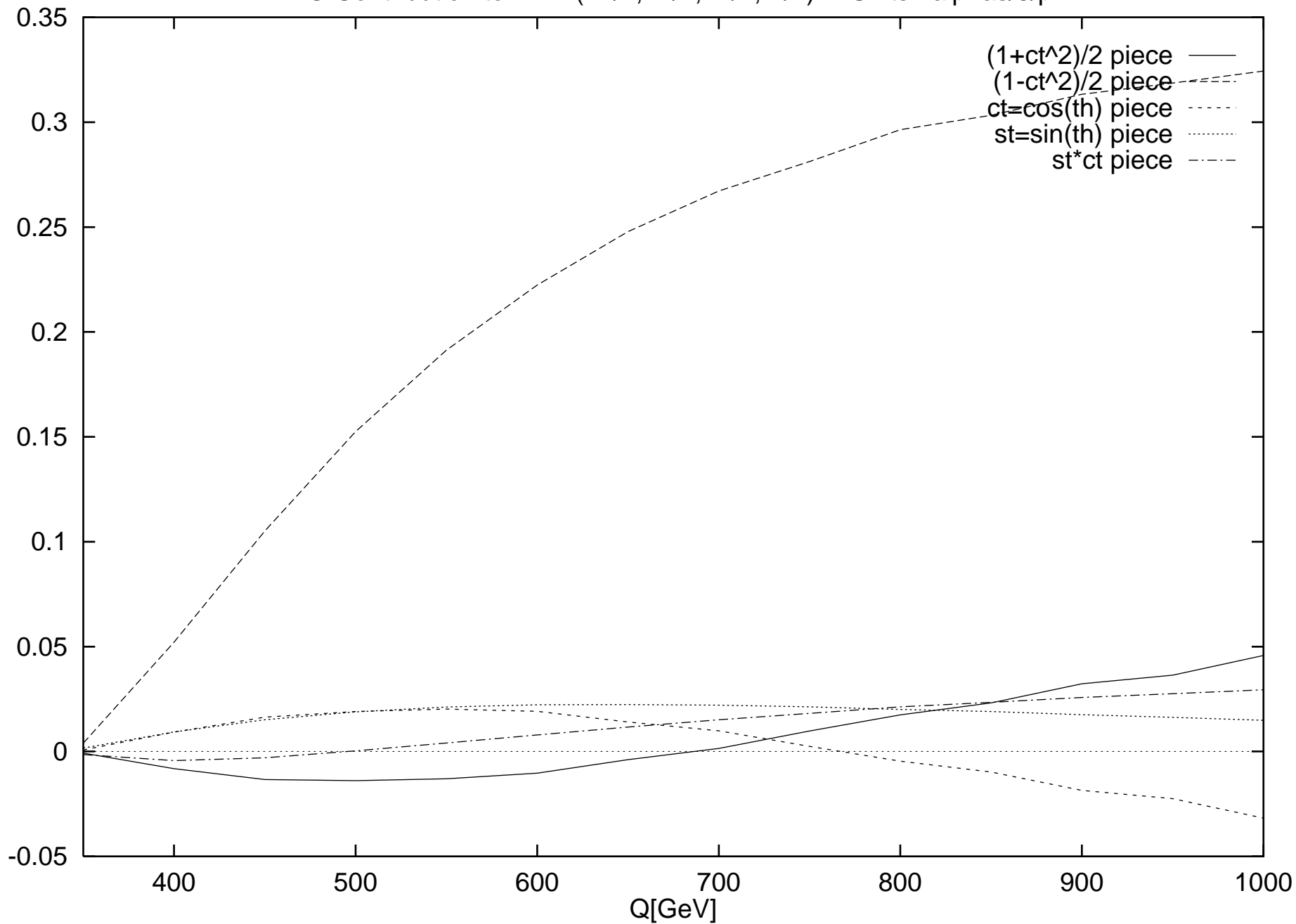
HO Contribution to R-VAAVAA(+1/2,+1/2,-1/2,+1/2) in Units $2\alpha/3\pi$



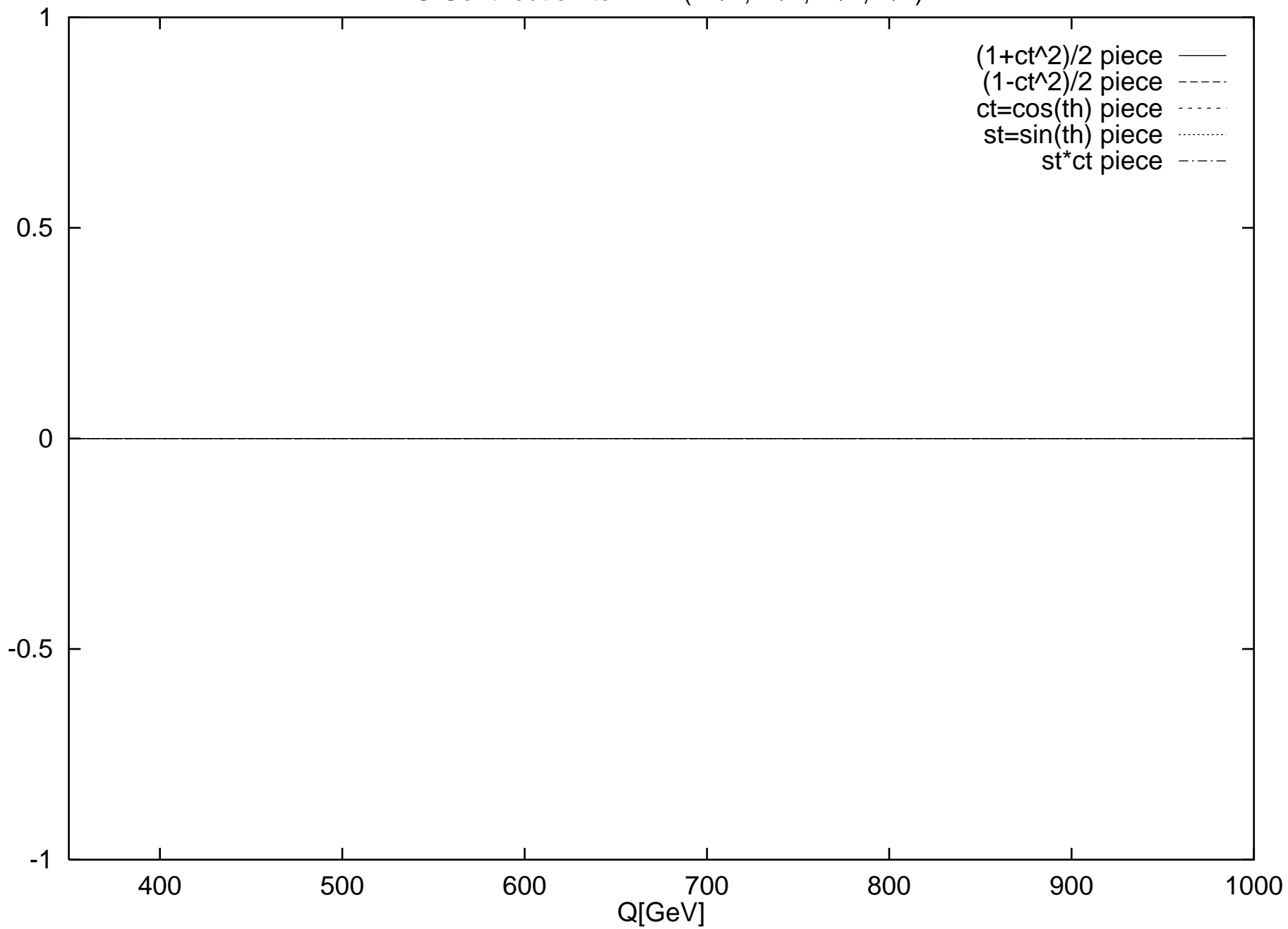
LO Contribution to R-VV(+1/2,+1/2,+1/2,-1/2)



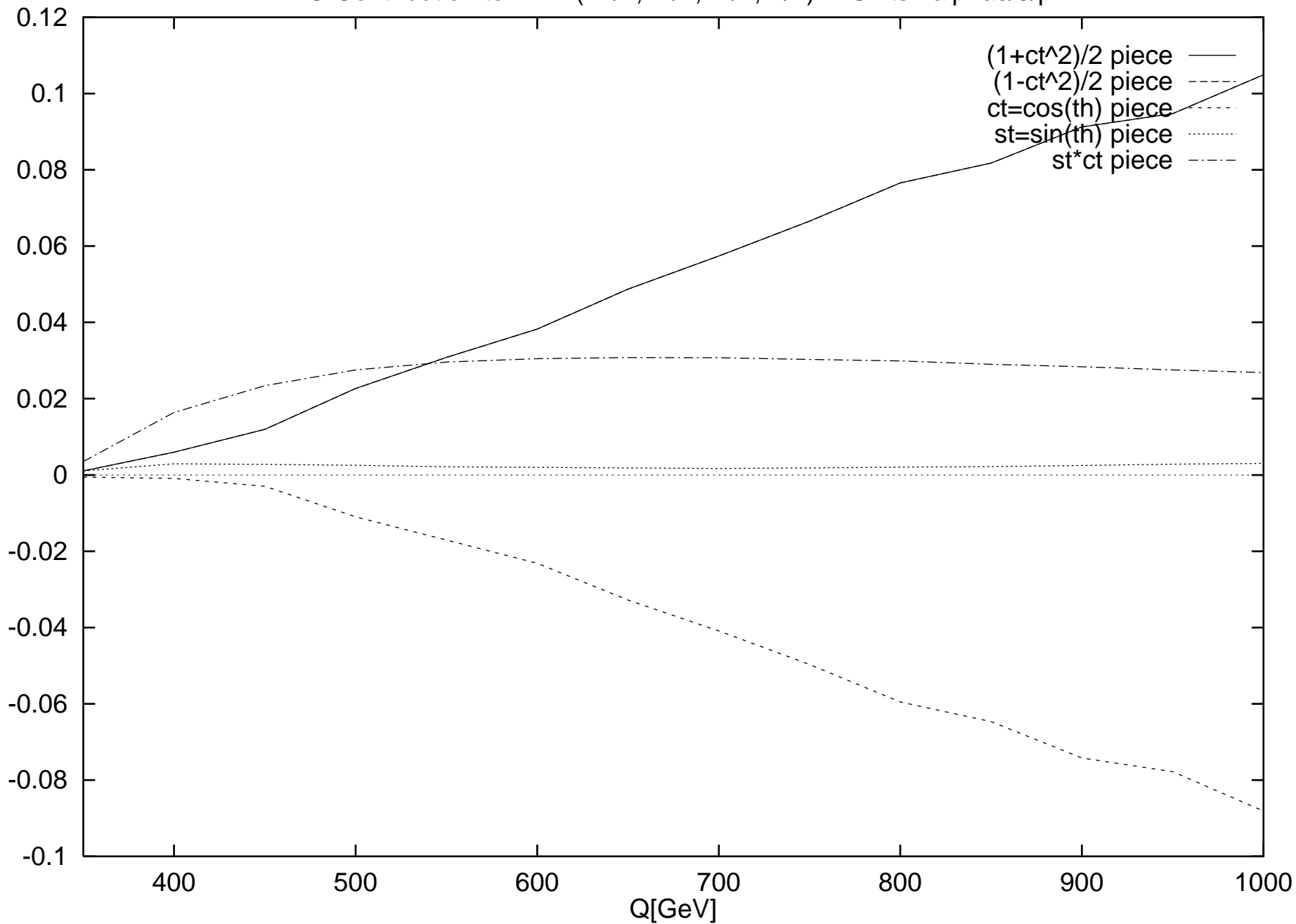
HO Contribution to R-VV(+1/2,+1/2,+1/2,-1/2) in Units $2\alpha/3\pi$



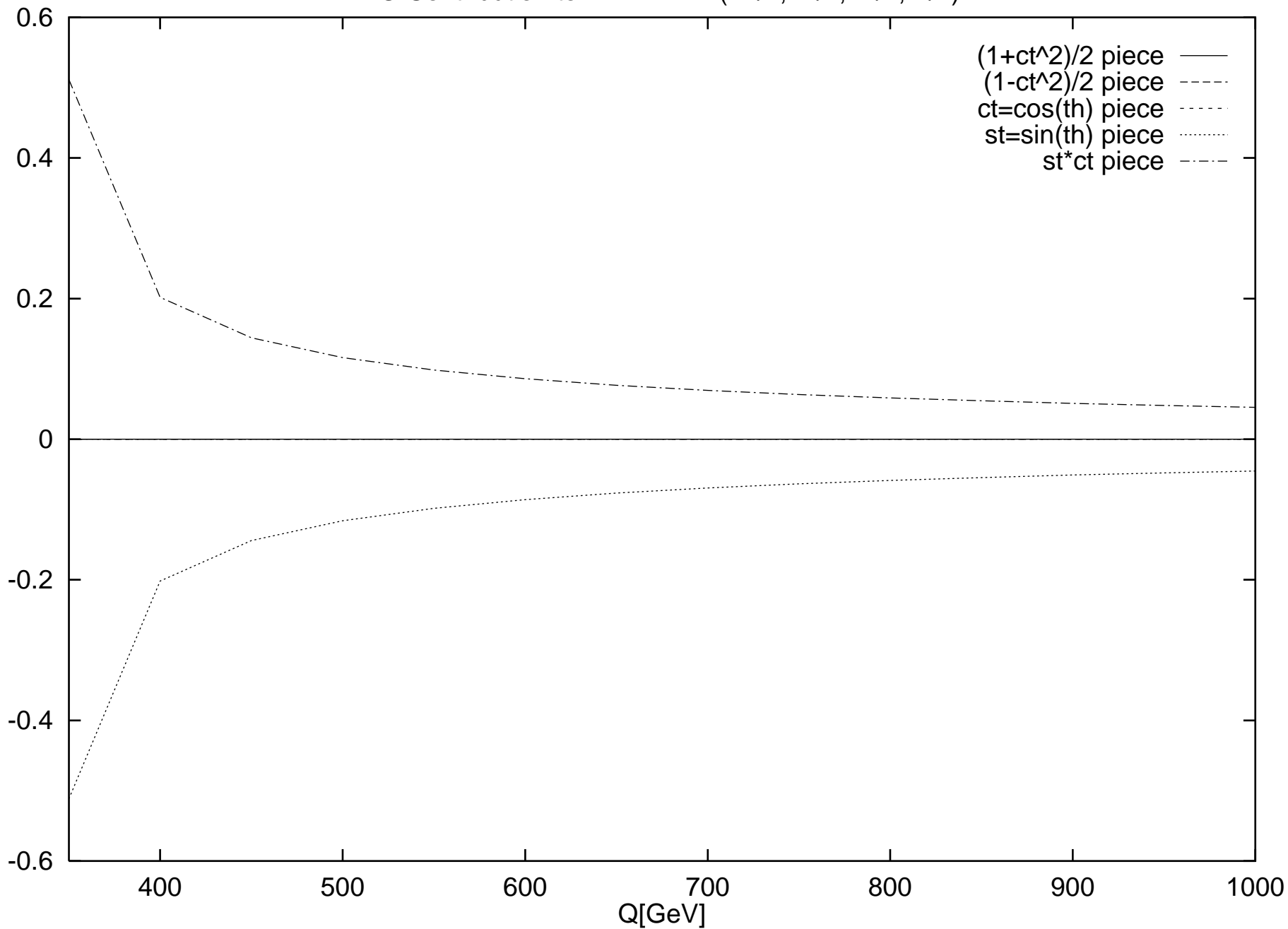
LO Contribution to R-AA(+1/2,+1/2,+1/2,-1/2)



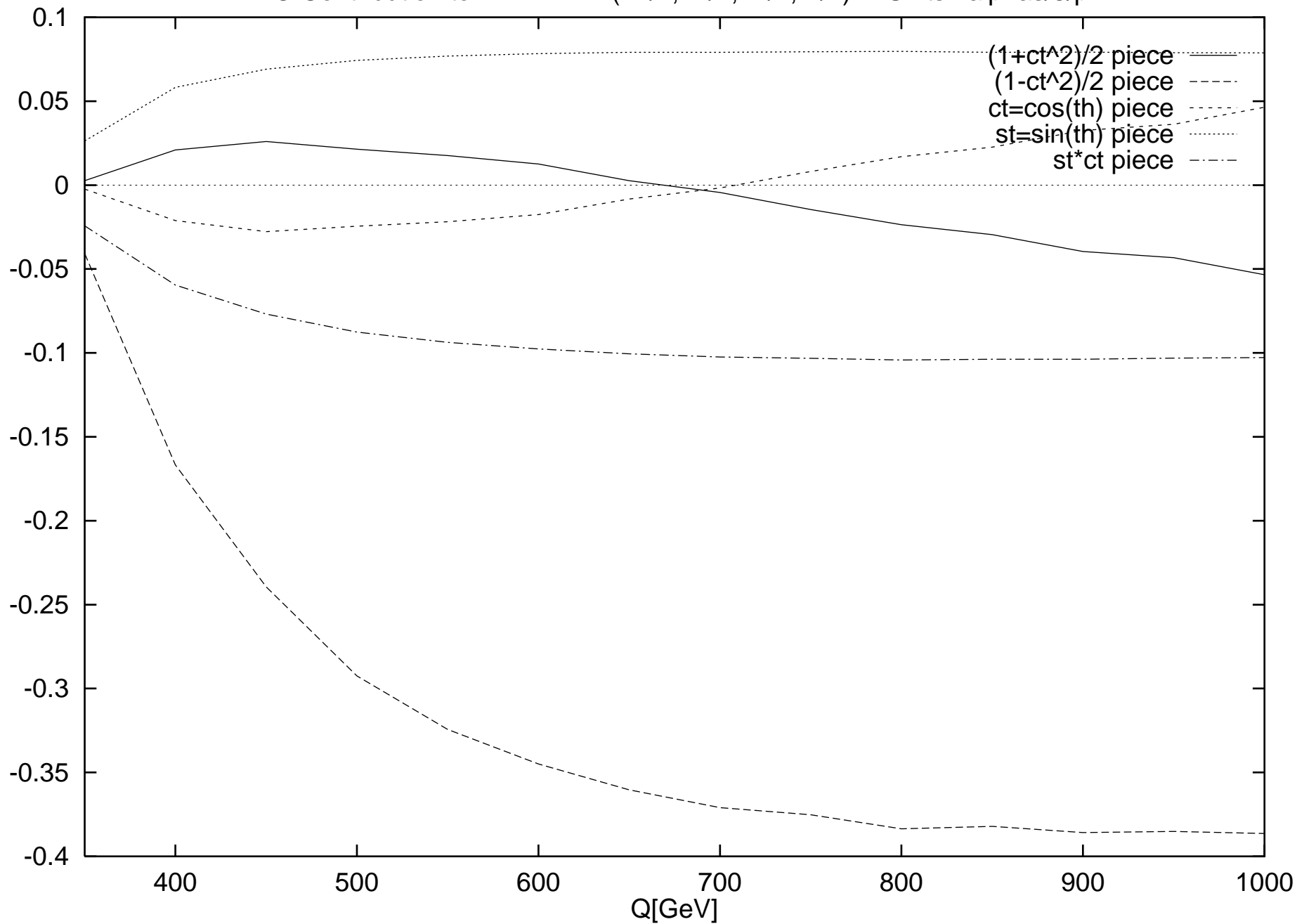
HO Contribution to R-AA(+1/2,+1/2,+1/2,-1/2) in Units $2\alpha_s/3\pi$



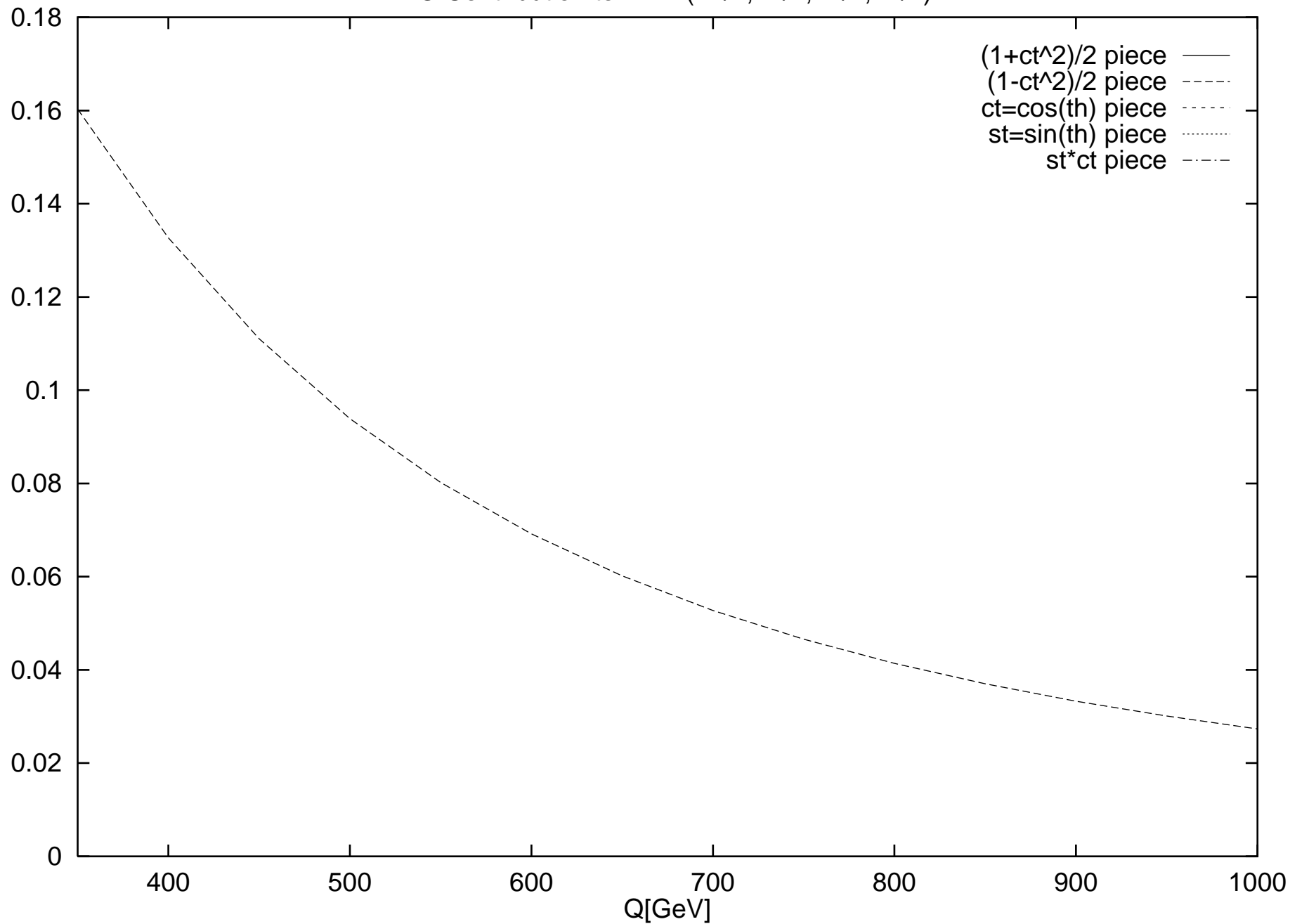
LO Contribution to R-VAAVAA(+1/2,+1/2,+1/2,-1/2)



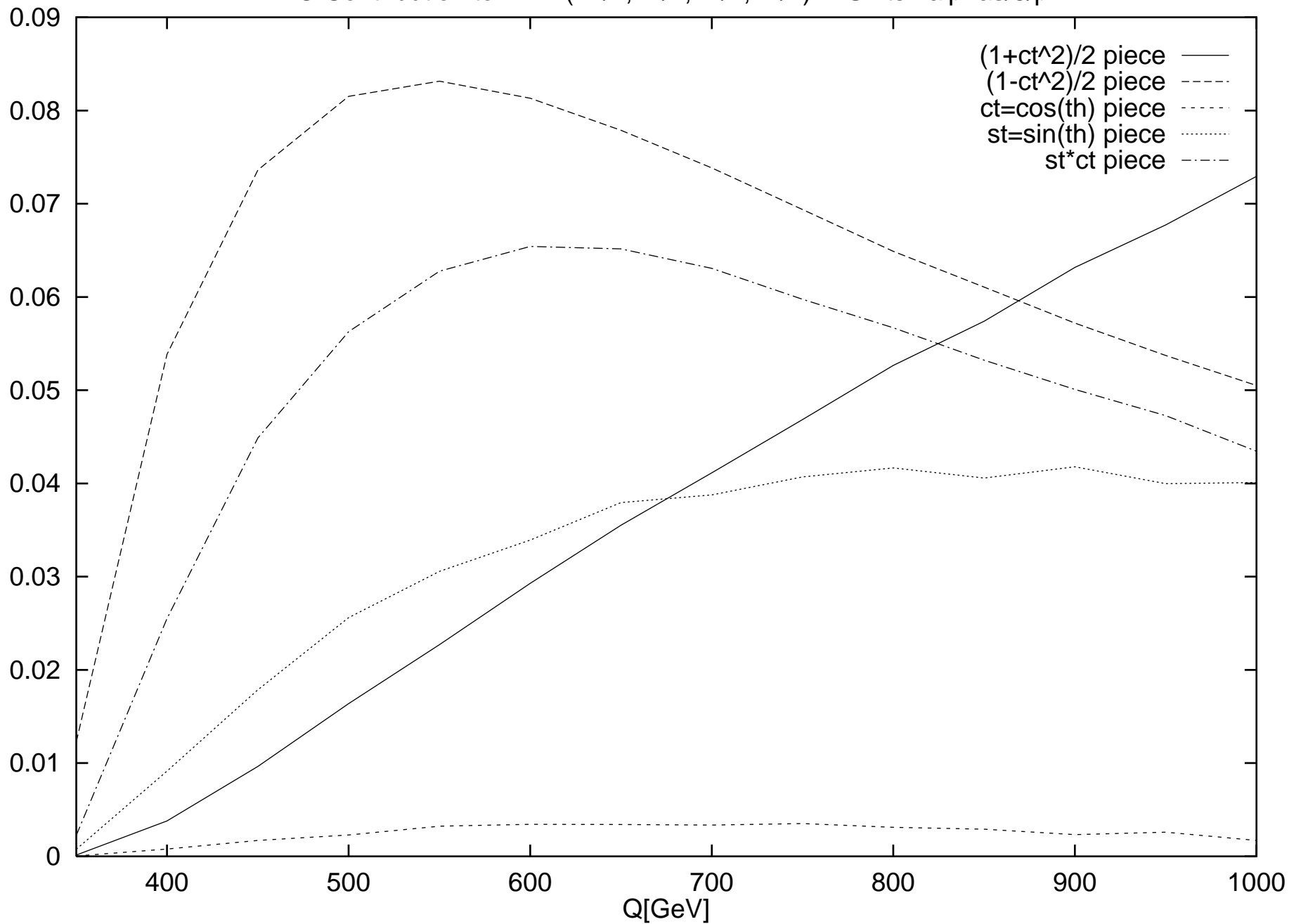
HO Contribution to R-VAAVAA(+1/2,+1/2,+1/2,-1/2) in Units $2\alpha/3\pi$



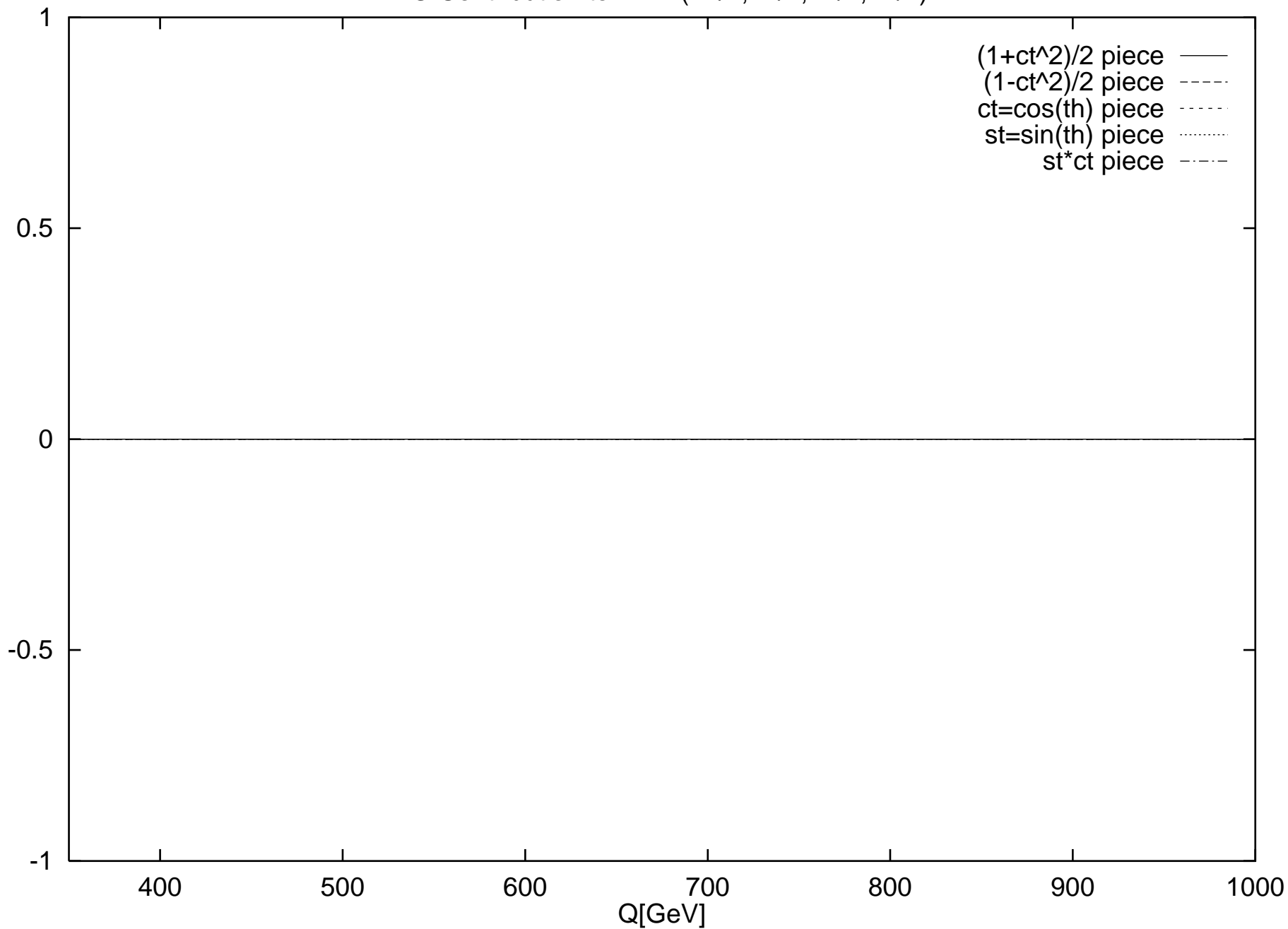
LO Contribution to R-VV(+1/2,+1/2,+1/2,+1/2)



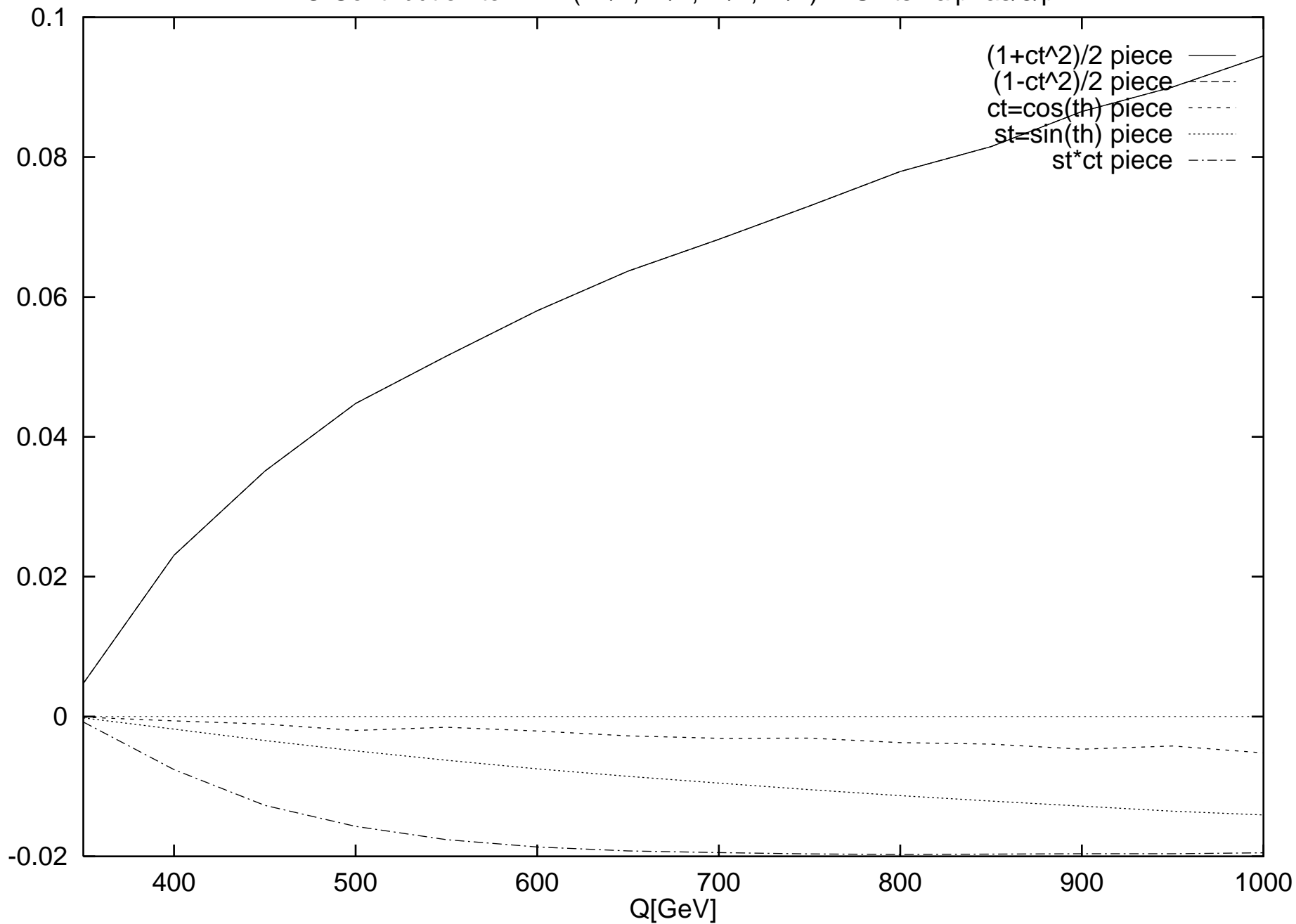
HO Contribution to R-VV(+1/2,+1/2,+1/2,+1/2) in Units $2\alpha/3\pi$

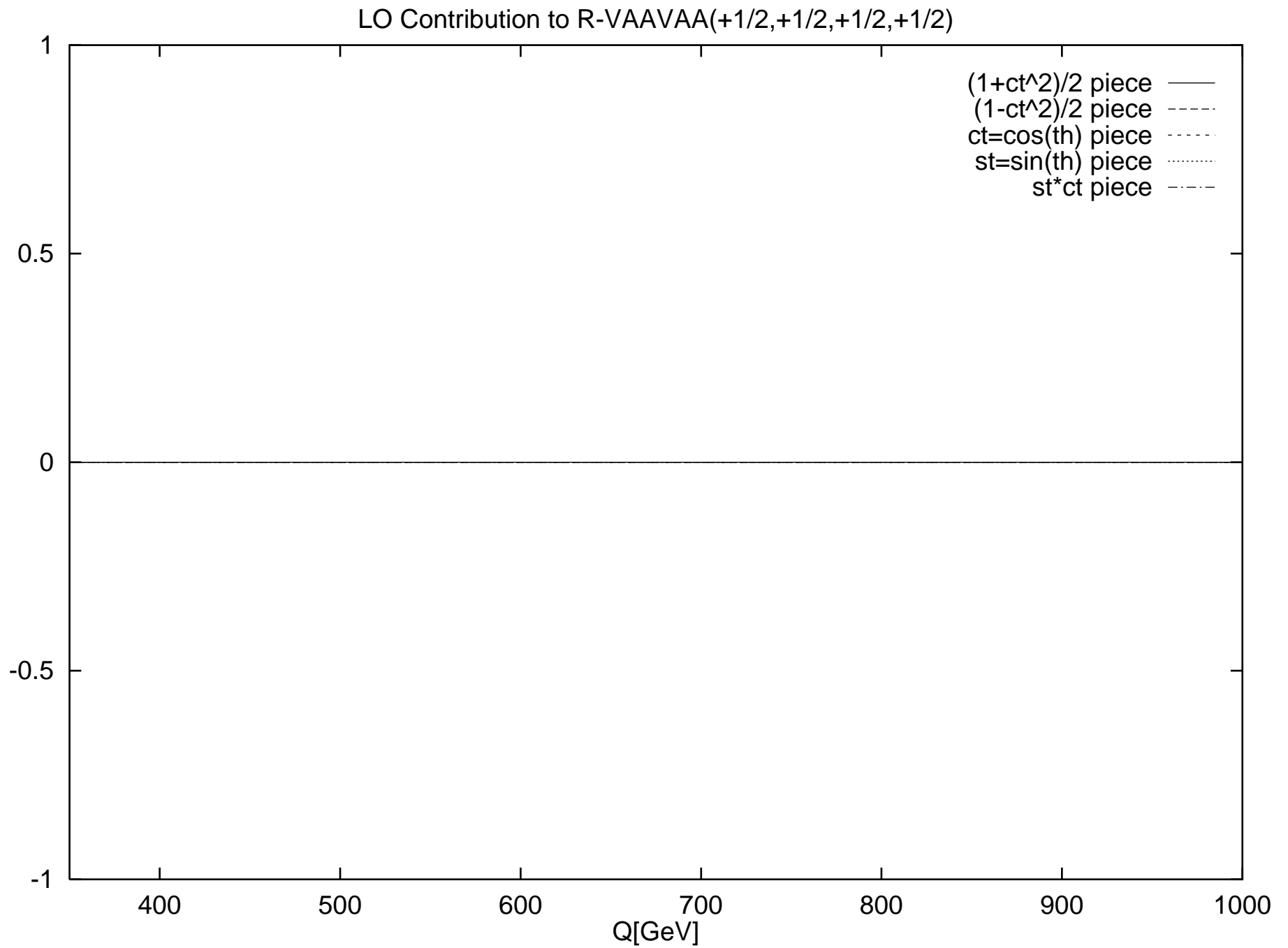


LO Contribution to R-AA(+1/2,+1/2,+1/2,+1/2)

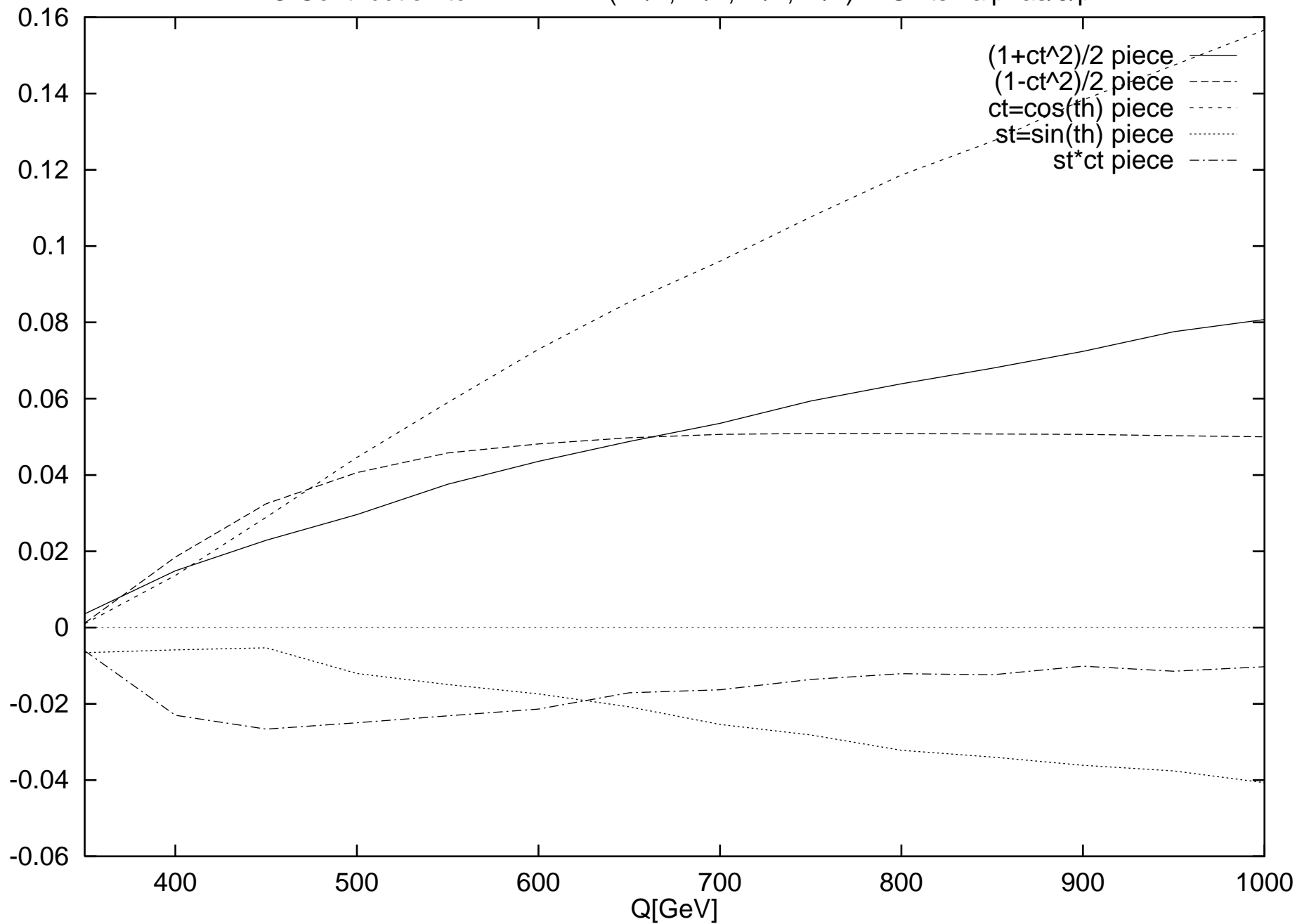


HO Contribution to R-AA(+1/2,+1/2,+1/2,+1/2) in Units $2\alpha_s/3\pi$

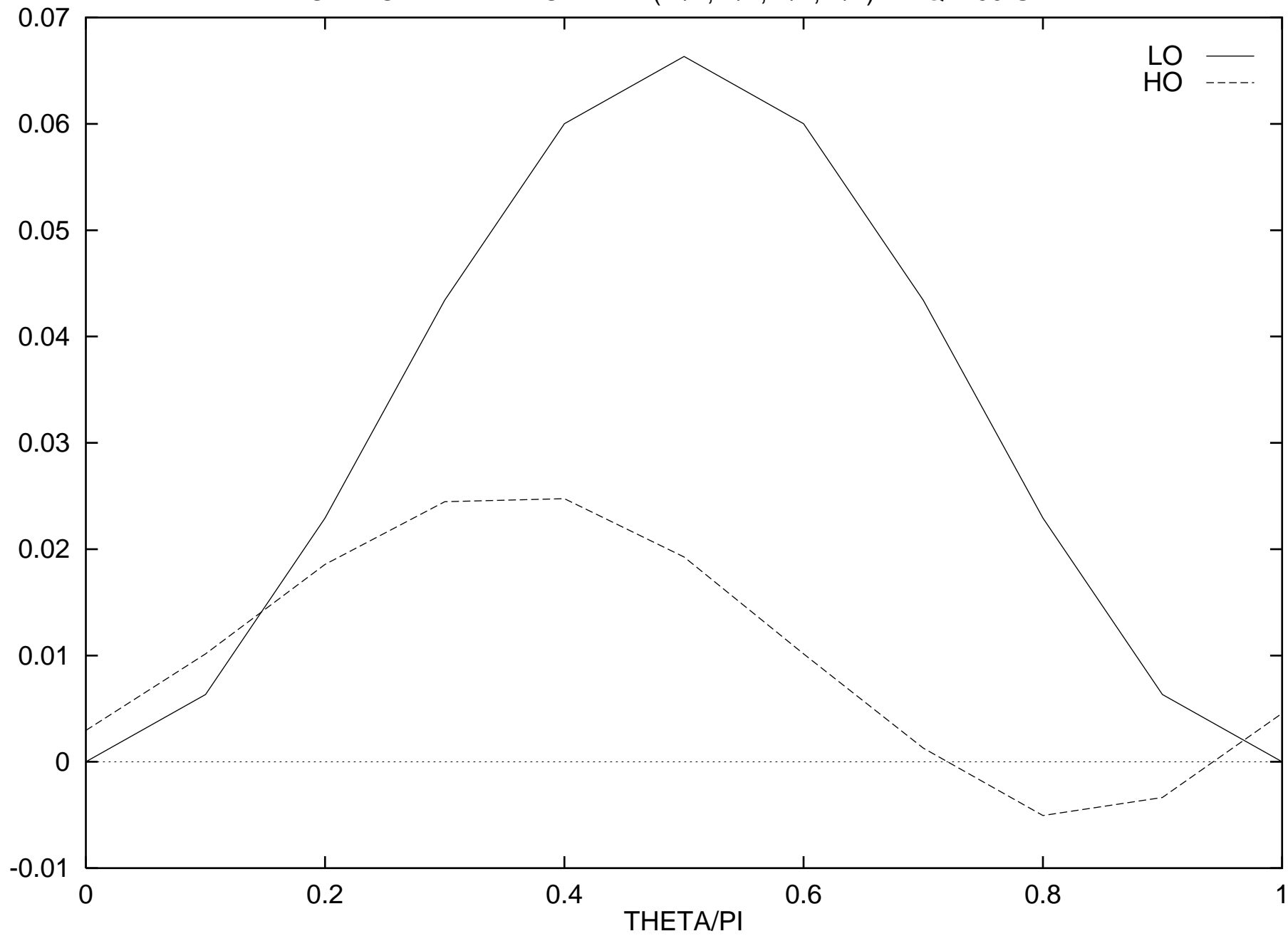




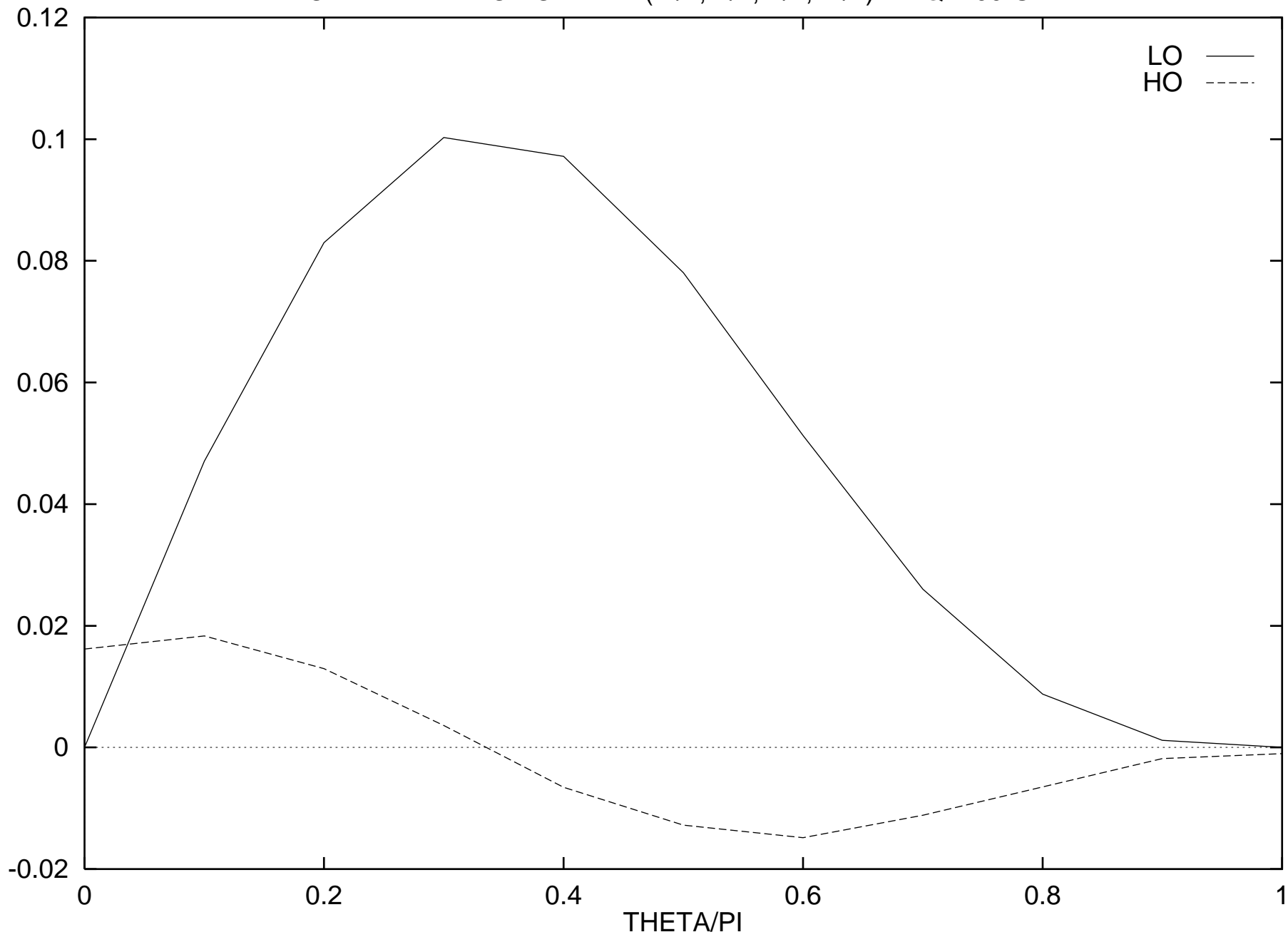
HO Contribution to R-VAAVAA(+1/2,+1/2,+1/2,+1/2) in Units $2\alpha/3\pi$



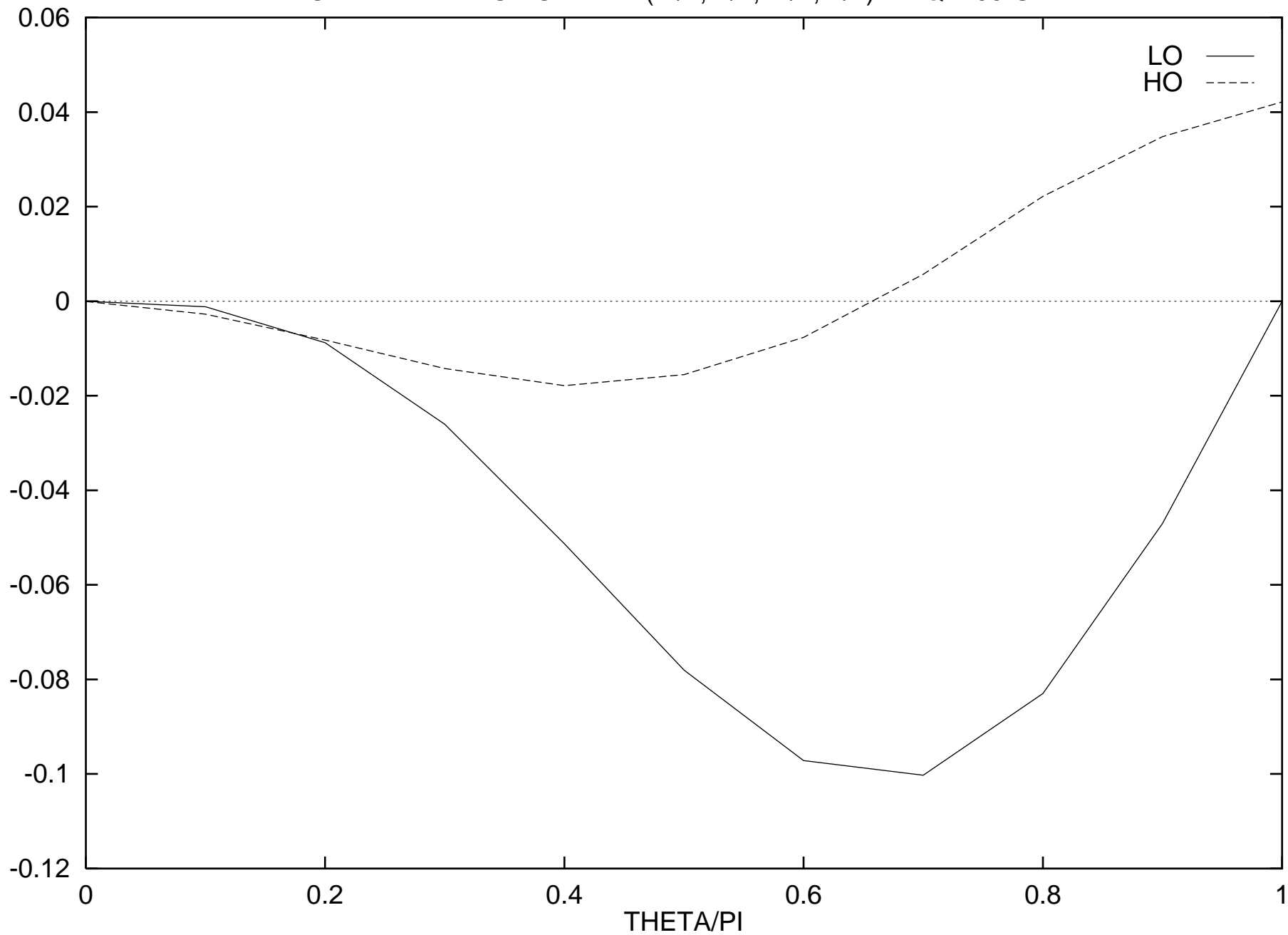
LO + HO * ALPHA FOR R-VV(-1/2,-1/2,-1/2,-1/2) AT Q=400 GEV



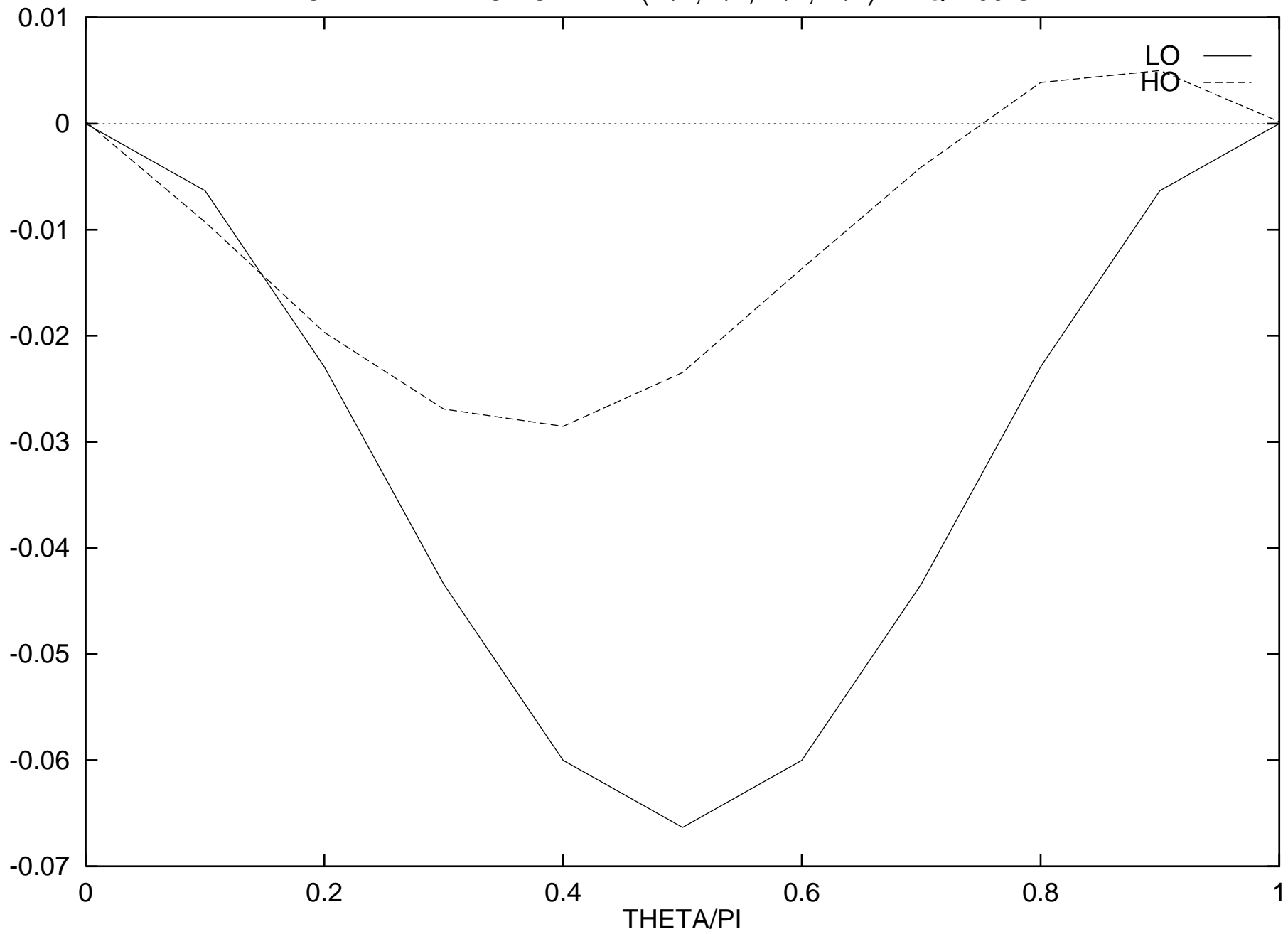
LO + ALPHA * HO FOR R-VV(-1/2,-1/2,-1/2,+1/2) AT Q=400 GEV



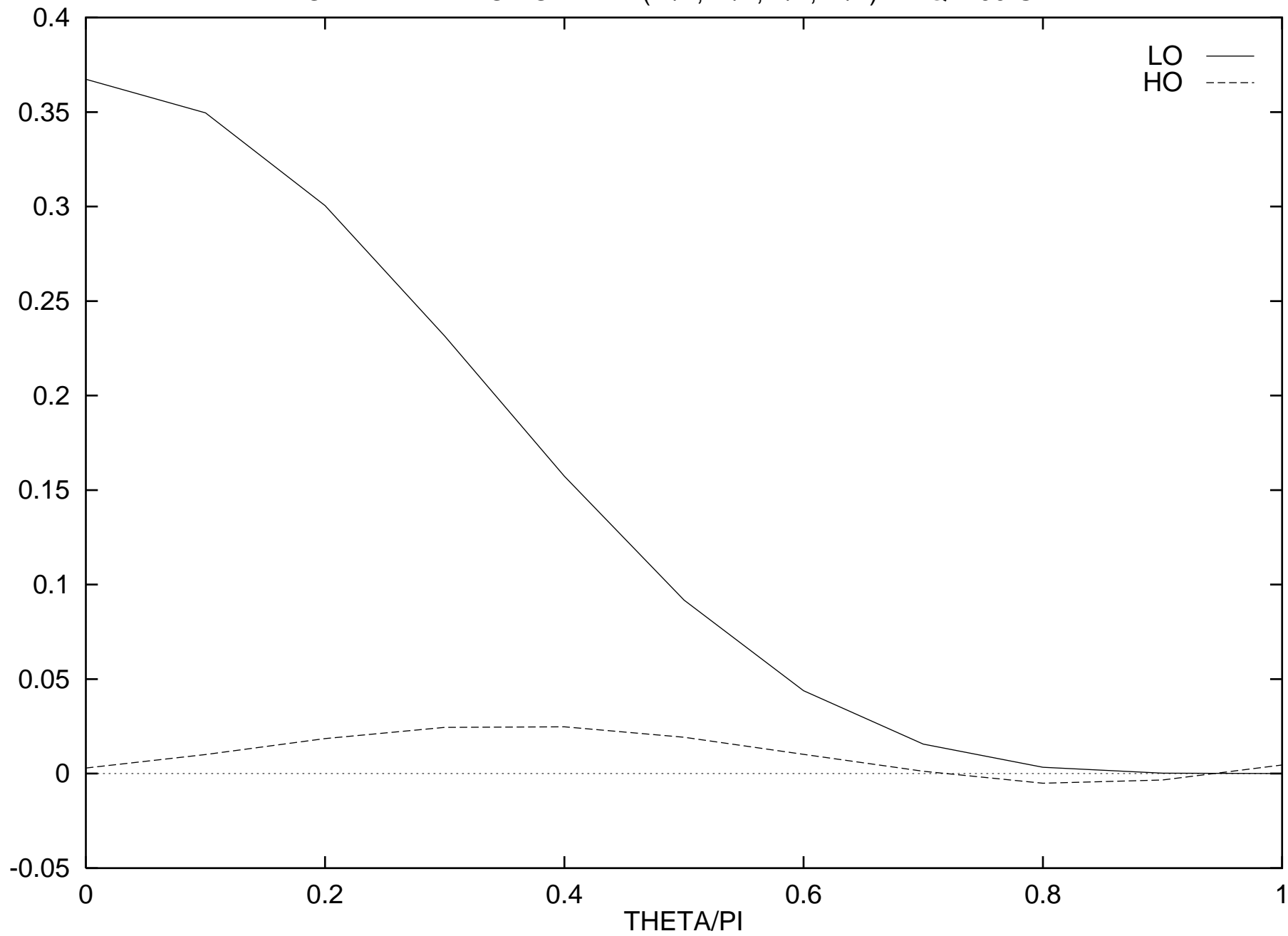
LO + ALPHA * HO FOR R-VV(-1/2,-1/2,+1/2,-1/2) AT Q=400 GEV



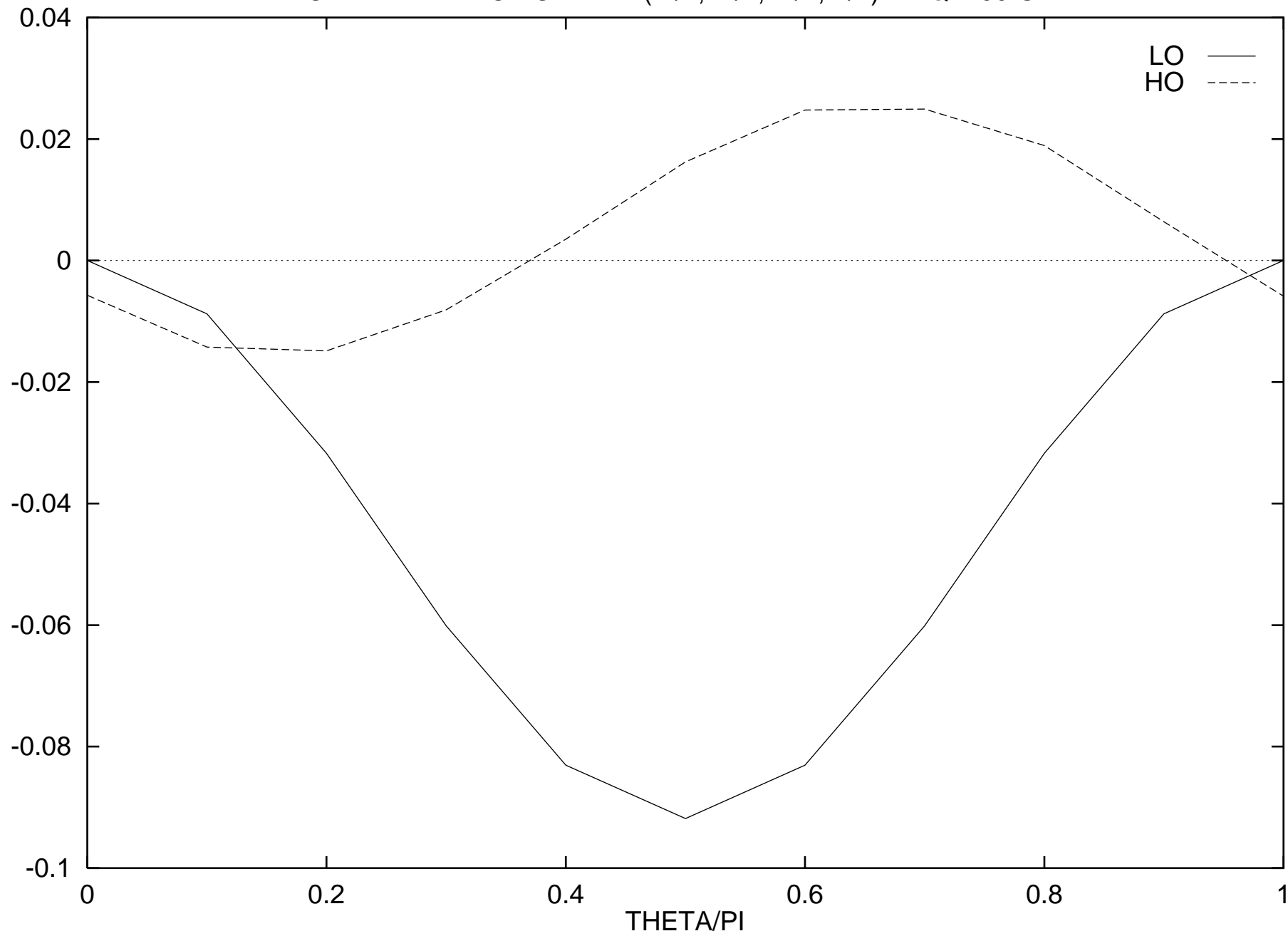
LO + ALPHA * HO FOR R-VV(-1/2,-1/2,+1/2,+1/2) AT Q=400 GEV



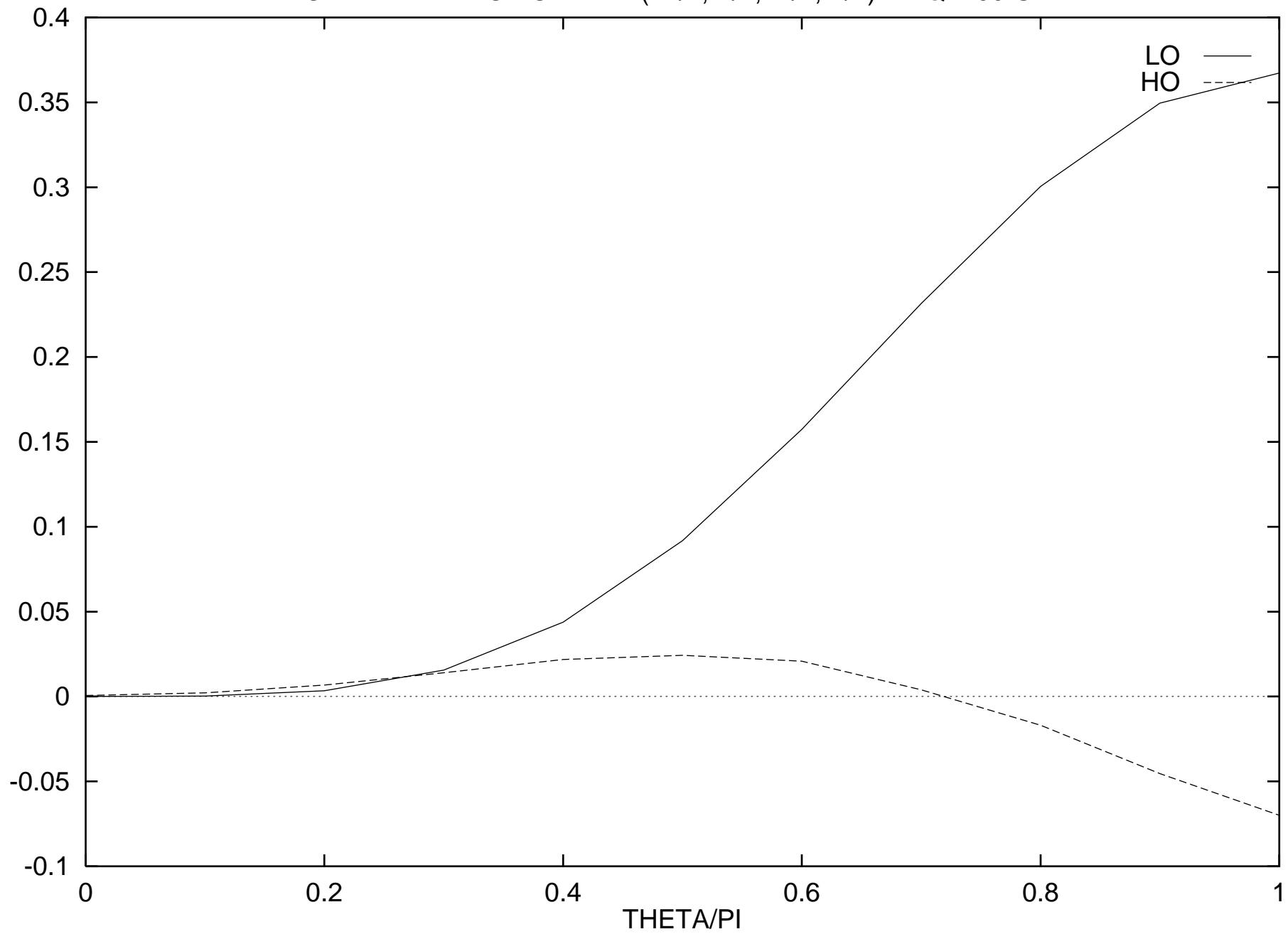
LO + ALPHA * HO FOR R-VV(-1/2,+1/2,-1/2,+1/2) AT Q=400 GEV



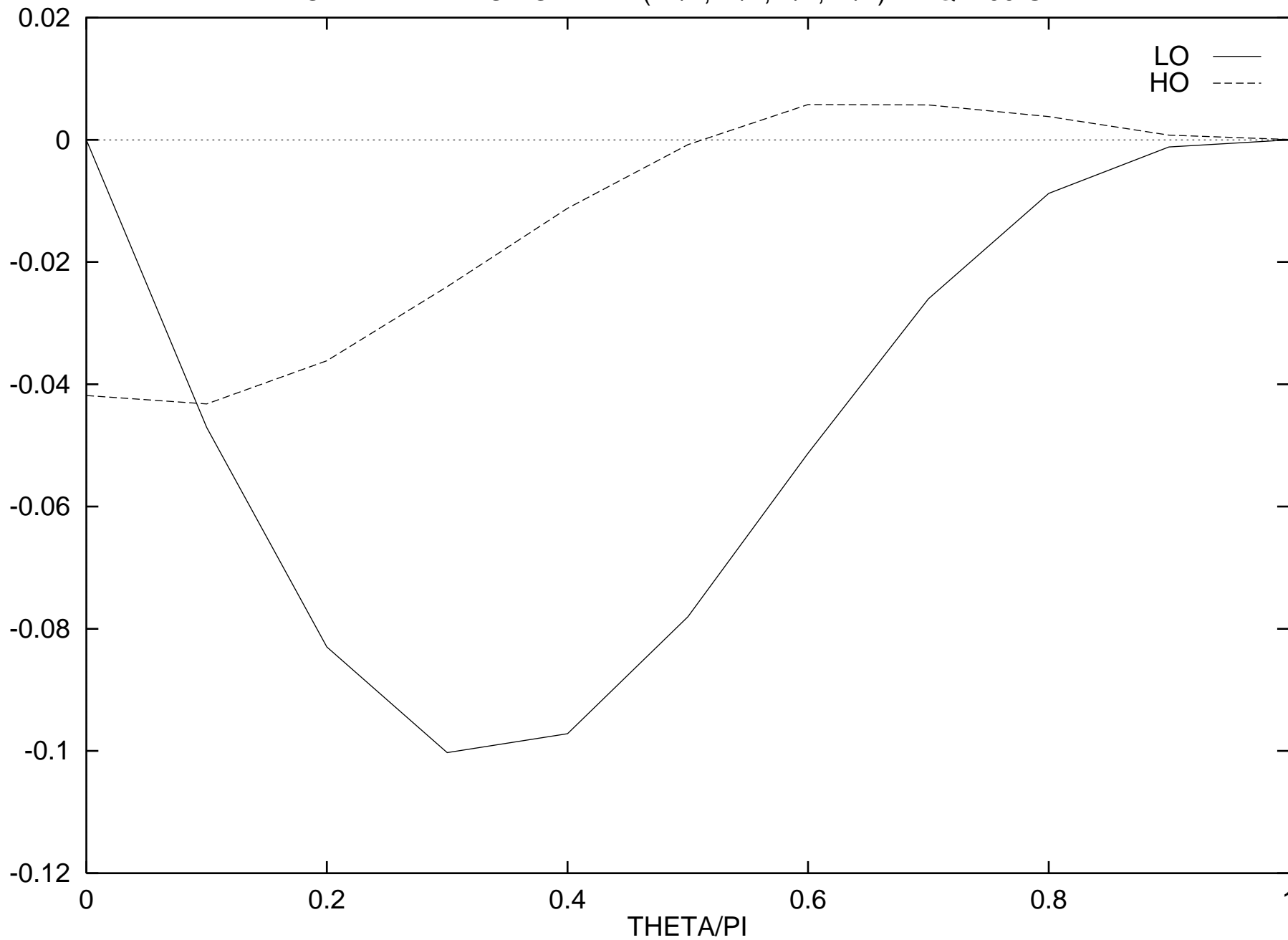
LO + ALPHA * HO FOR R-VV(-1/2,+1/2,+1/2,-1/2) AT Q=400 GEV



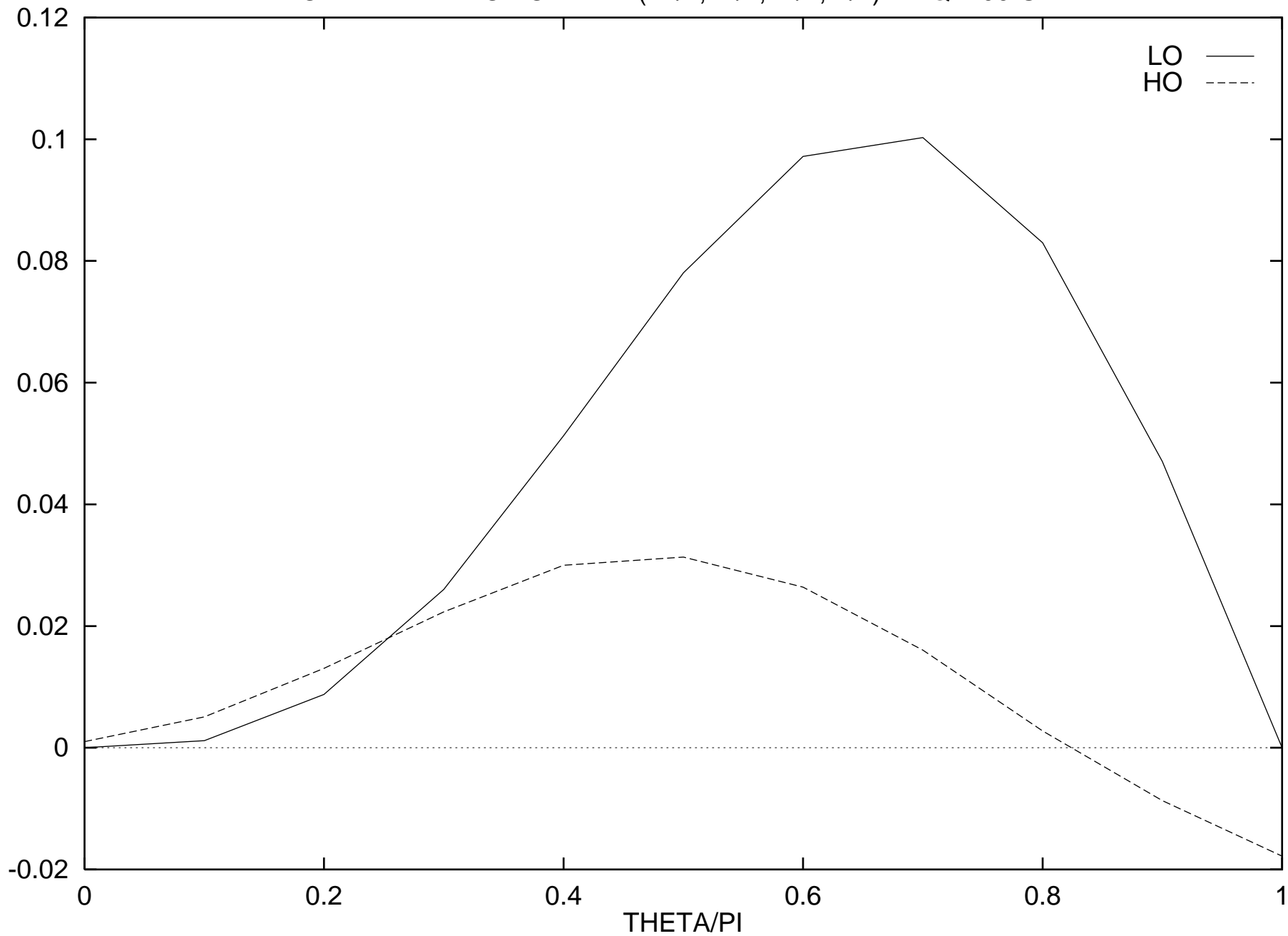
LO + ALPHA * HO FOR R-VV(+1/2,-1/2,+1/2,-1/2) AT Q=400 GEV



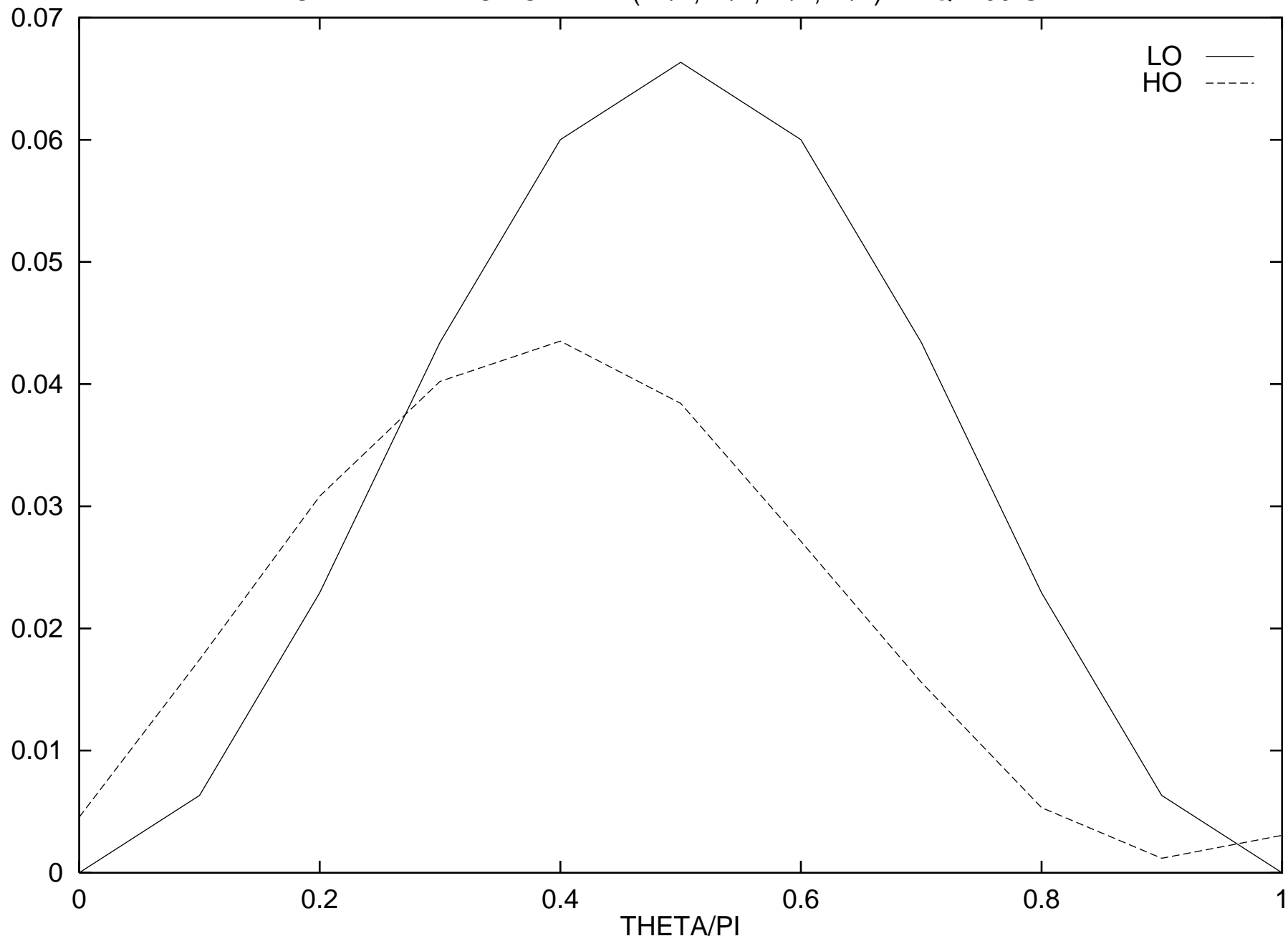
LO + ALPHA * HO FOR R-VV(+1/2,+1/2,-1/2,+1/2) AT Q=400 GEV



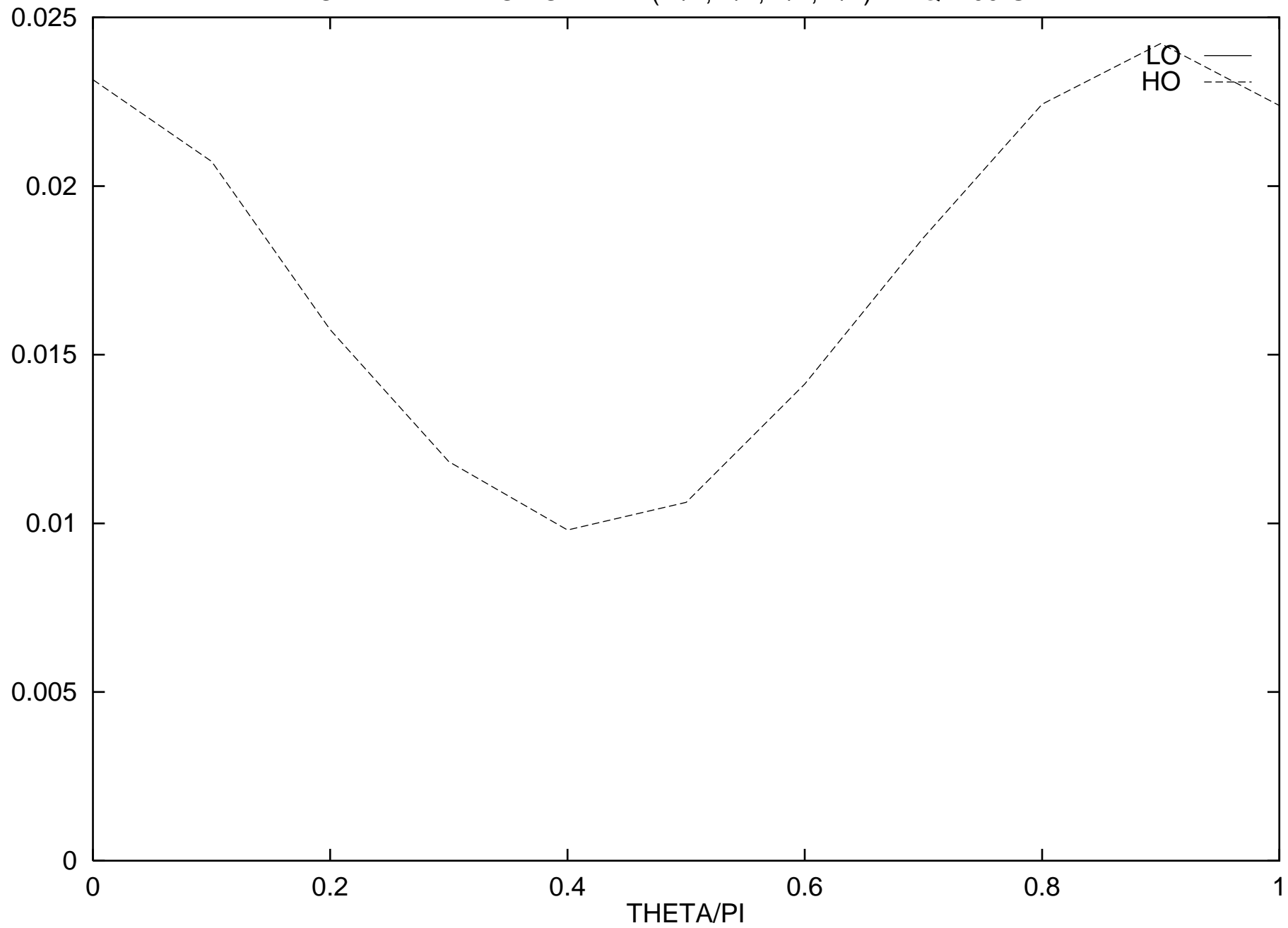
LO + ALPHA * HO FOR R-VV(+1/2,+1/2,+1/2,-1/2) AT Q=400 GEV



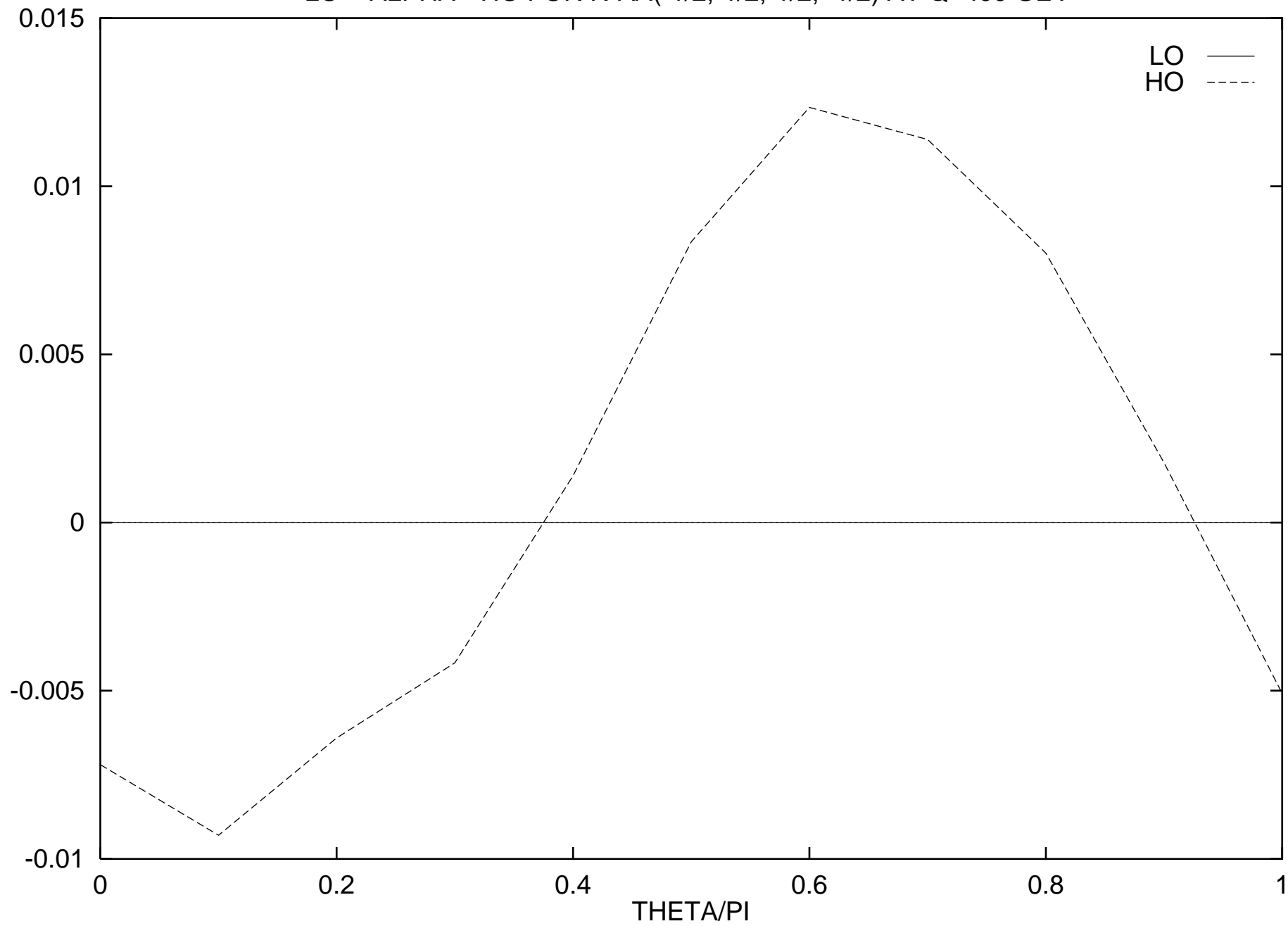
LO + ALPHA * HO FOR R-VV(+1/2,+1/2,+1/2,+1/2) AT Q=400 GEV



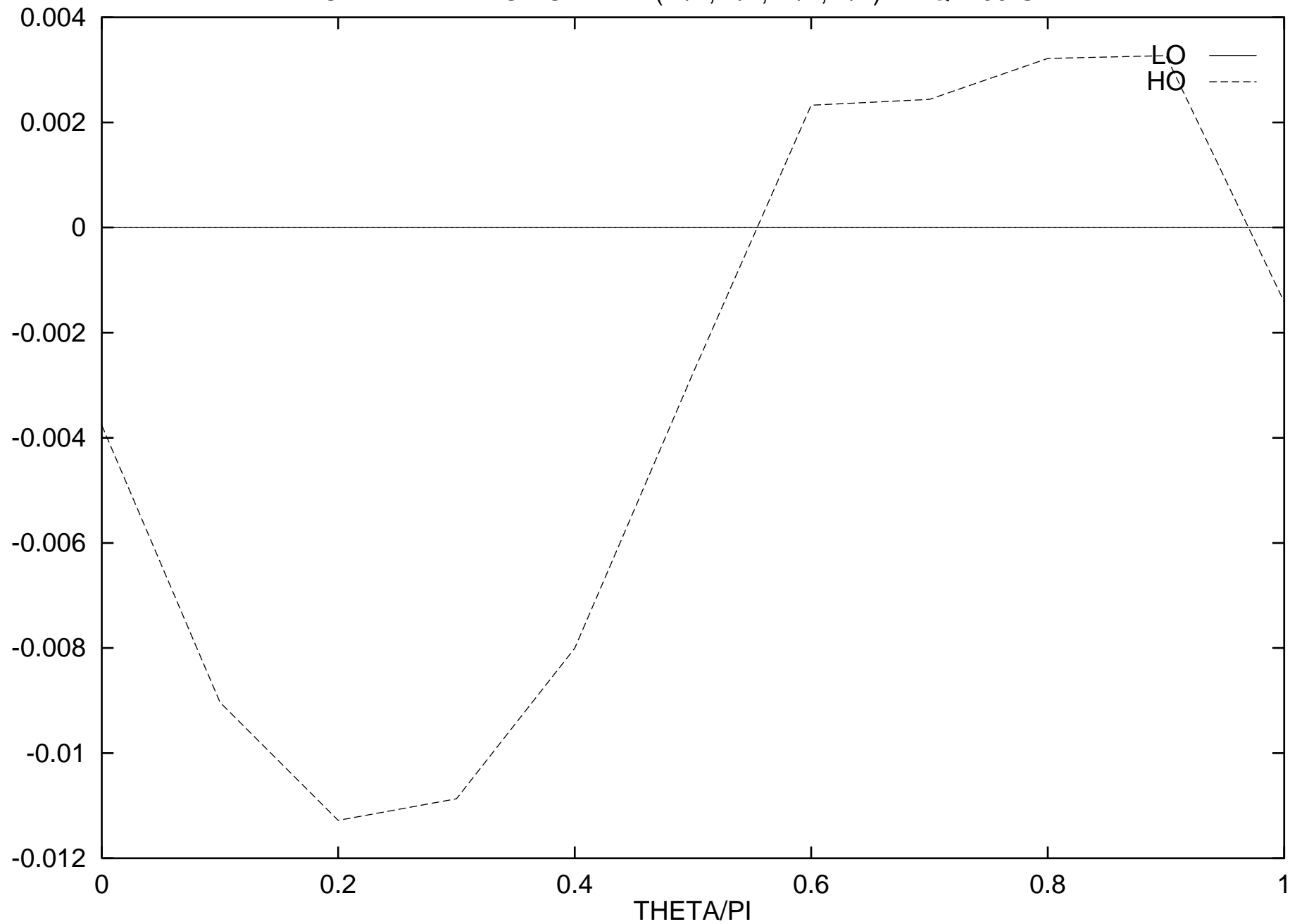
LO + ALPHA * HO FOR R-AA(-1/2,-1/2,-1/2,-1/2) AT Q=400 GEV



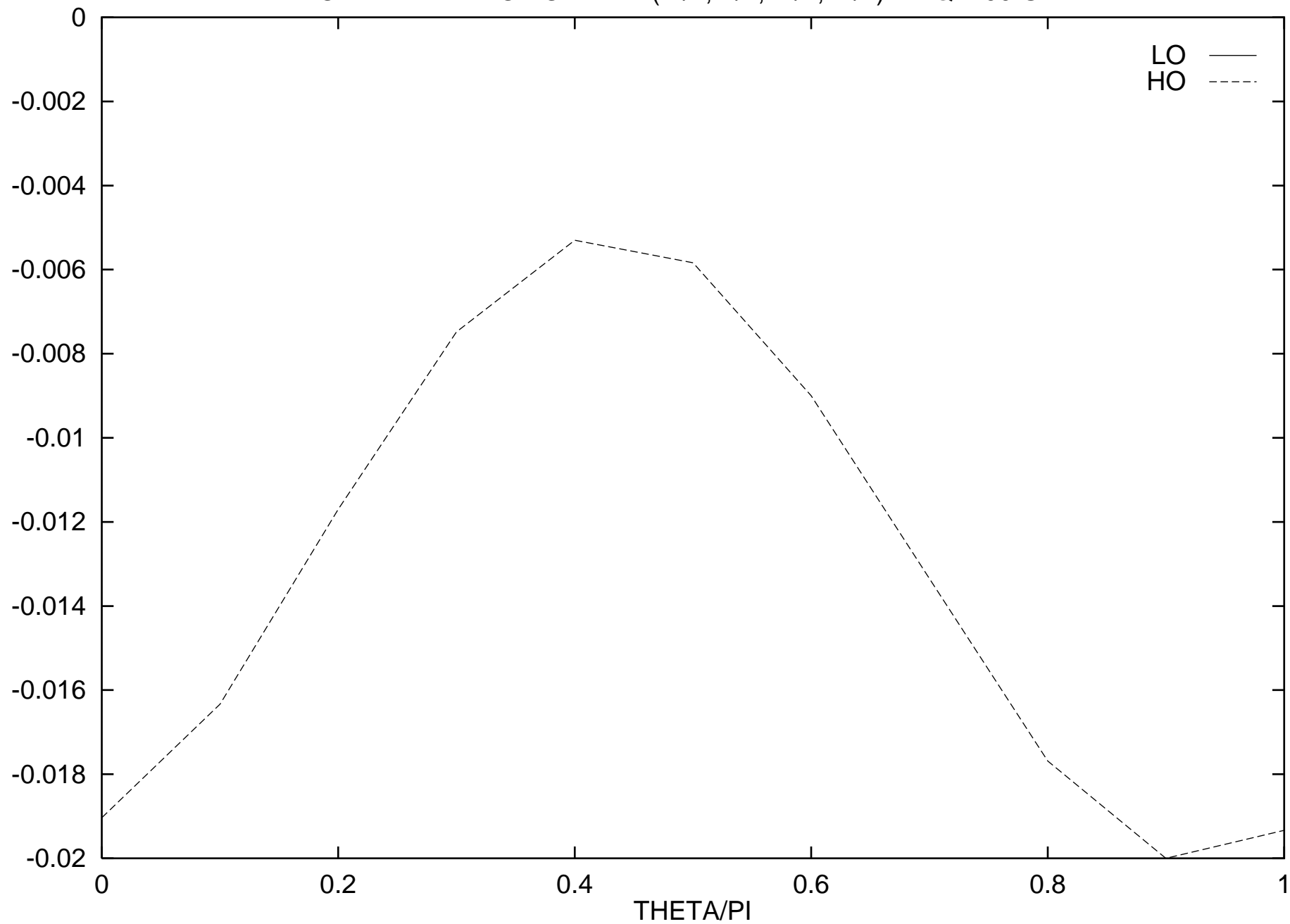
LO + ALPHA * HO FOR R-AA(-1/2,-1/2,-1/2,+1/2) AT Q=400 GEV



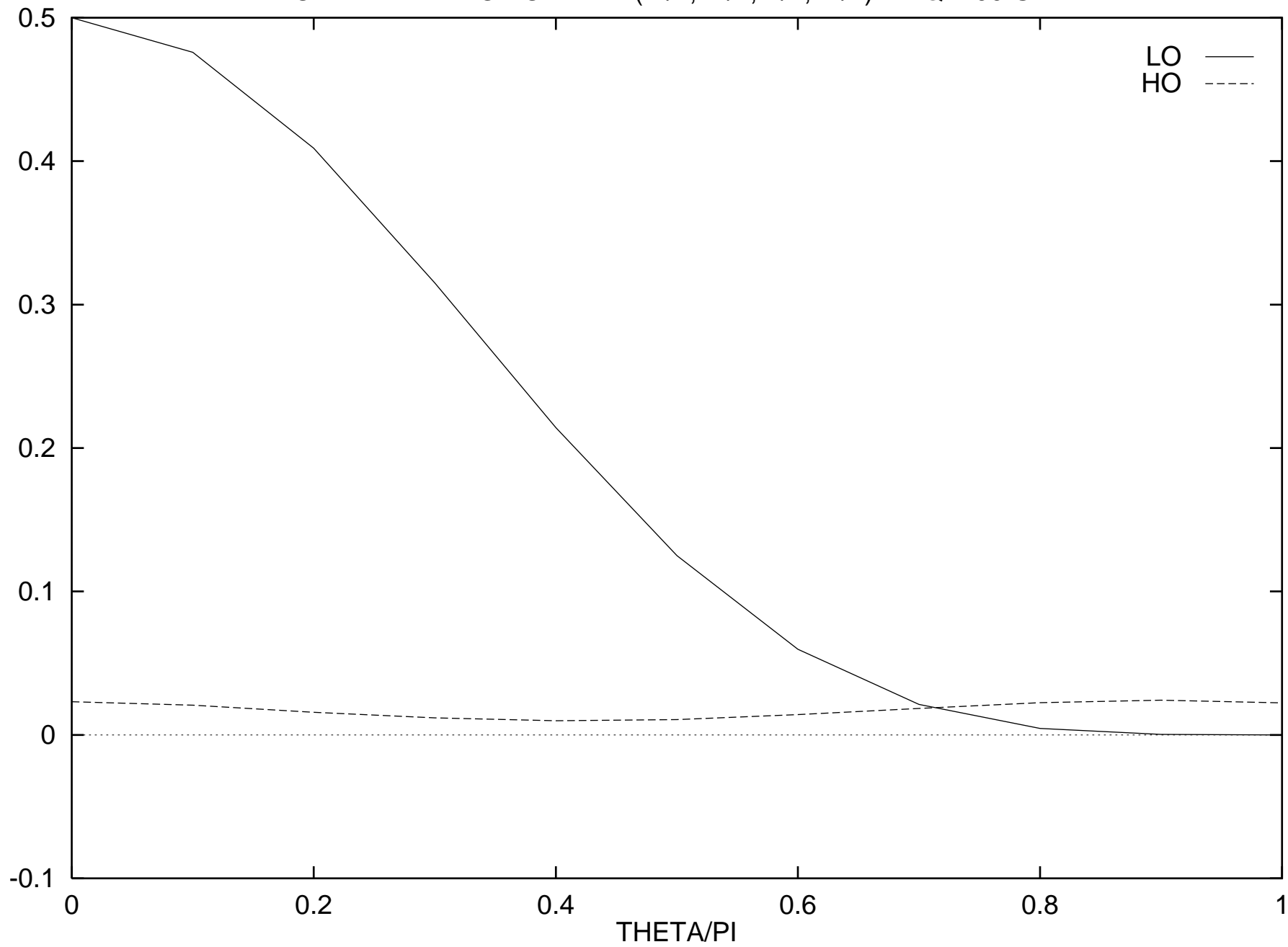
LO + ALPHA * HO FOR R-AA(-1/2,-1/2,+1/2,-1/2) AT Q=400 GEV



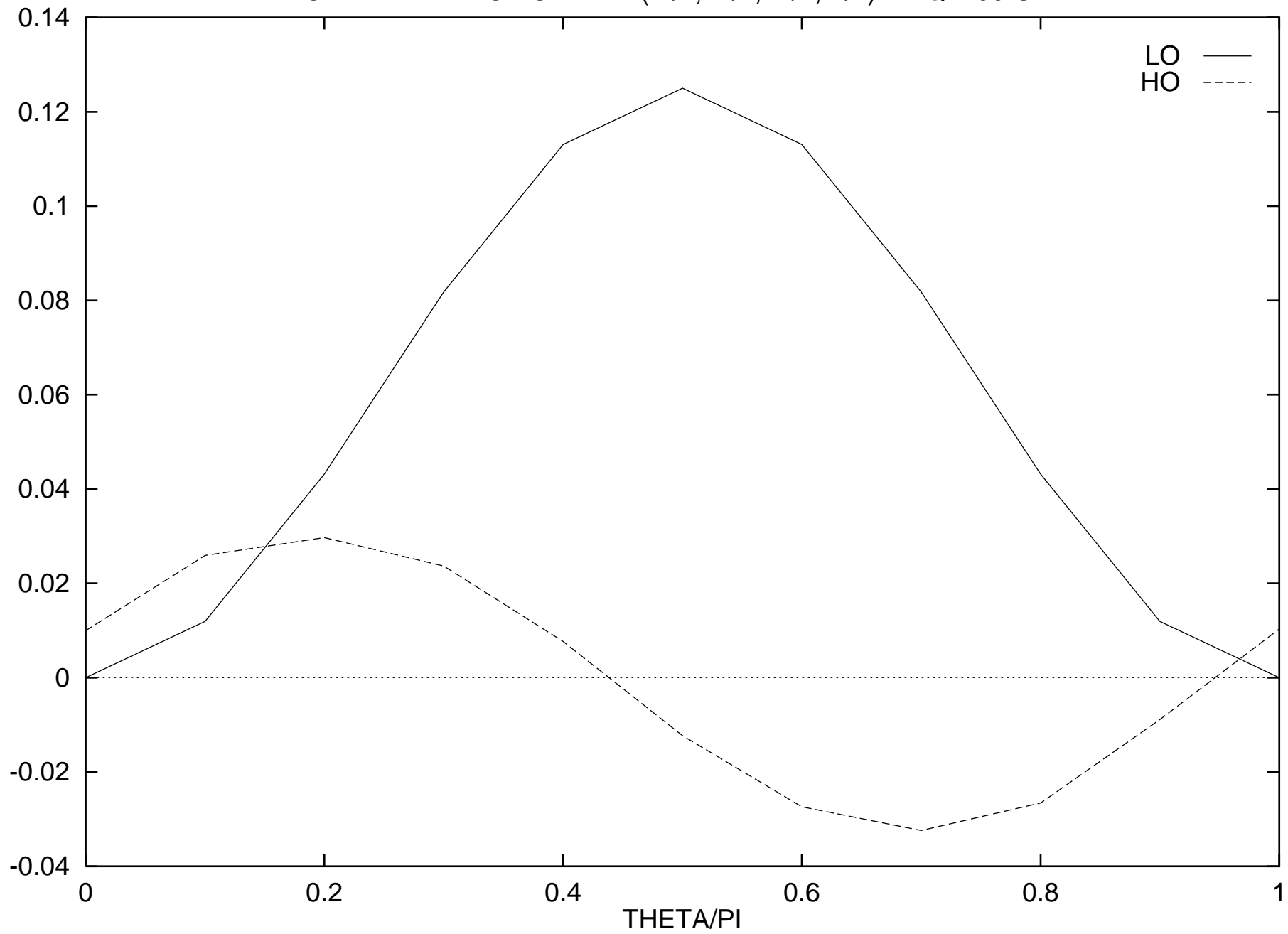
LO + ALPHA * HO FOR R-AA(-1/2,-1/2,+1/2,+1/2) AT Q=400 GEV



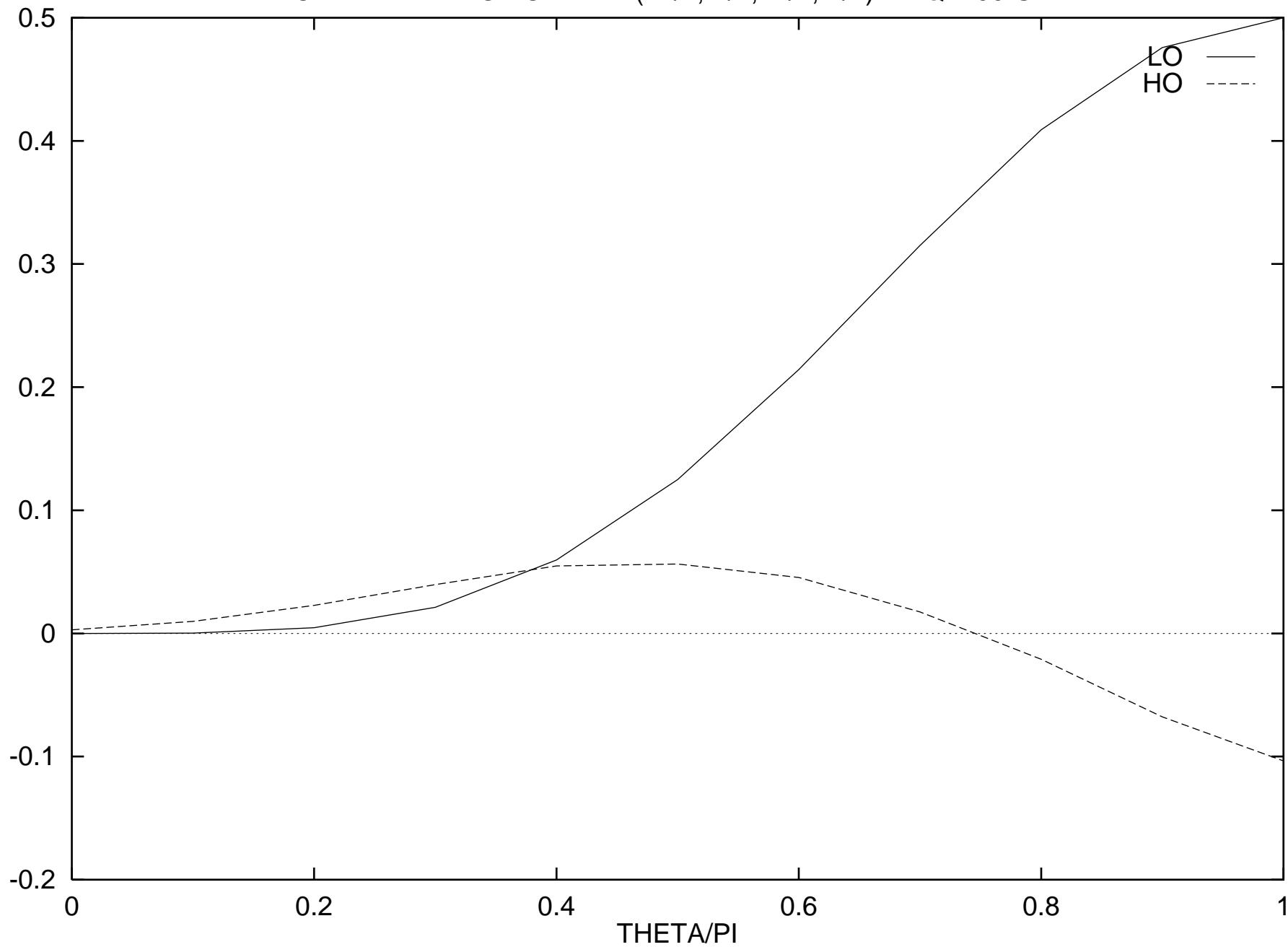
LO + ALPHA * HO FOR R-AA(-1/2,+1/2,-1/2,+1/2) AT Q=400 GEV



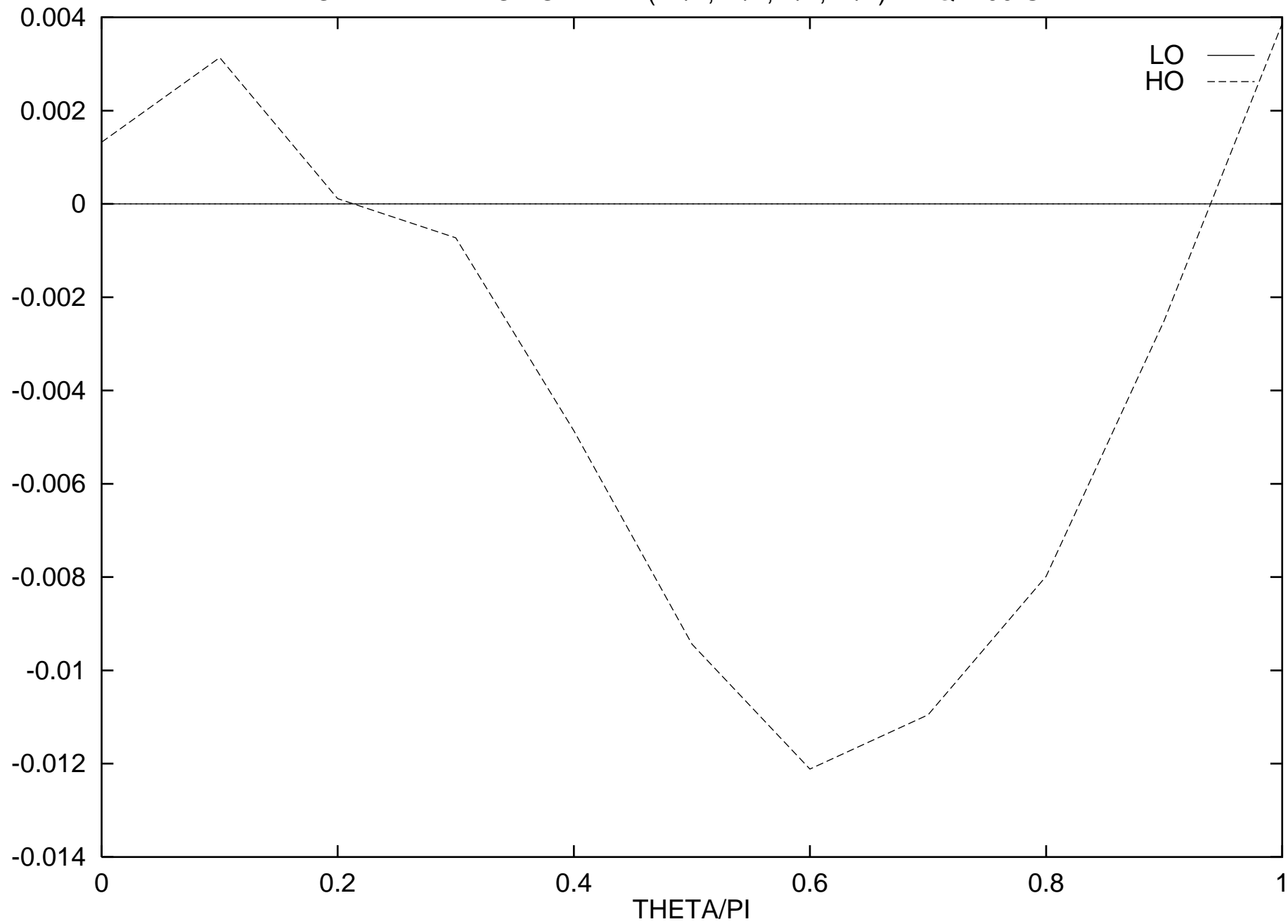
LO + ALPHA * HO FOR R-AA(-1/2,+1/2,+1/2,-1/2) AT Q=400 GEV



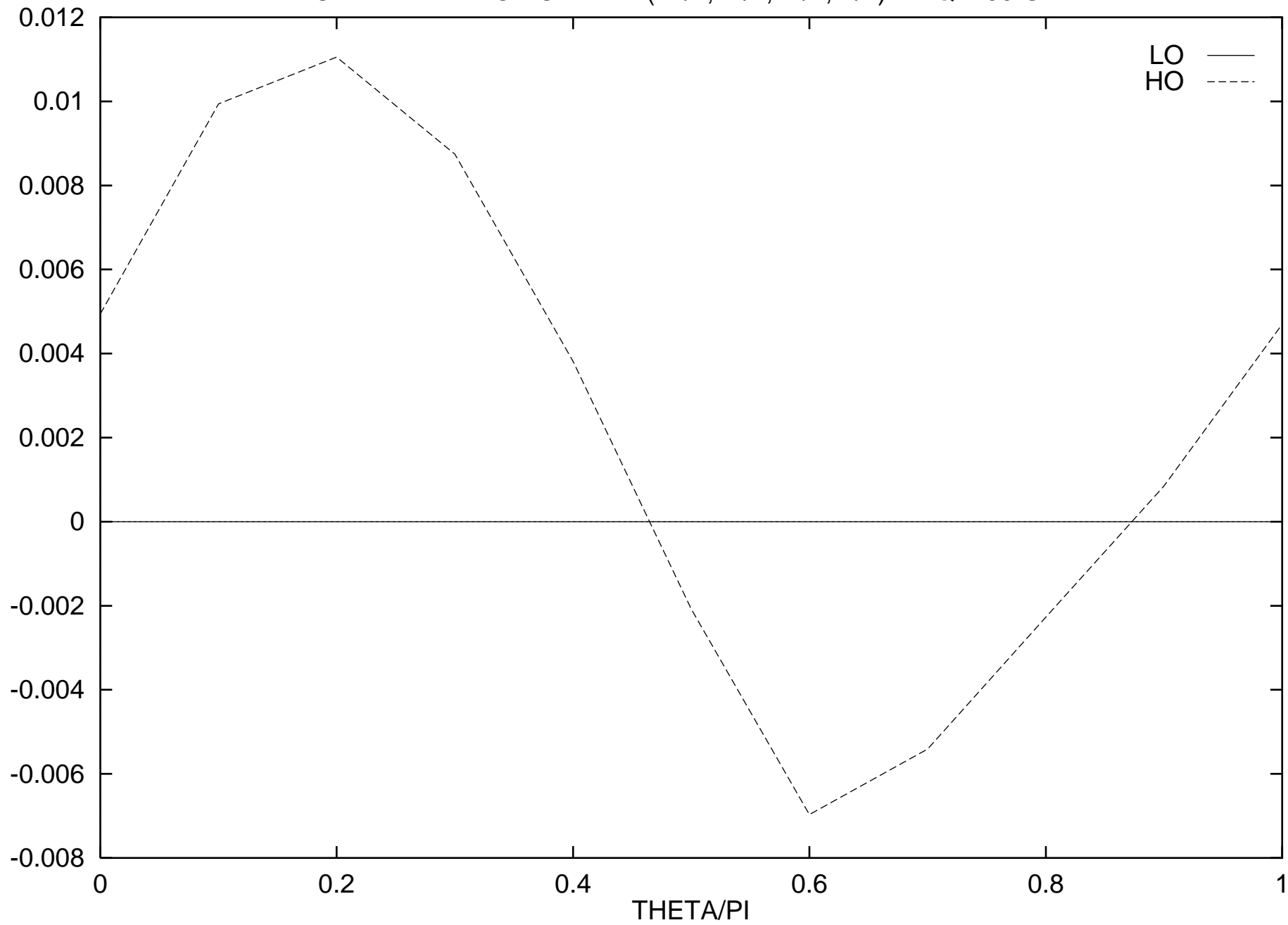
LO + ALPHA * HO FOR R-AA(+1/2,-1/2,+1/2,-1/2) AT Q=400 GEV



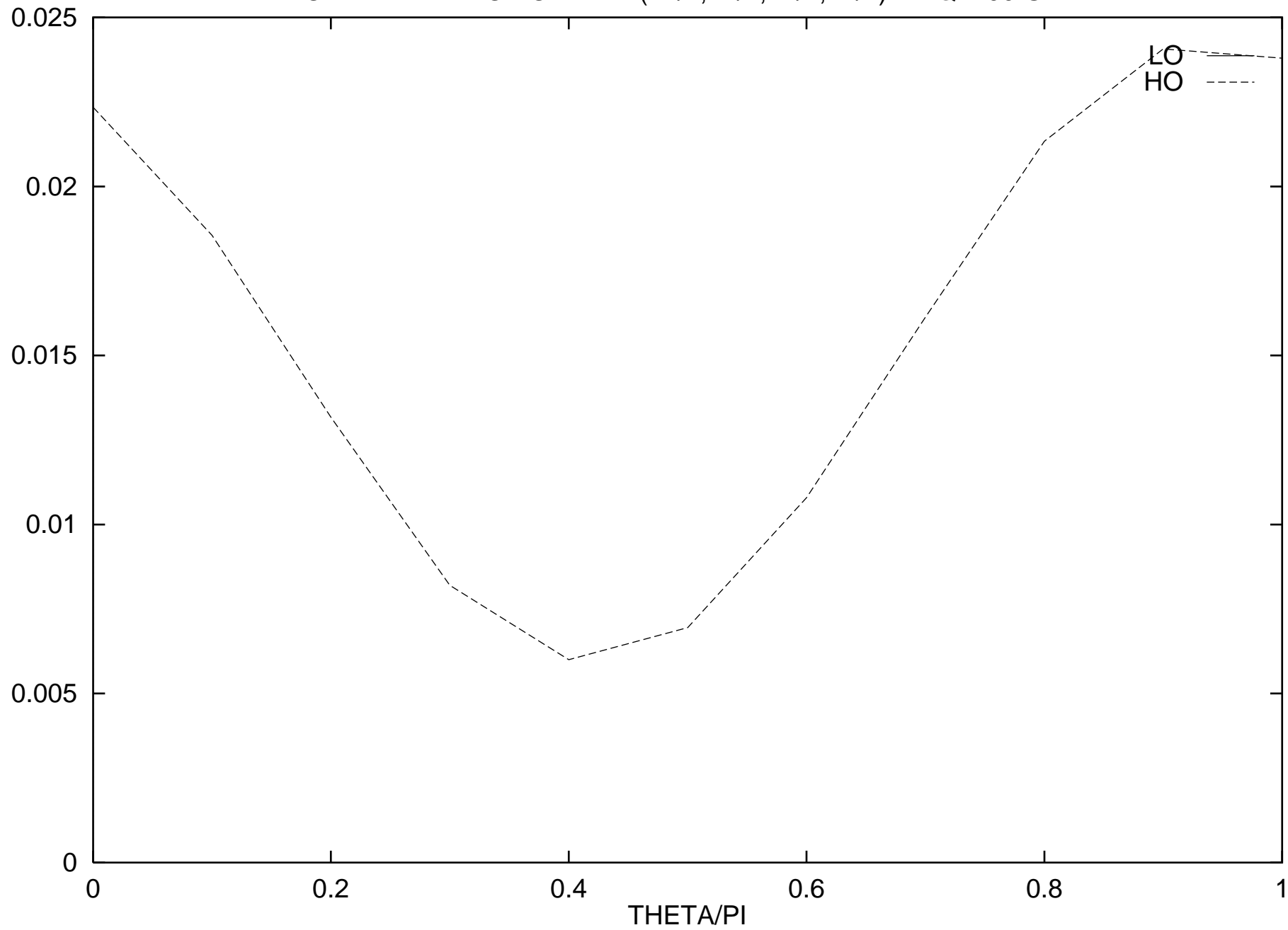
LO + ALPHA * HO FOR R-AA(+1/2,+1/2,-1/2,+1/2) AT Q=400 GEV



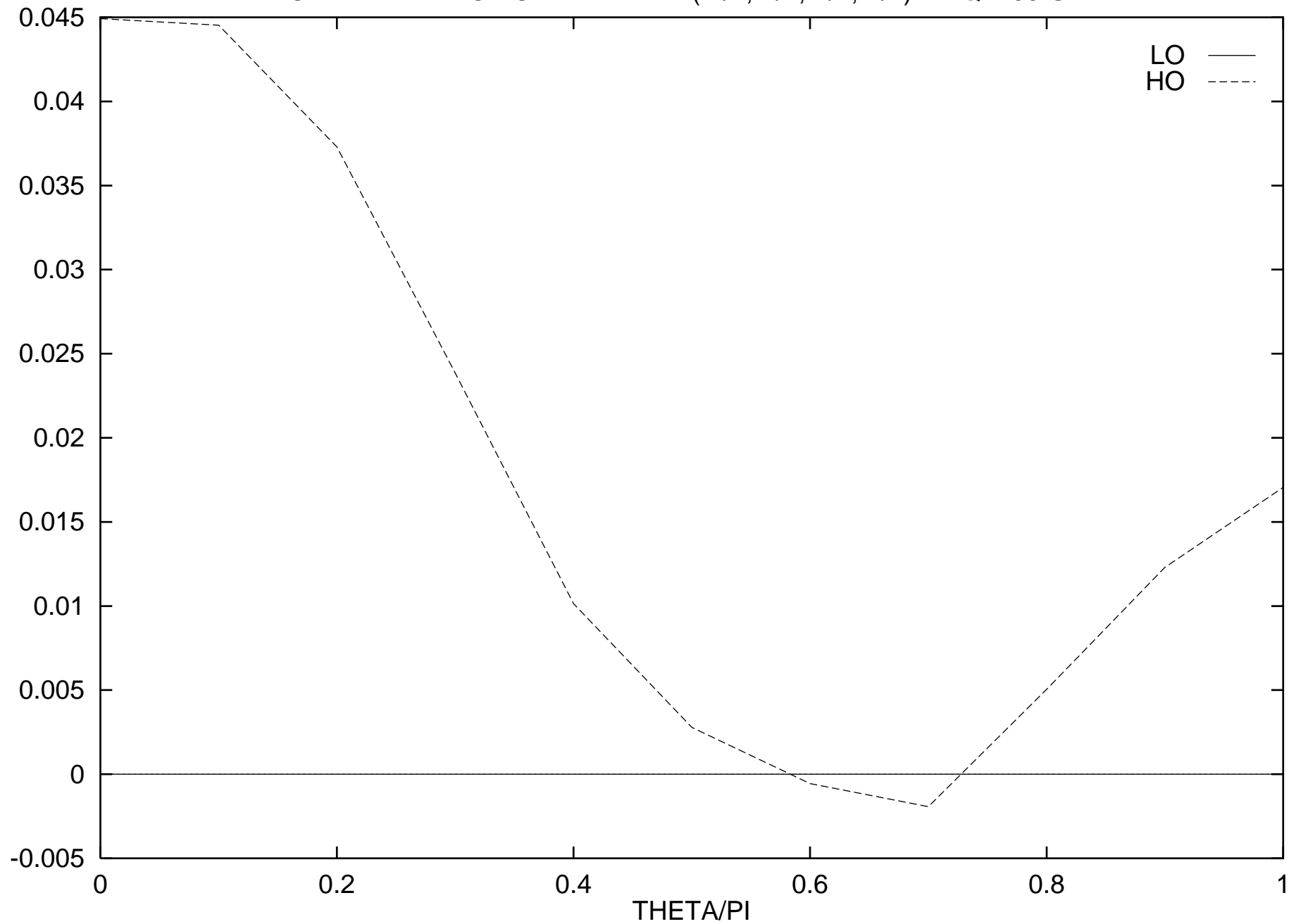
LO + ALPHA * HO FOR R-AA(+1/2,+1/2,+1/2,-1/2) AT Q=400 GEV



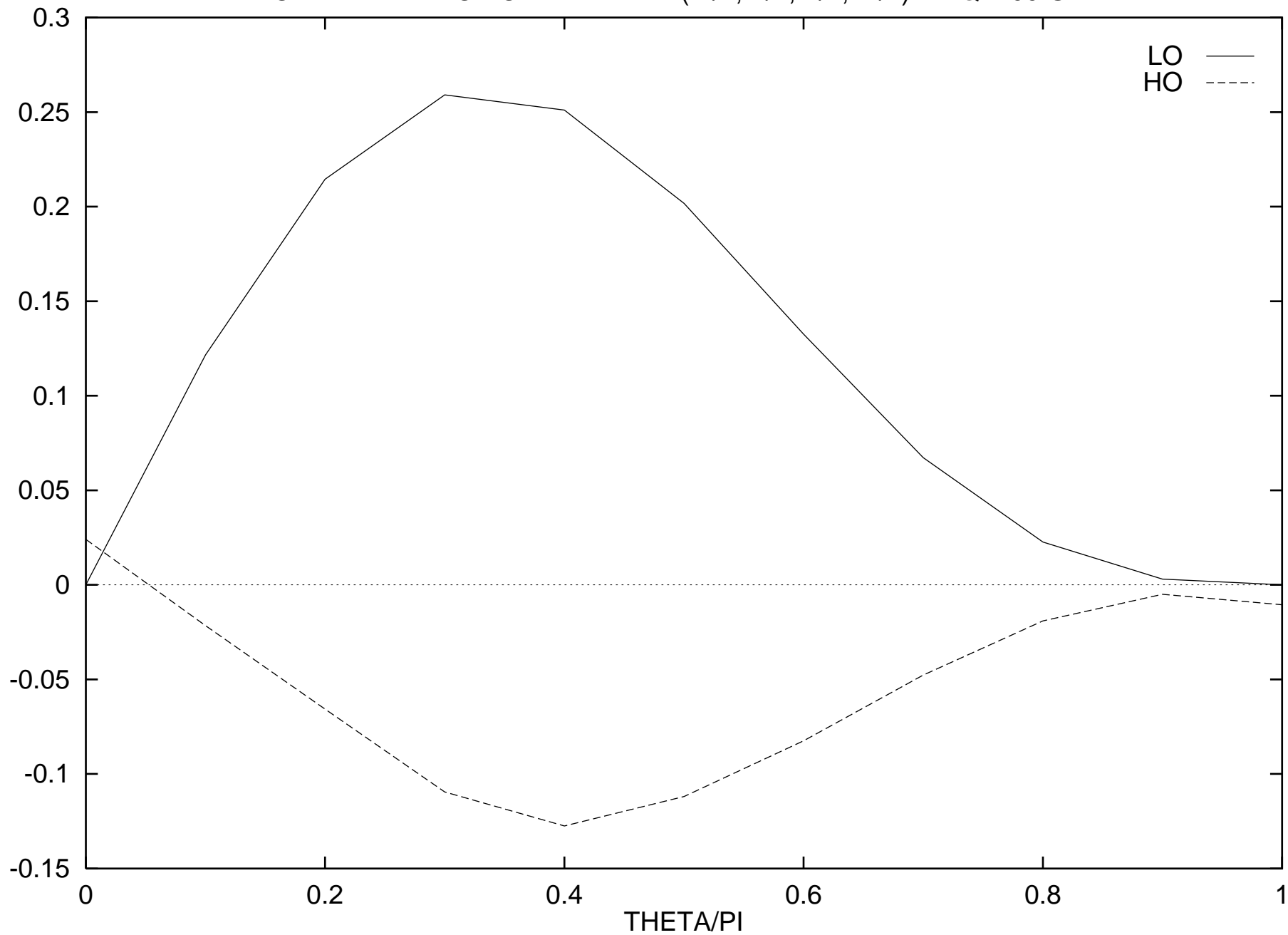
LO + ALPHA * HO FOR R-AA(+1/2,+1/2,+1/2,+1/2) AT Q=400 GEV



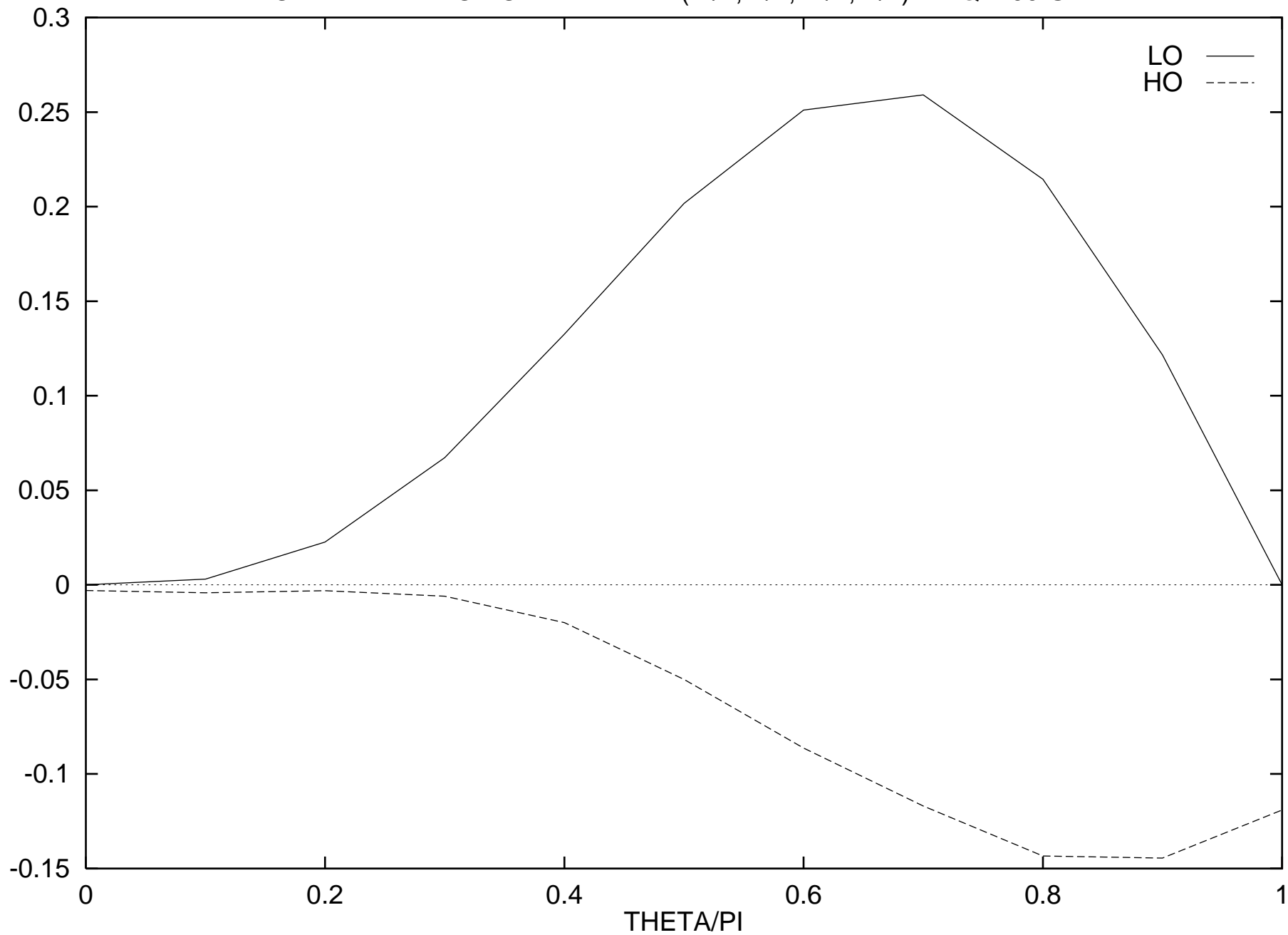
LO + ALPHA * HO FOR R-VAAVAA(-1/2,-1/2,-1/2,-1/2) AT Q=400 GEV



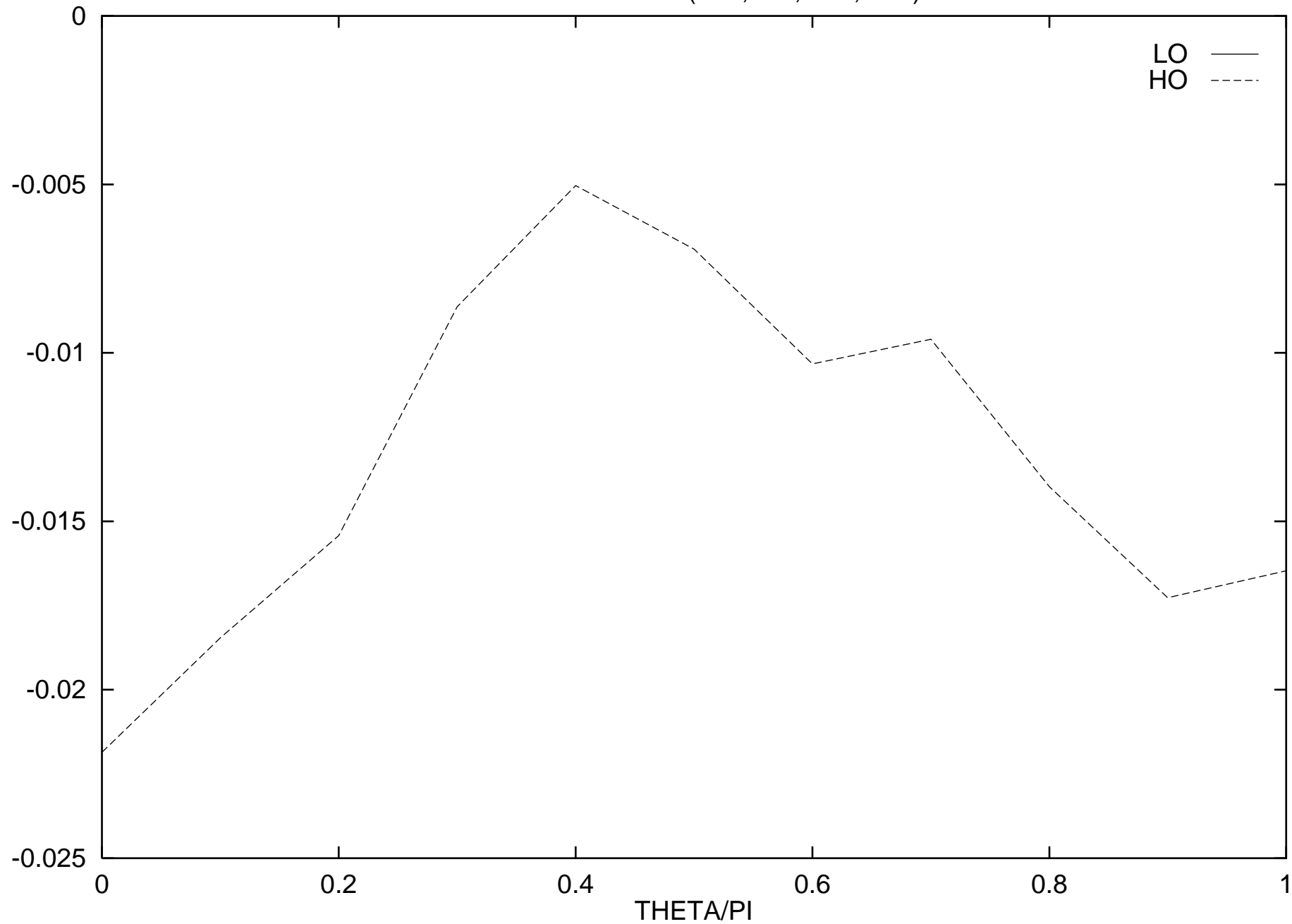
LO + ALPHA * HO FOR R-VAAVAA(-1/2,-1/2,-1/2,+1/2) AT Q=400 GEV



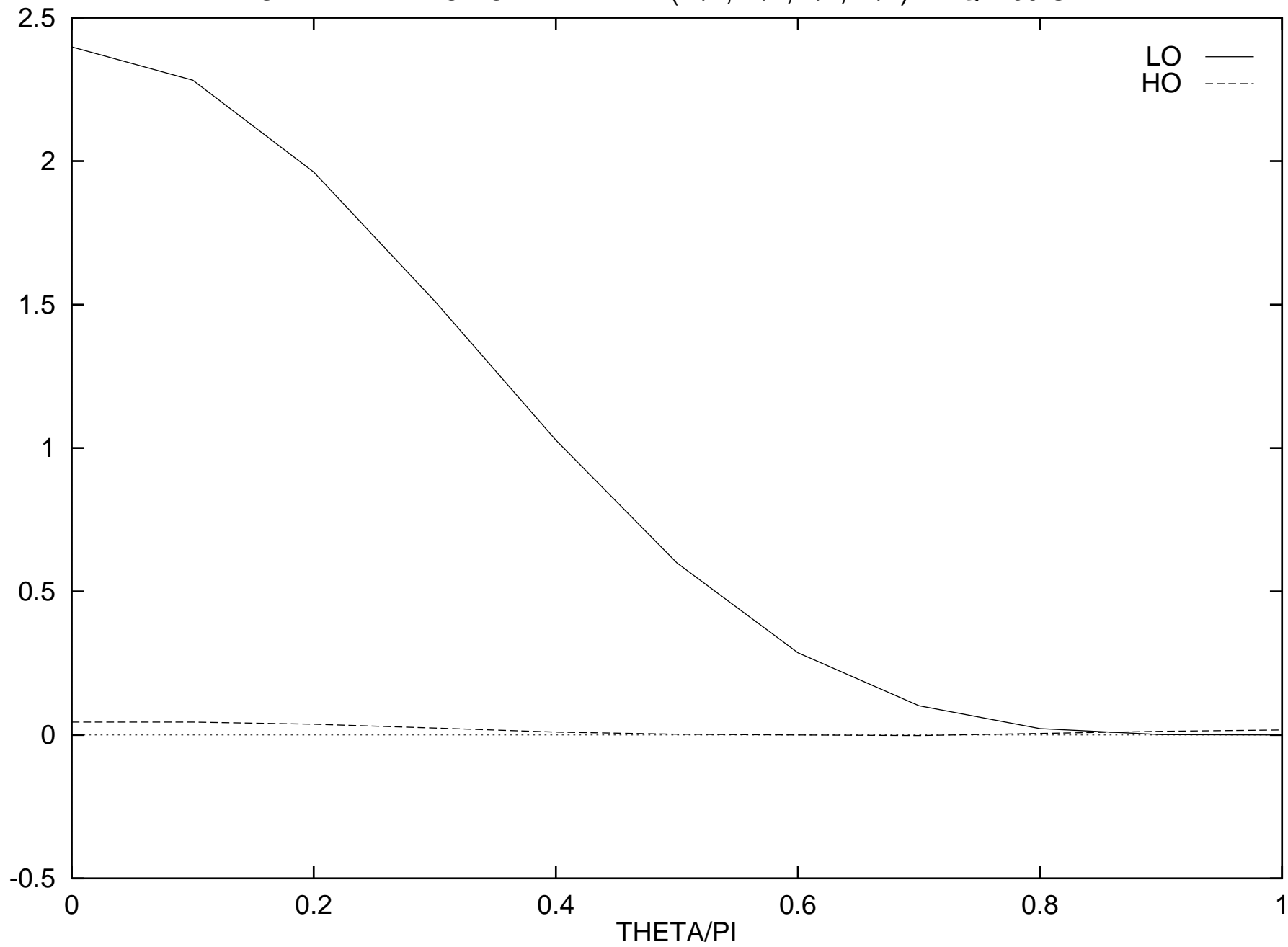
LO + ALPHA * HO FOR R-VAAVAA(-1/2,-1/2,+1/2,-1/2) AT Q=400 GEV



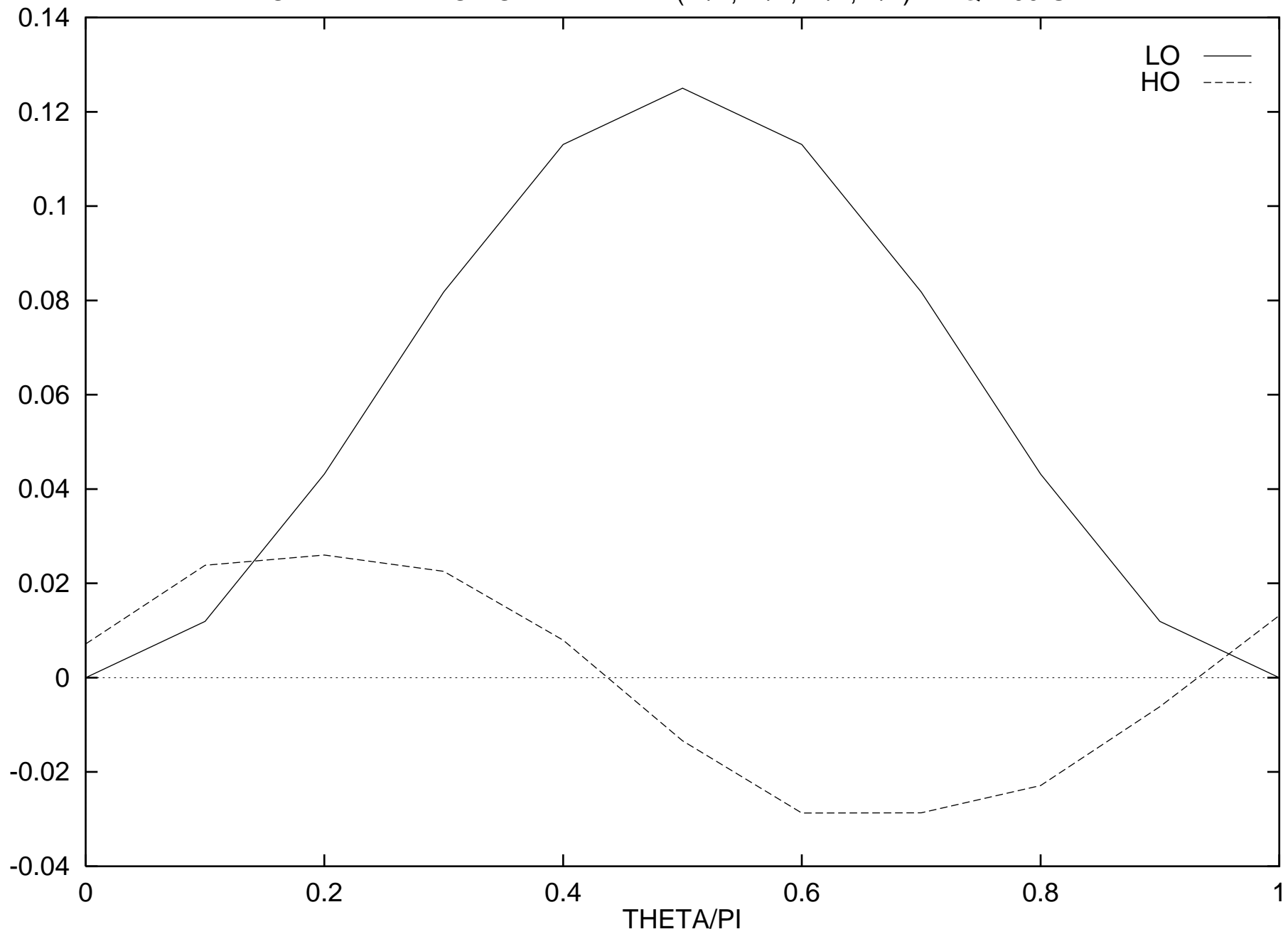
LO + ALPHA * HO FOR R-VAAVAA(-1/2,-1/2,+1/2,+1/2) AT Q=400 GEV



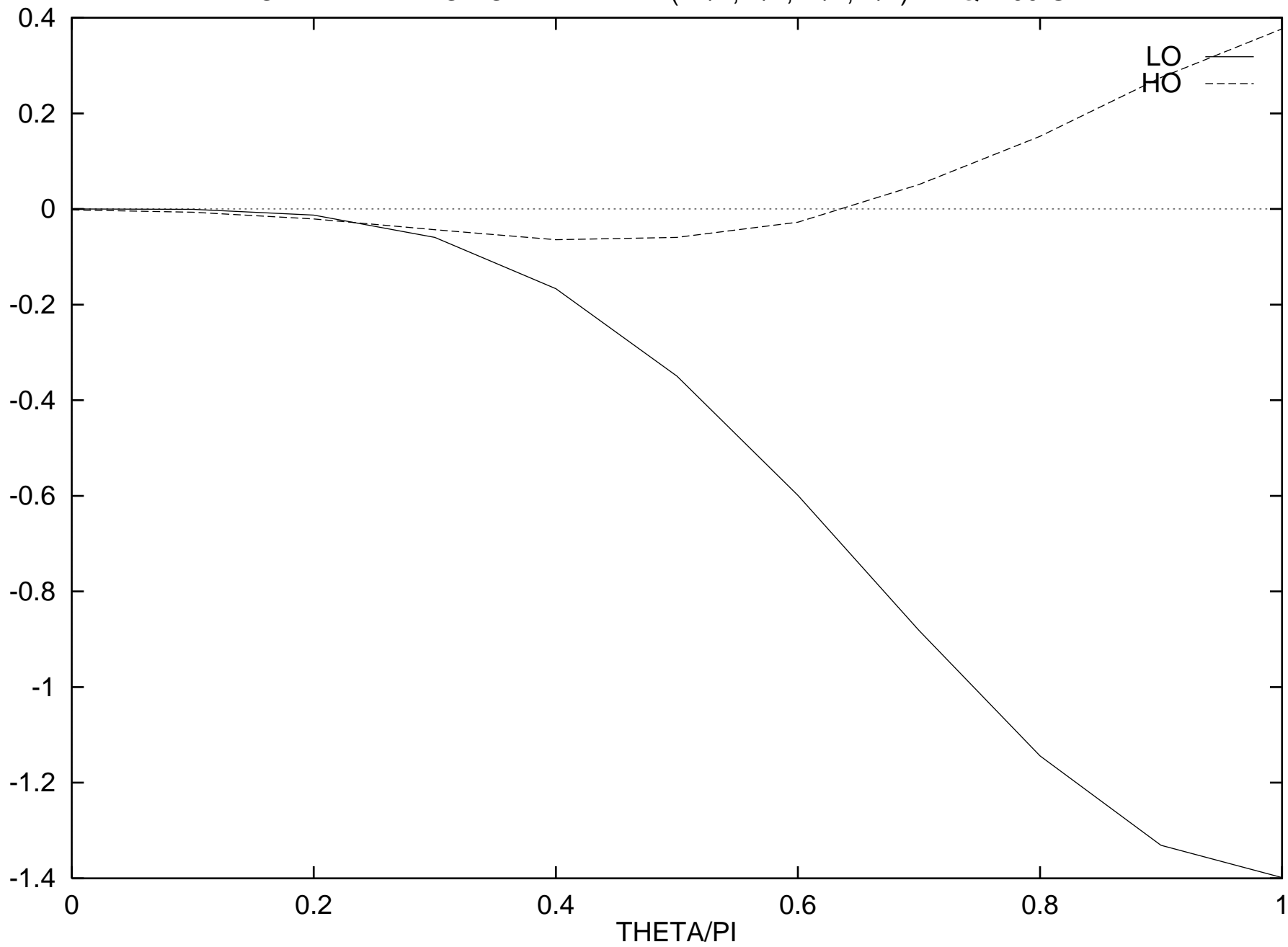
LO + ALPHA * HO FOR R-VAAVAA(-1/2,+1/2,-1/2,+1/2) AT Q=400 GEV



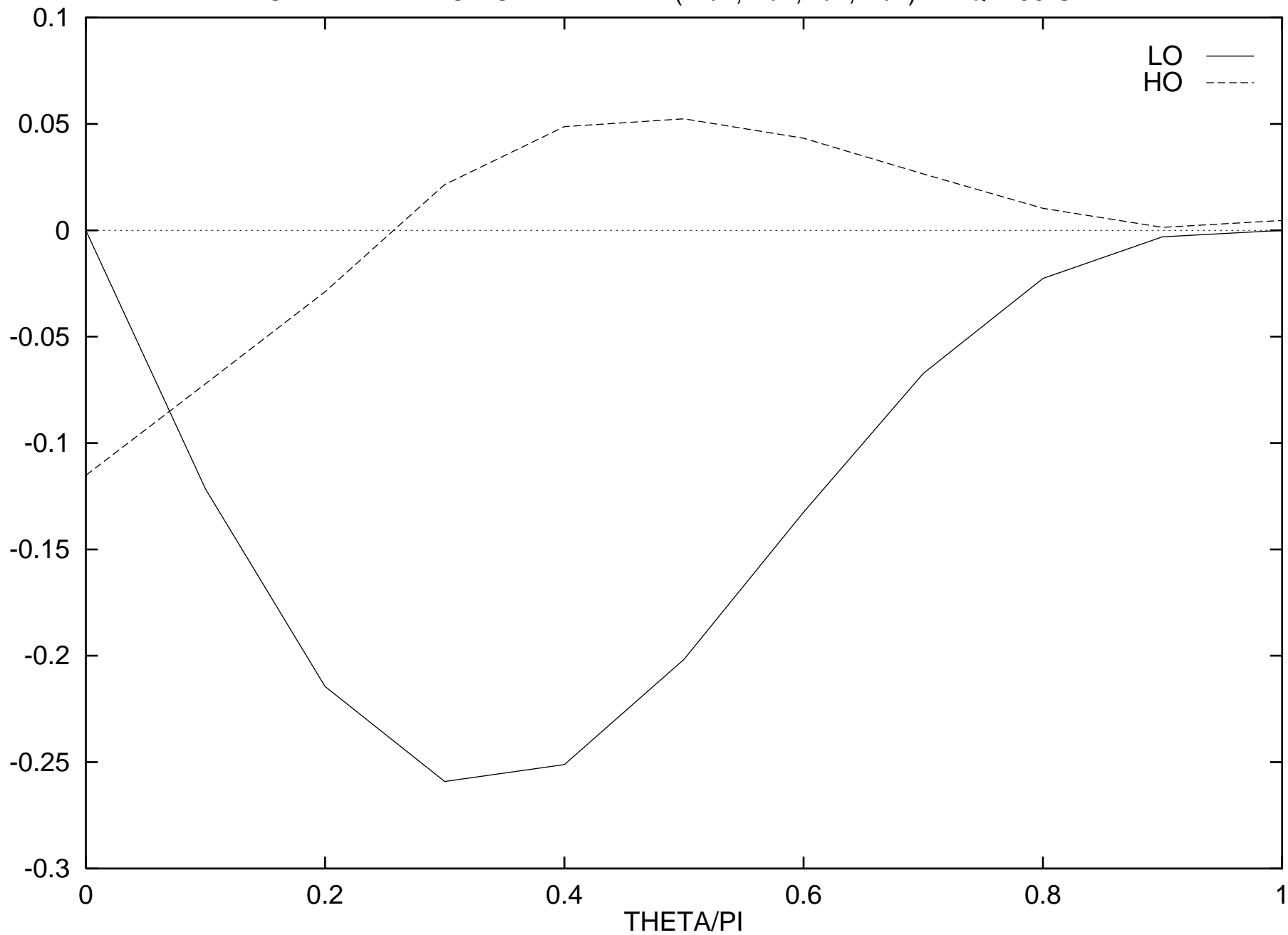
LO + ALPHA * HO FOR R-VAAVAA(-1/2,+1/2,+1/2,-1/2) AT Q=400 GEV



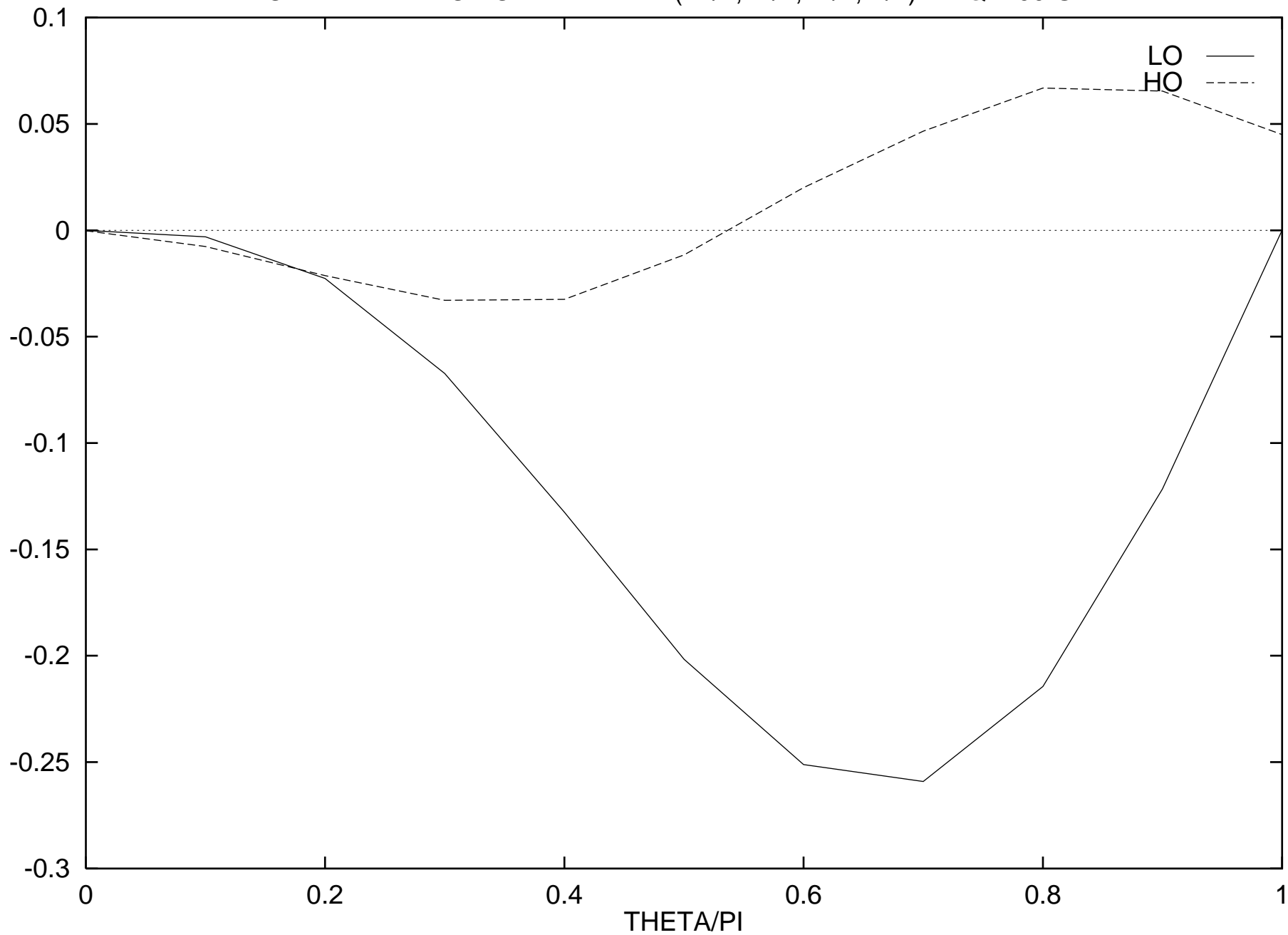
LO + ALPHA * HO FOR R-VAAVAA(+1/2,-1/2,+1/2,-1/2) AT Q=400 GEV



LO + ALPHA * HO FOR R-VAAVAA(+1/2,+1/2,-1/2,+1/2) AT Q=400 GEV



LO + ALPHA * HO FOR R-VAAVAA(+1/2,+1/2,+1/2,-1/2) AT Q=400 GEV



LO + ALPHA * HO FOR R-VAAVAA(+1/2,+1/2,+1/2,+1/2) AT Q=400 GEV

